Cellular localization and mechanism of Amyloid Precursor Protein (APP) homodimer formation in an oxidizing environment

Dissertation
zur Erlangung des Grades
„Doktor der Naturwissenschaften“

am Fachbereich Biologie
der Johannes Gutenberg-Universität Mainz

von

Simone Isbert
geboren am 11. August 1979 in Troisdorf

Mainz, im November 2011

Dekan:

1. Berichterstatter:

2. Berichterstatter:

Tag der mündlichen Prüfung: 23.01.2012

Table of contents

Abbreviations

AD	Alzheimer´s Disease
ADAM	A disintegrin and metalloprotease
AICD	APP intracellular domain
ANOVA	Analysis of variance
APH	Anterior pharynx defective
APLP	Amyloid precursor protein-like protein
APP	Amyloid precursor protein
APPL	Amyloid precursor protein like
APPs	APP soluble ectodomain
APPsw	Swedish mutant APP
Aβ	Amyloid-β
BACE	β-site APP cleaving enzyme
BFA	Brefeldin A
BiFC	Bimolecular Fluorescence Complementation
BME	β-Mercaptoethanol
bp	Base pair
BSA	Bovine serum albumin
°C	Degrees celsius
cDNA	Complementary deoxyribonucleic acid
CHO	Chinese hamster ovary
Ci	Curie
CPZ	Chlorpromazine
C-terminal	Carboxy-terminal
CTF	Carboxy-terminal fragment
CuBD	Copper binding domain
Cys	Cysteine
DAPT	N-[N-(3,5-Difluorophenacetyl-L-alanyl)]-S-pheylglycine t-butyl ester
DMSO	Dimethylsulfoxid
D/N	Dominant/Negative
DNA	Deoxyribonucleic acid
ECL	Enhanced chemiluminescence
E.coli	*Escherichia coli*
EGF	Epidermal growth factor
ER	Endoplasmic Reticulum
ERGIC	Early Golgi and Intermediate Compartments
EtOH	Ethanol
FAD	Familial Alzheimer's disease
FRET	Fluorescence resonance energy transfer

g	Gram
GFLD	Growth factor like domain
GFP	Green fluorescent protein
GSK3-β	Glycogen-synthase 3-β
h	Hour
HEK	Human embryonic kidney
HRP	Horse raddish peroxidase
ICD	Intracellular domain
IgG	Immunoglobulin G
IP	Immunoprecipitation
kDa	Kilo Dalton
KK*XX*	Dilysine ER retention motif
KPI	Kunitz type protease inhibitor
LB	Luria-bertani Broth
LRP	Low density lipoprotein receptor related protein
LTP	Long-term potentiation
M	Molar
MES	2-(N-morpholino)ethanesulfonic acid
m	Milli
min	Minute
mM	Millimolar
n	Nano
NaCl	Sodium Chloride
NaN_3	Sodium Azide
NEM	*N*-ethylmaleimide
NFTs	Neurofibrillary tangles
NICD	Notch intracellular domain
NP-40	Nonidet P-40
NPxY	Asparagin-Prolin-x-Tyrosine-motif
NSAID	Non-steroidal anti-inflammatory drug
N-terminal	Amino-terminal
OD	Optical density
p	Pico
PAGE	Polyacrylamide gel electrophoresis
PBS	Phosphate-buffered saline
PCR	Polymerase chain reaction
PD	Parkinson's disease
PD	Pull down
PDI	*Protein disulfide isomerase*
Pen-2	Presenilin enhancer 2
PFA	Paraformaldehyde

PHFs	Paired helical filaments
PID	Phosphotyrosine interaction domain
PM	Plasma membrane
PS	Presenilin
RIP	Regulated intramembrane proteolysis
rpm	Rounds per minute
RT	Room temperature
s	Second
S2	*Schneider* cells
sAPP	Soluble amyloid precursor protein ectodomain
SAXS	Small-angle X-ray scattering
SDS	Sodium dodecyl sulfate
SEM	Standard error of the mean
SP	Signal peptide
Sw	Swedish mutation
TACE	TNF-alpha converting enzyme
TAE	Tris acetic acid
TBS	Tris-buffered saline
TE	Tris-EDTA
TEMED	N,N,N'N'-Tetramethylethylendiamine
TGN	*Trans*-Golgi network
TM	Transmembrane
µg	Microgram
µl	Microlitre
µM	Micromolar
UAS	Upstream activating sequence
UV	Ultra violet
v/v	Volume per volume
WB	Western blot
w/v	Weight per volume
wt	Wildtype
ZnBD	Zink binding domain

1 Introduction

1.1 Alzheimer´s disease

Alzheimer's disease (AD) is a progressive neurodegenerative disorder that begins as mild short-term memory deficits and culminates in total loss of cognition and executive functions. It is the most prevalent neurodegenerative disorder, affecting 10% of the population over the age of 65 and 50% of the population over the age of 85 (Brookmeyer et al. 2007). A small subset (<10%) of AD cases result from inherited autosomal dominant gene mutations and has an early-onset (the fourth to sixth decade) (Sloane et al. 2002). It is currently estimated that 20-30 million people worldwide suffer from dementia today, with over 4 million new cases every year (Wancata et al. 2003). Regarding these numbers it can be predicted that the amounts will double every 20 years to 42 million by 2020 and over 80 million by 2040 (Ferri et al. 2005). The onset of Alzheimer's disease is usually gradual, and it is slowly progressive. Problems of memory, particularly for recent events (short-term memory) are common early in the course of AD. Mild personality changes such as apathy, withdraw from social interactions (Landes et al. 2001), or a progressive decline in language functions (Taler and Phillips 2008), may also occur early in the illness (Waldemar et al. 2007). As the cognitive decline continues, a slowing of motor functions and coordination often leads to a picture resembling extrapyramidal motor disorders such as Parkinson's disease (PD) (Waldemar et al. 2000). Later in the course of the disorder affected individuals may become totally incapable of caring for themselves, finally leading to death, likely from some problem that occurs in severe states of health (Duncan and Siegal 1998). The German psychiatrist Alois Alzheimer was the first to demonstrate a relationship between specific cognitive changes, neurological lesions in the human brain, and clinical history (Alzheimer 1907). Alzheimer reported the results of an autopsy on a 55-year-old woman named Auguste Deter, who had died from a progressive behavioral and cognitive disorder. He noted the presence of two distinct pathological lesions in Deters brain, which now define Alzheimer's disease (AD): first, the neurofibrillary tangles (NFTs), which accumulate intraneuronal (later shown to be composed of paired helical filaments (PHFs) containing the microtubule-associated protein tau) (Goedert et al. 1988; Goedert et al. 1989); second, extracellular amyloid deposits in the form of diffuse or neuritic senile plaques (Price et al. 1997). Later it was shown that In the AD brain, tau is hyperphosphorylated and more than 30 phosphorylation sites have been identified in PHF-tau proteins (Grundke-Iqbal et al. 1986; Kosik et al. 1986; Wolozin et al. 1986). The formation of NFTs is thought to be associated with a collapse of the microtubule network (Iqbal et al. 2005), disturbances of axoplasmic transports, and massive neuron loss (Gendron and Petrucelli 2009) macroscopically culminating in brain atrophy (Unger et al. 1991) in the hippocampus and cortex, resulting in cognitive decline and dementia (McEvoy et al. 2009). Senile plaques however, as described by Alois Alzheimer, accumulate extracellular and were isolated and purified in 1984 by Glenner and Wong, who showed that it was a ~4-kDa peptide, primarily 40 or 42 amino acids in length, which they speculated was cleaved from a larger precursor (Glenner and Wong 1984). Subsequent research determined that this peptide fragment originated from a larger precursor protein, named somewhat predictably, the amyloid-β precursor protein (AβPP, or APP as used here) and was characterized from the analysis of a

full-length cDNA encoding a translational product of 695 residues (Kang et al. 1987). This protein is synthetized in neurons as a 100-kDa glycosylated type I transmembrane protein. The use of cellular models has clearly identified two catabolic pathways for APP (described under 1.2). A non amyloidogenic pathway, in which APP is cleaved by α-*secretase* within the sequence of the amyloid peptide, precluding the formation of the full-length Aβ which is found in the amyloid core of senile plaques (Zheng and Koo 2006). A second catabolic pathway of APP leads to the production of Aβ from its precursor, after the initial cleavage by β-*secretase* to release the full-length amyloid peptide (Nunan and Small 2000). The cause for the widespread neuron loss in AD patients has not been fully determined but accumulating evidence suggests that aberrant production of the Aβ peptides plays a causal role in disease onset and progression (Hyman et al. 1989; Hyman et al. 1989). These observations led to the formulation of the amyloid hypothesis (Hardy 1997; Hardy and Selkoe 2002), (Glenner and Wong 1984) which states that overproduction of Aβ and its aggregation in senile plaques promotes a cascade of secondary neurotoxic effects, such as formation of intracellular neurofibrillary tangles, synaptic dysfunction, enhanced oxidative stress, and inflammatory responses that eventually culminate in neurodegeneration and development of AD (Selkoe 1991; Hardy 2002). In the following, both, Aβ and Tau, have been extensively investigated. In studies on genetic inheritance of AD (familiar AD, FAD), several mutations were discovered in genes involved in Aβ production, which in general lead to an earlier age of onset (Bertram et al. 2010). FAD Mutations were found in the *app*, and *presenilin* 1 and 2 genes (encoding components of a proteolytic complex involved in APP processing and degradation), all of which directly influence the generation of Aβ (Annaert and De Strooper 2002). The main effect of mutations in these genes is the overproduction of Aβ42, which was shown to be especially prone to aggregation (Suzuki et al. 1994). The first mutation within the *app* gene to cause FAD was discovered in 1991 (Goate et al. 1991). Today, there are 27 known mutations in APP found in 75 different families (http://www.alzforum.org/res/com/mut/app/default.asp). All mutations within APP are located in proximity of the different cleavage sites and either affect the quantity and length of Aβ that is formed, or alternatively the properties of Aβ. For example the Swedish mutation Lys595-Met596 → Asn595-Leu596 (Mullan et al. 1992) is located N-terminally of the β-*secretase* site and makes APP a better substrate for β-*secretase,* consequently resulting in a higher overall production in Aβ (Citron et al. 1992). The London mutation Val642 → Ile642 (Chartier-Harlin et al. 1991; Goate et al. 1991) on the other hand, which is located C-terminally of the γ-*secretase* cleavage, affects the γ-*secretase* in such a way that more Aβ42 is produced (Suzuki et al. 1994) which is more prone to aggregate into fibrils (Hilbich et al. 1991; Burdick et al. 1992), and thus drives Aβ deposition and formation of plaques (Jarrett et al. 1993). As mentioned above, mutations linked to an autosomal and highly penetrant form of early-onset AD were also found in the presenilin genes, coding for PS1 (encoded by *PSEN1* on chromosome 14), or its homologue PS2 (encoded by *PSEN2* on chromosome 1). In general PS, mutations highly affect the processing of APP (Citron et al. 1997) in such a way that the longer and more amyloidogenic Aβ42 is generated to a higher degree (Selkoe 2002) causing a faster disease progression with symptoms presented earlier in life (mean age of onset 40-50 years) (Bertram and Tanzi 2004). However, APP mutations linked with FAD account for less than 5% of total AD cases, whereas the clinical and pathological symptoms are nearly identical to that of the more

frequent, late-onset sporadic AD (Scacchi et al. 1995). Thus, the main risk factor for developing the disease is considered to be high age (Herrup 2010). Moreover, in patients with Down's syndrome (trisomy 21), overexpression of the normal APP gene which is located on the long arm of chromosome 21 (Korenberg et al. 1989) causes AD-like pathology and symptoms during middle adult years (Glenner and Wong 1984). Although some researchers now believe that oligomeric Aβ42 is the crucial trigger causing the disease (Selkoe 2002) the precise molecular mechanism leading to AD is still unknown. Until recently, it was also unclear, whether tau hyperphosphorylation and tangle formation are cause or effect of Aβ production and deposition, or vice versa. The twist in the Aβ-hypothesis rather suggests that the sequence of pathophysiological events may have more to do with the Aβ form i.e. soluble Aβ oligomers as opposed to monomers and insoluble amyloid fibrils (Suzuki et al. 1994; Tucker et al. 2002; Qahwash et al. 2003). Several recent studies have reported a correlation between the levels of soluble Aβ oligomers and the severity of the disease (Caughey and Lansbury 2003; Oddo et al. 2006; Li et al. 2011).

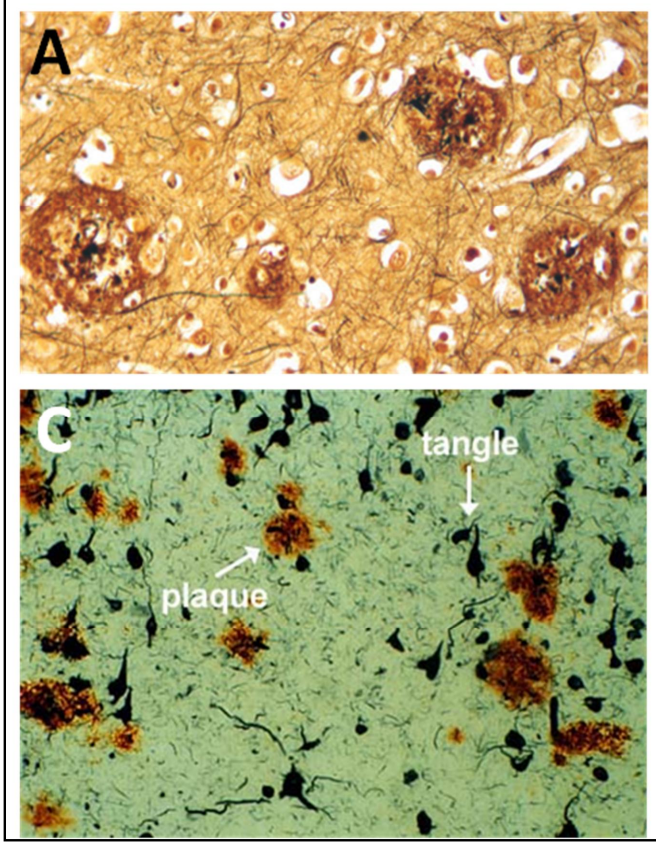

Fig. 1: The characteristic pathological features in an AD brain, plaques and tangles: (A) AD is pathologically characterized by the presence of extracellular amyloid plaques, composed of aggregated amyloid-β peptide and intracellular neurofibrillary tangles (B) (NFTs), which consist of intraneuronal lesions made up of aggregated, hyperphosphorylated microtubule-associated tau. (C) The mature plaques contain in addition to amyloid-β peptides, degenerating axons and dendrites, and are surrounded or invaded by microglia and reactive astrocytes. Adapted from Khalifa et al., 2007)

1.2 The amyloid precursor protein and its proteolytic processing

Full-length APP is a type I 110 – 130 kDa single pass transmembrane protein with a large ectodomain and a shorter cytoplasmic carboxy-terminal (C-terminal) tail (Kang et al. 1987). In addition to many post-translational modifications (outlined below), APP is further modified through a series of cleavage events generating a variety of fragments, including the Aβ peptide (Marks and Berg 2003). APP processing occurs via two different pathways, the amyloidogenic and the non-amyloidogenic pathway (Fig. 2). The first pathway, originally described by Esch and co-workers (Esch et al. 1990) is initiated by a protease referred to as α-*secretase*, which cleaves APP between lysine 612 and leucine 613 (APP695 numbering; Fig. 2A). Cleavage of APP by α-*secretase* precludes Aβ generation as the cleavage site is within the Aβ domain (at the Lys16-Leu17 bond), and releases a large soluble ectodomain of APP called sAPPα and an 83-amino-acid-long C-terminal membrane-bound fragment C83 (Fig. 2B). This pathway is commonly referred to as the nonamyloidogenic pathway for it precludes generation of the Aβ peptide. Later it was determined that α-*secretase* is a zinc metalloproteinase (Rosendahl et al. 1997) being a member of the so called ADAM-(a disintegrin and metalloproteinase) family. These include TACE (tumor necrosis factor-α converting enzyme), also known as ADAM17 (Moss et al. 1997; Killar et al. 1999) as well as ADAM10 (Lammich et al. 1999) and MDC-9, also known as ADAM9 (Hotoda et al. 2002). The APP cleavage by α-*secretase* was shown to occur preferably in the trans-Golgi compartment (Sinha and Lieberburg 1999), or at the cell surface (Lammich et al. 1999). The second known proteolytic pathway leads to the production of Aβ, and is typically referred to as the amyloidogenic pathway. The first step in Aβ generation is cleavage of APP by the β-*secretase*, which was identified by independent approaches (Hussain et al. 1999; Sinha et al. 1999; Vassar et al. 1999; Yan et al. 1999) as BACE1 (β-site APP-cleaving enzyme). It is a membrane-bound aspartyl protease with a characteristic type I transmembrane domain near the C-terminus (Sinha et al. 1999; Vassar et al. 1999). Cleavage of APP by BACE1 (Vassar 2002) occurs between methionine 596 and aspartate 597 of APP695 (Figure 2A), producing two fragments, the secreted N-terminal ectodomain sAPPβ and a remaining 10 kDa, 99-amino-acid-long fragment C99 (Figure 2B), encompassing the N-terminus of the Aβ peptide. The optimal pH of BACE activity is approximately 4.5, suggesting that the β-site cleavage of APP occurs preferentially in more acidic compartments, such as in endosomes (Vassar et al. 1999). It has also been suggested that BACE1 cleavage can occur in lipid rafts (Ehehalt et al. 2003). After α- or β-cleavage, the carboxyl terminal fragments (CTFs) of APP, known as αCTF (C83) and βCTF (C99), respectively, remain membrane-associated and are further cleaved by the γ-*secretase*-complex (Edbauer et al. 2003). The γ-*secretase* is an aspartyl protease complex (Wolfe et al. 1999), which unlike α- and β- *secretases*, acts within the membrane and cleaves APP at multiple sites (Zhao et al. 2004), releasing either, Aβ and intracellular C-terminal domain fragments (ICDs) or p3 and ICDs (Fig. 2B). This process is called regulated intramembrane proteolysis (RIP) (Brown et al. 2000). However, while the two predominant forms of Aβ and p3 terminate at valine 637 (Aβ40 and p3/40) and alanine 639 (Aβ42 and p3/42) (Haass et al. 1992), isolated ICDs are shorter than expected and begin at sites 9-10 amino acid downstream of those residues (Gu et al. 2001).

Figure 2

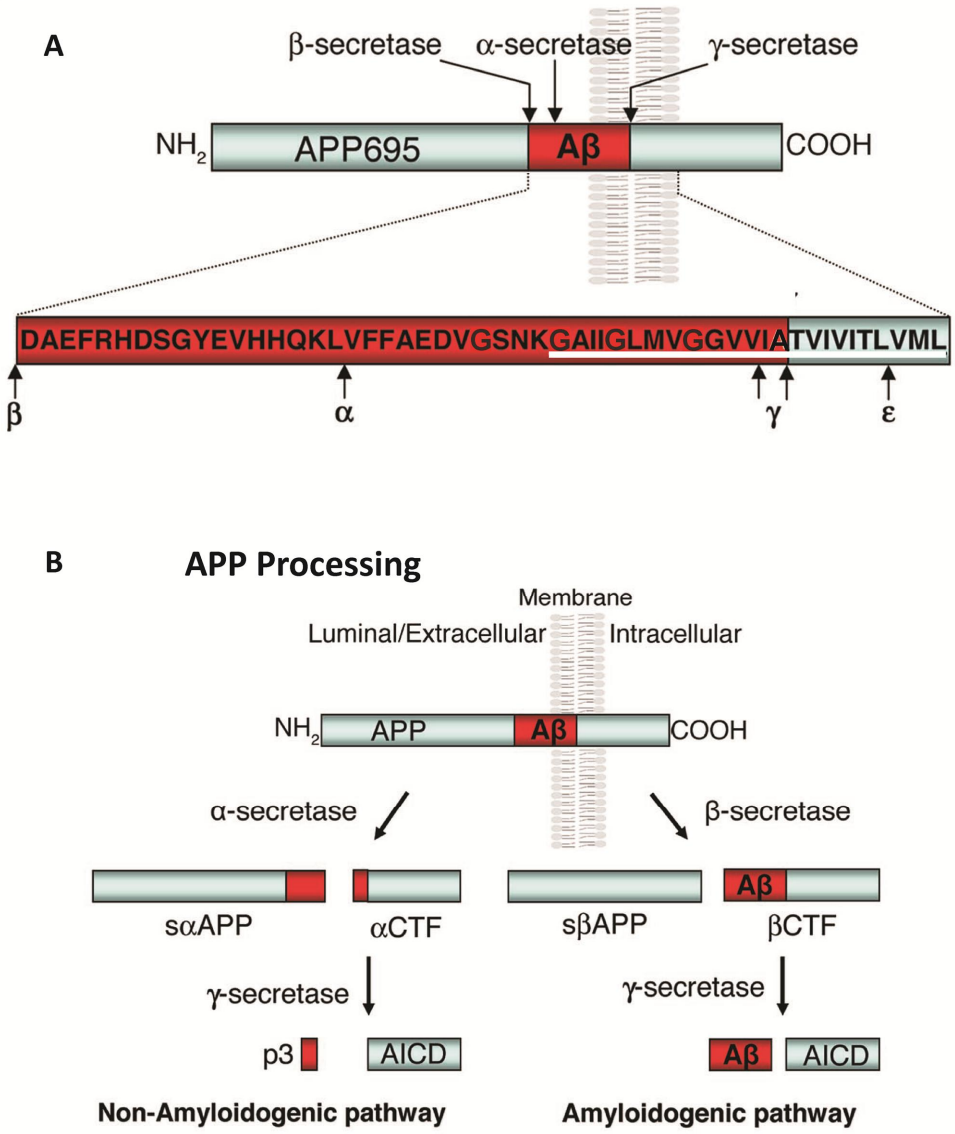

Fig. 2: The metabolism of the amyloid precursor protein (APP695) with amyloid-β and p3 generation

(A) Schematic illustration of APP isoform 695, with the Aβ sequence, shown in red and enzyme cleavage sites as indicated. The first 28 residues of the Aβ domain are located outside the membrane whereas the remaining 12–14 residues are in the transmembrane domain of APP (underlined in white). **(B)** APP can be processed along two main pathways: In the non-amyloidogenic pathway, α-secretase cleaves APP around residue 16 within the Aβ domain, which releases a soluble fragment of APP (α-sAPP), thus precluding Aβ generation. The remaining C-terminal fragment (α-CTF, C83) is further cleaved by γ-secretase, releasing the 3 kDa short p3 peptide into the extracellular space and the AICDfragment into the cytoplasm, which can enter the nucleus regulating gene transcription. In the amyloidogenic pathway, β-secretase (BACE1) cleaves APP just before the Aβ domain, releasing the soluble βAPPs. The membrane anchored, β-CTF fragment (C99) is further cleaved by the γ-secretase complex, generating the 4 kDa, 40–42 amino acid Aβ peptide. Analogous to the non-amyloidogenic pathway, the remaining AICD can enter the nucleus where it might be involved in nuclear signaling. (Aβ: Amyloid-β; AICD: APP intracellular domain; APP: amyloid precursor protein; CTF: C-terminal fragment; sAPP: Soluble APP; (illustration was modified from Khalifa et al., 2010).

Overall, several Aβ species are generated and have been isolated, including Aβ40, Aβ42, Aβ43, Aβ45, Aβ48 and Aβ49, whereas only two species of ICDs, C49 and C50 (Kakuda et al. 2006) have been identified so far. Released AICD has been shown to possess transactivation activity (Cao and Sudhof 2001, 2004) and can regulate transcription of multiple genes including APP, GSK-3β, KAI1, neprilysin,

BACE1, p53, EGFR, and LRP1 (Kim et al. 2003; von Rotz et al. 2004; Pardossi-Piquard et al. 2005; Slomnicki and Lesniak 2008). Multiple lines of biochemical evidence have shown γ-*secretase* being a multiprotein complex consisting of at least four different components: nicastrin (Yu et al. 2000), anterior pharynx defective-1 (APH-1) (Goutte et al. 2002), presenilin enhancer-2 (PEN2) and the presenilin proteins, PS1 or PS2. These four proteins are necessary and sufficient to form an active γ-*secretase* complex in vitro (Edbauer et al. 2003). At the subcellular level, γ-*secretase* activity has been shown to reside in multiple compartments including the ER, late-Golgi/TGN, endosomes and the plasma membrane (Baulac et al. 2003; Capell et al. 2005; Dries and Yu 2008) whereas 6% of total γ-*secretase* activity had been detected at the cell surface (Wang et al. 2004; Chyung et al. 2005; Hansson et al. 2005). However, recent biological evidence suggests that γ-*secretase* components assemble into the proteolytically active complex in the Golgi/TGN compartments (Baulac et al. 2003). Since the discovery of APP as a γ-*secretase* substrate, many other integral membrane proteins have been identified such as a series of functionally important transmembrane proteins, including the Notch receptor (Okochi et al. 2002), E-cadherin (Ferber et al. 2008), ErbB4 (Vidal et al. 2005), and CD44 (Pelletier et al. 2006). Therefore, therapeutic strategies targeting the γ-*secretase* complex to prevent Aβ generation causes unpredictable side effects. Under normal conditions, the cleavage of APP by α-*secretase* predominates (> 90%) over that achieved by β-*secretase* (Cordell 1994; Furukawa et al. 1996). Over 20 pathogenic mutations in the APP gene causing FAD have been identified to date and can be divided into mutations that improve BACE1 cleavage (Citron et al. 1992), e.g. the so called Swedish mutation, where the K670N/M671L (APP770) amino acid exchanges at the BACE cleavage site make APP a better substrate for BACE and the enzyme cleaves more efficiently, resulting in more overall Aβ production. On the other hand, there are mutations at the γ-cleavage site, which increase production of specifically Aβ42 (Murrell et al. 2000), as well as mutations in the middle of the Aβ region, which enhance the aggregation properties of the peptide (Nilsberth et al. 2001).

1.3 APP isoforms and domain organization

The human APP gene is located on chromosome 21 and was cloned independently by several laboratories in 1987 (Kang et al. 1987; Robakis et al. 1987; Tanzi et al. 1987). APP is encoded by 19 exons, of which exons 7, 8, and 15 can be alternatively spliced (Sandbrink et al. 1997) to produce three major protein isoforms APP770, APP751 and APP695 (Kitaguchi et al. 1988), reflecting the number of amino acids encoded for by their respective complementary DNAs (Smith et al. 1990). APP695 is the only isoform that lacks a Kunitz Protease Inhibitor (KPI) domain in its extracellular portion whereas the two larger APP isoforms contain the 57-amino-acid KPI insert. Additionally, APP770 comprises another 19 amino acid long insert (encoded by exon 8) with striking homology to the immunoregulatory OX-2 antigen (Richards et al. 1995). Alternative splicing, by excision of exon 15 of the APP gene, generates a recognition site for chondroitin sulfate glycosaminoglycans (CS-GAG), and the corresponding L-APP forms have been characterized to be expressed in a variety of peripheral tissues, but not in the nervous system such as the brain and spinal cord (Sandbrink et al. 1993). The differences between the isoform domains are shown in Figure 3A. Variations in APP alternate transcripts also alter the primary amino acid sequences (Fig. 3B), highlighting the areas of

variation in each isoform, as illustrated in Figure 3B, and C. APP is widely expressed throughout the body, in many cell- and tissue types including endothelia, glia and neurons of the brain (Schmechel et al. 1988). In non-neuronal cells (e.g. astrocytes), the longer isoforms containing exon 7 (APP751) or exons 7 and 8 (APP770) predominate (LeBlanc et al. 1991) while neurons express principally the isoform lacking exons 7 and 8 (APP695) (Ponte et al. 1988; Kang and Muller-Hill 1990). Structurally, APP resembles a ubiquitously expressed cell surface receptor with a large N-terminal ectodomain, a single transmembrane domain and a short cytoplasmic C-terminal tail (Tanzi et al. 1988). However, the extracellular part of APP can be regarded as several individual domains, most of them also representing independent folding units, which have been structurally characterized in the last years (Gralle and Ferreira 2007). Furthermore the extracellular region, which is much larger than the intracellular part, can be divided into the E1 and E2 domains, linked by an acidic domain (AcD) (see Fig. 3). The very N-terminal region, also designated as the E1 domain, is localized immediately after the signal sequence and comprises 172 amino acids, which is very cysteine-rich, containing 12 cysteine residues. Furthermore it can be divided into a number of subdomains, encompassing a heparin-binding/-growth-factor-like domain (HFBD/GFLD), a copper-binding domain (CuBD) and a zinc-binding domain (ZnBD), also referred to as the metal binding domain (MBD). In 1999, a 96-residue N-terminal subfragment was crystallized, by Rossjohn and colleagues (Rossjohn et al. 1999) which contains six cysteine residues that are well conserved across the APP family and is capable of binding to heparin (Mok et al. 1997). The disulfide bridge between Cys98 and Cys105 has been shown to stabilize a so called beta-hairpin loop, which seems to be critical for neurite outgrowth (Small et al. 1994), or dimerization properties (Rossjohn et al. 1999; Kaden et al. 2008). The HFBD/GFLD is followed by the well-studied copper-binding domain (CuBD) (Hesse et al. 1994), which is able to reduce bound Cu^{2+} to Cu^{+} (Multhaup et al. 1996), possibly leading to the formation of intramolecular disulfide bonds (Multhaup et al. 1998). A peptide sequence that binds Zn^{2+} in vitro is also present in this amino acid sequence of APP (Bush et al. 1993). Other studies have revealed that the N-terminal part of APP could bind heparin in vitro (Multhaup et al. 1994; Small et al. 1994). Therefore, a region close to the N-terminus of APP (residues 96-110) was identified as a potential heparin-binding domain based on secondary structure predictions and molecular modeling. Interestingly, its heparin binding capacity was enhanced by zinc (Multhaup et al. 1995). Recent studies by Dahms and co-workers indicated that two E1 fragments can come together to form a dimer in the presence of heparin, because the protein dimer interface comprises positively charged amino acid side chains that are held in place by the negatively charged heparin molecule (Dahms et al. 2010), depending on different pH values in solution. The E1 domain is connected via a flexible acidic region (rich in aspartic acid and glutamic acid) to the carbohydrate domain, which is also called the E2-, or central APP domain (CAPPD). The E2 domain is the largest region within the ectodomain of APP (aa 365-566) and contains a high-affinity binding site for the extracellular matrix protein heparin sulfate proteoglycan (HSPG), as well as a sequence that might display growth factor-like capabilities upon soluble APP (Wang and Ha 2004). Wang and colleagues found evidence that E2 is folded independently of the rest of APP, and their X-ray crystallography data indicate that the tertiary structure of E2 contains two coiled-coil substructures connected through a continuous helix.

The researchers further found that the E2 domain invariably dimerizes in solution in an antiparallel orientation.

1.4 The KPI domain

As mentioned above, only the longer two APP isoforms contain a so called Kunitz type protease inhibitor (KPI) domain, which was the first APP fragment to be crystallized in 1990 (Hynes et al. 1990).

Figure 3

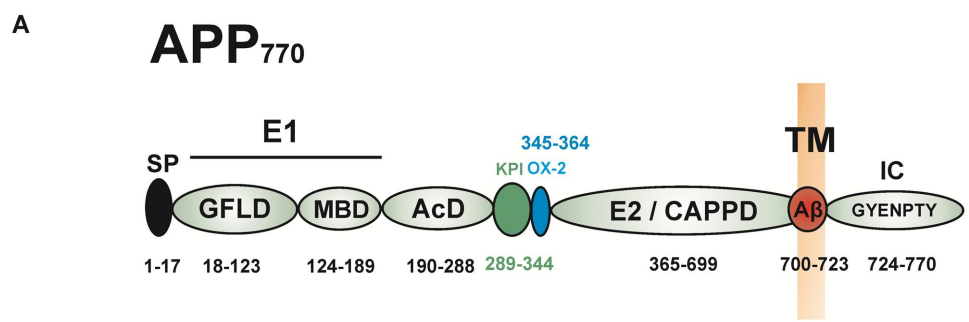

B

Human APP770:

MLPGLALLLLAAWTARALEVPTDGNAGLLAEPQIAMFCGRLNMHMNVQNGKWDSDPSGTK
TCIDTKEGILQYCQEVYPELQITNVVEANQPVTIQNWCKRGRKQCKTHPHFVIPYRCLVG
EFVSDALLVPDKCKFLHQERMDVCETHLHWHTVAKETCSEKSTNLHDYGMLLPCGIDKFR
GVEFVCCPLAEESDNVDSADAEEDDSDVWWGGADTDYADGSEDKVVEVAEEEEVAEVEEE
EADDDEDDEDGDEVEEEAEEPYEEATERTTSIATTTTTTTESVEEVVREVCSEQAETGPC
RAMISRWYFDVTEGKCAPFFYGGCGGNRNNFDTEEYCMAVCGSAMSQSLLKTTQEPLARD
PVKLPTTAASTPDAVDKYLETPGDENEHAHFQKAKERLEAKHRERMSQVMREWEEAERQA
KNLPKADKKAVIQHFQEKVESLEQEAANERQQLVETHMARVEAMLNDRRRLALENYITAL
QAVPPRPRHVFNMLKKYVRAEQKDRQHTLKHFEHVRMVDPKKAAQIRSQVMTHLRVIYER
MNQSLSLLYNVPAVAEEIQDEVDELLQKEQNYSDDVLANMISEPRISYGNDALMPSLTET
KTTVELLPVNGEFSLDDLQPWHSFGADSVPANTENEVEPVDARPAADRGLTTRPGSGLTN
IKTEEISEVKMDAEFRHDSGYEVHHQKLVFFAEDVGSNKGAIIGLMVGGVVIATVIVITL
VMLKKKQYTSIHHGVVEVDAAVTPEERHLSKMQQNGYENPTYKFFEQMQN

Fig. 3: Domain structure of the amyloid precursor protein APP770 and its amino acid sequence

Panel **(A)** depicts the overall APP domain structure including the relative amino acid positions of the growth factor-like domain (GFLD), metal-binding domains (MBD) for Zn^{2+} and Cu^{2+}, acidic region (AcD), E2/central APP domain (CAPPD), amyloid beta region (Aβ), transmembrane domain (TM), and the intracellular domain (IC). The cytoplasmic region of APP contains a protein interaction motif, namely the GYENPTY sequence, including the NPXY internalization signal. The longest APP isoform 770, comprises two alternatively spliced exons, encoding a Kunitz-type protease inhibitor (KPI) consensus sequence (exon 7) and an alternatively spliced 19-residue (exon 8), encoding for an OX-2 homologous sequence. The APP695 isoform lacks the KPI-and OX-2 exons. **(B)** Full length amino acid sequence of APP770 (Accession No. P05067). Highlighted areas differ from isoforms APP695 and APP751. The amino acids in green (KPI-domain), or blue (OX-2 domain) font are missing from APP695. Amino acids indicated in blue font (OX-2 domain) are missing from APP751.

This domain is coded for by a single exon (exon 7 of APP), translated into a 57-amino-acid insert in the middle of the APP sequence (see Fig. 3A and B), showing strong homology to other Kunitz-type protease inhibitors (Oltersdorf et al. 1989; Hynes et al. 1990). Therefore it seems likely that the KPI domain of APP constitutes an independent folding unit and that the structure obtained for the

isolated domain represents well the structure of the domain in the context of full-length APP (Hynes et al. 1990; Gralle and Ferreira 2007). The structure is a disulfide rich alpha and beta fold, containing six cysteine residues. KPI is one of the main serine protease inhibitors or serpins (short for serine protease inhibitor), comprising a group of proteins that inhibit peptidases and are defined by the presence of a serine residue in their active site. In the brain three forms of APP have been described and are referred to as APP695, APP751 and APP770, whereas APP (-) KPI account for less than 14% of total brain APP (Van Nostrand et al. 1989). It has been shown that the KPI inhibits the activity of trypsin or plasmin forming a stable, noncovalent, 1:1 molar complex with the enzyme (Oltersdorf et al. 1989), whereby the post-translational modifications of APP, including glycosylation, improve the inhibition of trypsin by the KPI domain (Godfroid and Octave 1990). Nevertheless the physiological function(s) of the KPI domain within APP remains a matter of debate. Several sorts of studies provide evidences about the involvement of KPI containing APP in neurodegenerative diseases, thus mRNA and protein levels of KPI-APP are elevated in AD brain and are associated with increased Aβ production (Palmert et al. 1988; Hyman et al. 1992). Furthermore it has been shown that APP containing the KPI domain acts as a ligand of the LDL-receptor-related protein 1 (LRP1), a large transmembrane endocytic receptor that can bind and internalize many functionally distinct ligands (Herz et al. 1988). APP containing a KPI domain can be internalized through interaction with this receptor (Kounnas et al. 1995). Interestingly, an extracellular portion of the LRP can bind to APP through its KPI domain (Santiago-Garcia et al. 2001). The KPI domain is immediately followed by a seemingly random short stretch of 19 amino acids without significant homology to other known proteins and without a recognizable structure (Richards et al. 1995). This is followed by the transmembrane domain (TM), which includes part of the β-amyloid peptide (Aβ) sequence. Lastly, the cytoplasmic tail (IC) of APP contains a protein interaction motif, namely the -GYENPTY- sequence, encompassing the NPXY internalization signal (Lai et al. 1995), conserved in all APP homologues. NMR studies have shown that the C-terminal cytoplasmic tail of APP has no rigid structure (Bertrand et al. 2001), while an α-helical structure is assumed for the transmembrane segment (Kang et al. 1987).

1.5 The amyloid precursor like proteins APLP1 and APLP2

The amyloid precursor protein (APP) belongs to an evolutionary highly conserved gene family, which in addition includes two mammalian paralogues, APLP1 (Wasco et al. 1992; Paliga et al. 1997) and APLP2 (Sprecher et al. 1993; Wasco et al. 1993) (APP-like protein 1 and 2). APP-like proteins have also been identified in other species, including APPL (APP like) in *Drosophila melanogaster* (Rosen et al. 1989) and APL-1 in *Caenorhabditis elegans* (Daigle and Li 1993). Both APLPs are also are single transmembrane glycoproteins, sharing striking amino acid and domain homology to APP, as illustrated in Figure 4 (Coulson et al. 2000).

Figure 4

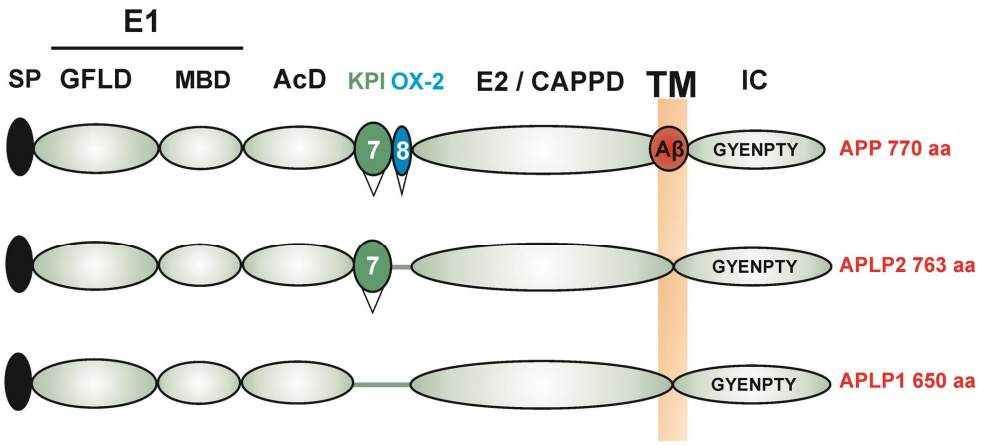

Fig.4: Schematic reperesentation of the APP protein family

All APP family members contain a signal peptide sequence (SP), growth factor like (GFLD)-, metal binding (MBD) domain for copper and zinc, followed by the E2 domain, a transmembrane region (TM) and a C-terminal part encompassing an NPXY motif. Alternative splicing of APP and APLP2 (exons 7 and/or 8) produces multiple protein isoforms that differ in the presence of the Kunitz protease inhibitor (KPI) and OX-2 domains. APLP1 however, is not alternatively spliced. The shortest APP isoform 695 lacks both, exon 7 (KPI domain) and exon 8 OX-2 domain, whereas APP 751 only lacks the OX-2 domain. Here, only the longest isoform APP770 is depicted. Note that the Aβ region and OX-2 domain are unique to APP.

All members of the APP family are single transmembrane glycoproteins, with a large exoplasmic domain and a short, highly conserved cytoplasmic domain that contains an NPXY (Asn-Pro-X-Tyr) clathrin internalization signal and putative phosphorylation sites (Kang et al. 1987; Dyrks et al. 1988). On the extracellular side, there is a cysteine rich E1 domain showing also heparin and collagen binding properties, followed by zinc and copper binding domains, an acidic region, and a carbohydrate domain (see illustration in Figure 4). APP and APLP2 are ubiquitously expressed throughout the organism while the expression of APLP1 seems to be restricted to the peripheral (PNS) and central nervous system (CNS) (Slunt et al. 1994; Lorent et al. 1995). APLP1 has been found to consist of 650 amino acids and undergoes no alternative splicing, thus no additional isoforms have yet been detected (Wasco et al. 1992; Paliga et al. 1997), as in the case of APPL and APL-1. APLP1 is viewed as the ancestral member of the mammalian APP gene family, since it is closest to the invertebrate paralogues (Coulson et al. 2000). APLP2 on the other hand, is alternatively spliced and expressed in a similar pattern as APP (Slunt et al. 1994), while the major neuronal form of APLP2 with 763 amino acids contains the alternatively spliced Kunitz-type protease inhibitor (KPI) domain (Sandbrink et al. 1997). Despite a high degree of homology, the OX-2 and the Aβ region are unique to APP, although one recent study claims that APLP2 also gave rise to Aβ-like peptides (Eggert et al. 2004).

1.6 Functions of APP family proteins

The APP family proteins are highly conserved across species and ubiquitously expressed, suggesting that they fulfill important physiological functions. Due to their sequence and structure analogy, it has been suggested that the APP gene family proteins have, partly overlapping, if not redundant important physiological functions. In *Drosophila melanogaster*, knockout of the *App-l* homologue resulted in relative mild phenotypes, such as a phototaxis defect that can be rescued with human APP. In mice, the knockout of APP alone also caused a mild phenotype, resulting in reduced body weight, discrete anatomical, behavioral, and electrophysiologic changes, hypersensitivity to seizure-inducing stimuli, alterations in locomotor activity, and impairment in spatial learning and long-term potentiation (Muller et al. 1994). Nevertheless, the mice were apparently viable and fertile (Zheng et al. 1995) and the mild phenotype was rescued by the reintroduction of sAPP alone (Zheng et al. 1995; Dawson et al. 1999; Seabrook et al. 1999; Ring et al. 2007), suggesting a role for APP in neuronal cell function, although the molecular mechanism remains elusive. Further single knockout mice of APLP2$^{-/-}$ (von Koch et al. 1997) or APLP1$^{-/-}$ (Heber et al. 2000) mice were also found to be normal and viable, thus functional redundancy between the APP family members might explain the subtle phenotypes observed for single knockout mice, even though no compensatory upregulation of the homologous family members in single knock-out mice could be observed (Zheng et al. 1995; von Koch et al. 1997). To better understand the normal functions of APP family members, double and triple knock-out mice have been generated (Anliker and Muller 2006) and indeed, the combined knockouts APP$^{-/-}$/APLP2$^{-/-}$ and APLP1$^{-/-}$/APLP2$^{-/-}$ resulted in early postnatal death (postnatal day 1) (von Koch et al. 1997; Heber et al. 2000). These results provided genetic evidence for at least some distinct physiological roles for APP and APLP2 and suggest that APLP2 has the key physiological role among the family members. However, no major morphological abnormalities have been observed in these mice (von Koch et al. 1997; Heber et al. 2000; Wang et al. 2005), and the reason for the lethality remained unexplained. As expected, triple knockout mice of APP, APLP1 and APLP2 resulted in perinatal lethality (death *in utero)*, and showed severe cranial defects (81%) and cortical dysplasia (68%) (Herms et al., 2004), indicating that three proteins are required for embryonic development. In contrast, the APP-APLP1 (APP$^{-/-}$/APLP1$^{-/-}$) double knockout mice are viable (Heber et al. 2000), therefore these results suggested that APLP2 was crucial for survival, although APP and APLP1, in combination (but not alone) could compensate for the essential APLP2 function and rescue the lethal phenotype, which did not seem to be a consequence of compensatory expression of either APP or APLP1. Thus, a functional overlap between the three family members was suggested. Further in depth research concerning APP$^{-/-}$/APLP2$^{-/-}$ mice suggested fewer synaptic vesicles in the neuromuscular junctions and also differences in the expression pattern of the acetylcholine receptor (Wang et al. 2005; Yang et al. 2005). These mice exhibited defective synapses, displaying reduced number of synapses, reduced quantity of vesicles and active zones, and an aberrant neuronal sprouting (Wang et al. 2005; Yang et al. 2005). However, none of the lethal double mutants displayed obvious histopathological abnormalities in the brain or any other organ examined. A recent study, using in utero electroporation of small interfering RNA (siRNA) to knock down APP function in mice, resulted in an arrest of migration of neurons before cortical plate entry (Young-Pearse et al. 2007).

The reasons for these divergent phenotypes are not clear, but reveal that normal APP levels are obviously required for correct neuronal migration during development of the mammalian brain. However, cDNAs encoding human APP or its homologues, amyloid precursor-like protein 1 (APLP1) or APLP2, fully rescued the shRNA-mediated migration defect (Young-Pearse et al. 2007).

1.7 Post translational modifications, trafficking and processing of APP family proteins

APP and its homologues are synthesized in the endoplasmatic reticulum (ER) and then transported through the Golgi apparatus to the trans-Golgi-network (TGN) and to the cell surface (Turner et al. 2003). During its passage through the Golgi complex, APP is N-glycosylated, O-glycosylated, tyrosine sulfated and phosphorylated on several residues on both sides of the membrane, increasing the structural complexity of APP and APLPs (Dyrks et al. 1988; Weidemann et al. 1989; Hung and Selkoe 1994).

Figure 5

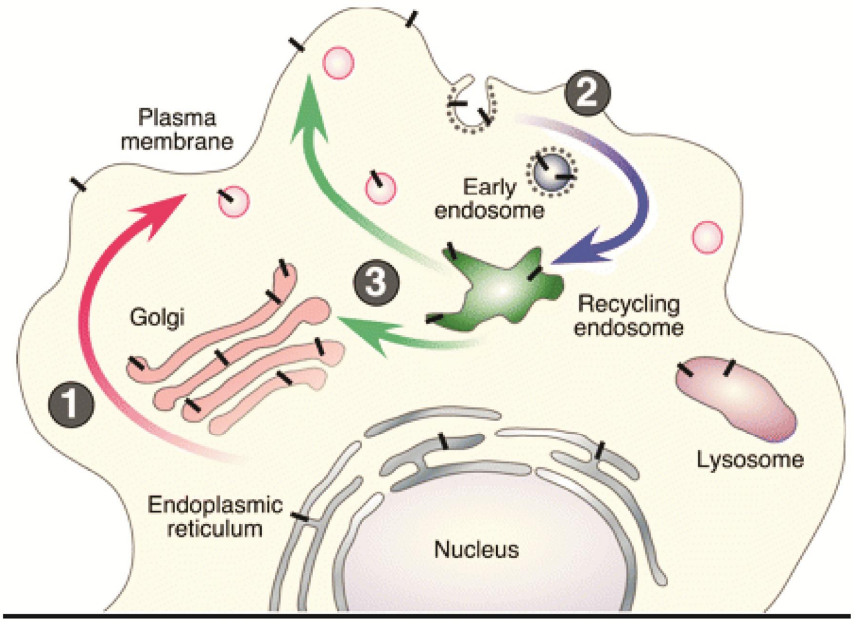

Fig. 5: Intracellular trafficking of APP and APLPs

Nascent APP/APLP molecules (black bars) mature through the constitutive secretory pathway (step 1). Once they reach the cell surface, they are rapidly internalized via an -NPXY- motif at the C-terminus (step 2) and subsequently trafficked through endocytic and recycling compartments back to the cell surface (step 3), or degraded in the lysosome. Non-amyloidogenic processing of APP occurs mainly at the cell surface, where *α-secretases* are present. Amyloidogenic processing involves transit through the endocytic organelles, where APP encounters *β- and γ-secretases.* (Adapted from Thinakaran and Koo, 2008).

Early studies indicated that both APLP1 and APLP2 undergo extensive post-translational modification (Thinakaran and Sisodia 1994; Paliga et al. 1997). Proteolytic cleavage of APP by *secretases* (section 1.2) mainly occurs at the plasma membrane and in the endosomes (Sambamurti et al. 1992; Parvathy et al. 1999). In non-neuronal cells, APP is internalized within minutes of arrival at the cell surface due to the presence of the -NPxY- internalization motif near the C-terminus of APP (residues 682–687 of

the APP695 isoform) (Thinakaran and Koo 2008). Only a small fraction of nascent APP molecules is present at the plasma membrane (estimated at ~10% based on APP overexpression in cultured cells), whereas the majority of APP at steady state localizes to the Golgi and TGN (Perez et al. 1999). Following endocytosis, APP is delivered to endosomes, and a fraction of endocytosed molecules is recycled to the cell surface (Fig. 5). Measurable amounts of internalized APP also undergo degradation in the lysosome. Moreover, processing represents another common feature of all APP family members, since recent evidence suggests that APLP1 and APLP2 undergo processing in a manner highly similar to APP, serving as substrates for α-, β- and γ-*secretases* (Scheinfeld et al. 2002; Eggert et al. 2004). It was reported that all homologues release their large extracellular domain, designated as sAPP, sAPLP1 and sAPLP2, as a result of proteolytic processing (Li and Sudhof 2004; Endres et al. 2005). In a different study, conducted by Eggert and colleagues, several C-terminal fragments with a size similar to α-CTF of APP were detected for both APLPs, generated by the action of α-or β-*secretase* (Eggert et al. 2004). First hints that both APLPs are also processed by γ-*secretase* came from findings that CTF levels were elevated in brain lysates of PS1 KO mice and in cells stably expressing dominant-negative PS1 and PS2 mutants (Naruse et al. 1998; Scheinfeld et al. 2002). Furthermore, γ-*secretase* inhibitors caused an accumulation of APLP1 and APLP2 CTFs, providing convincing evidence that both proteins are γ-*secretase* substrates (Walsh et al. 2003). In line with these observations, Eggert and colleagues found in a SH-SY5Y cell culture model that APLP1 and APLP2 secrete p3- or Aβ-like fragments, equivalent to those from APP, in a γ-*secretase*-dependent fashion, although they both lack the actual Aβ domain (Eggert et al. 2004). Cells expressing APLP1 secrete a 3.5 kDa a 4.5 kDa peptide, and cells expressing APLP2 generate peptides of 4.5 - 8 kDa size, whereas γ-*secretase* inhibitors prevented formation of these fragments, confirming that they are produced by γ-*secretase* complex (Eggert et al. 2004). However, BACE inhibitors, such as Merck compound 3 also completely blocked production of the 4 kDa peptide, derived from APLP2 and significantly diminished production of the 8 kDa fragment, whereas they had no effect on APLP1 p3-like fragment production (Eggert et al. 2004), suggesting that the 4 kDa peptide of APLP2 was generated by the action of both β- and γ-*secretases.* Furthermore, Eggert and colleagues could show that APLP1 p3-like peptide secretion was diminished upon treatment with ADAM inhibitors (such as metalloprotease inhibitor batimastat) and increased by treatment with phorbolesters, thus suggesting that this fragment was generated by consecutive α- and γ-cleavage (Eggert et al. 2004). Further manipulation with specific protease inhibitors confirmed that both homologues are processed by α- or β- *secretase,* and γ-*secretase*-like cleavages, and that their intracellular domains (ICDs) can be released by cleavage at epsilon-sites, whereas γ-*secretase* inhibitors decreased the production of these fragments significantly with a concomitant accumulation of C-terminal fragments of APLP1 and APLP2 (Scheinfeld et al. 2002; Walsh et al. 2003). Recent findings also demonstrated that APLP2 is constitutively shedded by ADAM10 or ADAM17 (A disintegrin and metalloproteinase) in HEK293 and in neuroblastoma SH-SY5Y cells (Endres et al. 2005; Hogl et al. 2011). Moreover, Hogl and co-workers also determined the proteolytic cleavage sites in the APLP2 sequence via mass spectrometry, indicating that ADAM10 was found to cleave APLP2 after arginine 670, whereas BACE1 cleaves after leucine 659 (methionine 596 in APP695). For APLP1 however, the situation is less clear, since another study by Li and colleagues could show that APLP1 is cut by BACE1 at a position that is

within 13 residues of the TM domain (Li and Sudhof 2004). In contrast to Eggert and colleagues they used different experimental setups, demonstrating that co-transfection of BACE 1 with APLP1 resulted in the production of a new CTF and increasing amounts of BACE 1 enhanced transactivation in a Gal4 assay, mediated by APLP1 (Li and Sudhof, 2004). However, Eggert et al. found no proof for BACE cleavage of APLP1 by pharmacological intervention. Taken together, APLP2 undergoes a processing, more similar to that of APP, also including *β-secretase*-like cleavages, which is not surprising since APP and APLP2 are evolutionarily more closely related to each other than to APLP1, representing the ancestral form of the APP gene family (Coulson et al. 2000).

1.8 Interactions of APP and APLPs with other proteins

When APP was first cloned (Kang et al. 1987), according to the primary structure, it was suggested that the APP family might work as cell surface receptors, similar to Notch (Kang et al. 1987). Since then, APP has been shown to interact with numerous proteins (Turner et al. 2003), via its C-terminus or its large extracellular part. Therefore, the short cytoplasmic domain encompassing the NPxY protein interaction motif, which is also a consensus sequence for clathrin coated pit-mediated internalization (Chen et al. 1990), gained a lot of interest. The initial observation that the Fe65 protein can interact with the APP cytoplasmic domain (Fiore et al. 1995), was followed by many research data that documented the existence of a protein-protein interaction network assembled around the APP C-terminus (Russo et al. 2005). All APP family proteins share a common NPxY motif, which provides a double function. On the one hand, it is important for clathrin mediated endocytosis from the cell surface (Koo and Squazzo 1994; Perez et al. 1999), on the other hand it also represents the binding site for phosphotyrosine-binding (PTB) domain containing proteins. PTB domains are functionally and evolutionary conserved modules, which play essential roles in signal transduction, or protein transport (Bork and Margolis 1995) and apparently recognize NPxY or related peptide motifs (Bork and Margolis 1995). One of the best described interaction partners for the APP C-terminus is Fe65, a highly conserved cytosolic protein, containing three protein-protein interaction domains, the PID/PTB domains 1 and 2 (Bork and Margolis 1995) and the WW domain (Sudol et al. 1995). Further *in vitro* and *in vivo* studies demonstrated that APP, APLP1 and APLP2 can bind to the PID2 element of Fe65 (Zambrano et al. 1997). So far, Disabled-1 (Dab1) (Trommsdorff et al. 1998; Homayouni et al. 1999; Howell et al. 1999), Shc (Tarr et al. 2002; Russo et al. 2005), Janus kinase interacting protein-1 (JIP-1), X11/Mint1 (Borg et al. 1996; Zhang et al. 1997), and Fe65, as well as Fe65 like proteins Fe65L1 and Fe65L2 (Fiore et al. 1995; Zambrano et al. 1997; Duilio et al. 1998; Trommsdorff et al. 1998; McLoughlin and Miller 2008) have been described to interact with the NPxY motif of at least one APP family member. Since the *γ-secretase* was shown to cleave both, APP, APLPs and Notch, the latter to generate the nuclear signaling-competent NICD fragment, prompted the notion that APP may play an analogous signaling role. Pioneering studies in 2001, using experimental approaches based on Gal4-dependent transcription of a reporter gene, demonstrated that the intracellular domain of APP (AICD) can form a complex with Fe65 and Tip60, a histone acetytransferase, and translocate to the nucleus to regulate the expression of artificial expression constructs in transfected cells (Cao and Sudhof 2001; Scheinfeld et al. 2002; Cao and Sudhof 2004; Zheng and Koo 2006). In addition, Fe65

appears to stabilize the highly labile AICD fragment (Kimberly et al. 2001). Moreover, Scheinfeld and colleagues found that intracellular domains of APLP1 and APLP2 denoted as AICD-like fragments ALID1 and ALID2, respectively, (containing the YENPTY motif) are also likely stabilized by Fe65 and that Gal4 fusion proteins of APLPs also activate reporter gene expression in an Fe65-dependent manner (Scheinfeld et al. 2002). They also found that JIP-1 activates transcription in cultured cells, when transfected with the C-terminus of APP, which neither, ALID1 nor ALID2 were capable of (Scheinfeld et al. 2003). Although many putative target genes for AICD (e.g KAI1, neprilysin etc.) have been documented, much controversy surrounds the part played by AICD in the transcription of these genes (Baek et al. 2002; von Rotz et al. 2004; Hebert et al. 2006). Interestingly, phosphorylation at threonine668 of APP has been reported to cause a conformational change, which negatively regulates APP binding to Fe65 and reduces the stability of AICD (Ando et al. 2001; Ramelot and Nicholson 2001). This phosphorylation has also been reported to modulate APP interaction with X11/Mint1 (Taru and Suzuki 2004; Zheng and Koo 2006). Furthermore, binding of some of these intracellular adaptor proteins does not only influence putative gene expression, but can also affect the processing of APP. Prominently, X11/Mint-1 and Fe65 seem to have antagonizing effects, influencing intracellular transport and function in a distinct way. X11 can stabilize the full length APP protein presumably by retaining it in early secretory compartments and decreases its turnover, APPs secretion and Aβ generation in a non-neuronal cell culture model (Borg et al. 1996; Sastre et al. 1998). In contrast, Fe65 expression and binding seems to affect APP shedding and secretion of Aβ (Sabo et al. 2001; Pietrzik et al. 2002; Pietrzik et al. 2004; Neumann et al. 2006). According to that came the observation that Fe65 links APP to the LDL receptor related protein 1 (LRP1), a multifunctional cell surface receptor for proteins involved in lipoprotein metabolism (Herz and Bock 2002). Pull down experiments demonstrated that the N-terminal PTB1 of Fe65 binds to LRP1 and the C-terminal PTB2 of Fe65 binds APP (Fiore et al. 1995). This suggested that Fe65 could act as an adaptor molecule between the two proteins (Pietrzik et al. 2002). The formation of an APP-Fe65-LRP1 complex allows efficient re-internalization of surface APP, thereby increasing APPsβ and Aβ generation, whereas disruption of the complex leads to an accumulation of APP at the cell surface, where it can undergo increased shedding by α-*secretase* and reduced BACE cleavage (Ulery et al. 2000; Pietrzik et al. 2002; Pietrzik et al. 2004), likewise reducing Aβ generation. Further studies confirmed that LRP1 can influence multiple steps in APP processing, as well as modulating APP trafficking along the secretory pathway (Waldron et al. 2008). Interestingly, it was also found that the APP-Fe65-LRP1 complex can be disrupted, when APP was functionally replaced through coexpression of its homologues APLP1 or APLP2, revealing a reduced endocytosis for APP, strongly promoting APP α-*secretase* cleavage and reducing BACE shedding, thus also diminishing Aβ secretion (Neumann et al., 2006). Specifically, the APLP1 effect on APP shedding was only observed in LRP1 expressing cells, demonstrating on the one hand that this effect was LRP1 dependent (Ulery et al. 2000; Pietrzik et al. 2002; Pietrzik et al. 2004) and on the other that APLPs can also form a triple complex with Fe65 and LRP1, mutually influencing APP processing. So far, solely cytoplasmic APP interactors have been discussed, but it has also been shown that soluble APP770 (APPs) associates via its KPI domain to LRP1 at the cell surface and is internalized by LRP1, hence modulating Aβ secretion (Kounnas et al. 1995).

1.9 Interactions between APP and APLPs

Another research field focused rather on the large extracellular part of APP and APLPs, than on cytosolic adapter proteins. Earlier studies reported that the ectodomains of APP family proteins have zinc- (Bush et al. 1993) and copper binding-properties (Simons et al. 2002) and that APP is able to reduce bound Cu^{2+} to Cu^{+} (Multhaup et al. 1996). Moreover, APP has been proposed to bind extracellular matrix proteins like heparin and collagen (Small et al. 1994), and to have a receptor-like function (Beher et al. 1996). In this context, it became more and more challenging, whether APP can form cellular *cis*-dimers (Scheuermann et al. 2001), reminiscent of classical receptor dimerization described for the EGF receptor (Schlessinger 2002). However, there is accumulating evidence from biochemical and structural data that APP can form homodimers (Scheuermann et al. 2001; Soba et al. 2005; Kaden et al. 2009) as well as heterodimers with its homologues APLP1 and APLP2 (Soba et al. 2005). In the following years, various experimental approaches have attempted to visualize dimerization between APP family proteins. First studies demonstrated the existence of APP-APP interactions at the cell surface, using the membrane impermeable crosslinker DTSSP to covalently link cell surface APP at the plasmamembrane (Scheuermann et al. 2001; Soba et al. 2005). Moreover, Scheuermann and colleagues also forced APP dimerization via a constitutive disulfide bond, introduced at the juxtamembrane region (Scheuermann et al. 2001), revealing for the first time that covalent disulfide bonds might be implicated in APP dimer formation. However, they did not further dissect single domains possibly involved in dimer formation (Scheuermann et al. 2001). To date, at least three domains have been reported to promote APP dimerization: the E1 domain containing the N-terminal Growth factor like domain (GFLD) and Copper binding domain (CuBD) (Soba et al. 2005), which is mainly responsible for full length APP dimerization (Kaden et al. 2009). A disulfide-bridged loop formed in that region, encompassing residues 91-111, seemed to be required and necessary for the stabilization of the homodimeric state (Kaden et al. 2008; Kaden et al. 2009), whereas APP interaction was gradually diminished by adding a small peptide mimicking the loop region (loop peptide) (Kaden et al. 2008). Interestingly, the loop peptide decreased the generation of sAPPβ as well as Aβ40 and Aβ42, when the synthetic peptide was added to APP-expressing cells, raising the possibility that APP monomer/dimer status might affect Aβ generation. Moreover, the strong homology and conserved domain organization between APP and the APP family members APLP1 and APLP2 imply that not only homo-oligomerization but also hetero-oligomerization might be possible as demonstrated recently (Soba et al, 2005). In this study it was elegantly demonstrated by co-immunoprecipitations and cell aggregation assays that APP family proteins display cell-adhesion-promoting functions, mediated through intercellular (*trans*-configuration) homo- and heterocomplexes of the APP family proteins (Soba et al., 2005). Moreover, Soba and co-workers identified the E1 domain as a major interaction interface, by deletion constructs, and demonstrated that the E1 *trans*-complexes promoted cell adhesion. Furthermore, in addition to the intercellular interactions, it was found that the APP and APLP2 proteins could also interact in an intracellular manner (*cis*-configuration), as homo- and heterodimers in living cells shown by FRET analysis (Kaden et al. 2009). The second dimerization interface is represented by the E2 domain (amino acids 365–699), the largest subdomain of the APP ectodomain, containing the carbohydrate- and the

juxtamembrane region. Crystallographic and X-ray structure modeling revealed that the E2 region can reversibly dimerize in an antiparallel orientation in solution (Wang and Ha 2004) and it has been reported that binding of extracellular matrix components, such as heparin, to this domain may also regulate dimerization (Gralle et al. 2006). However, in contrast to Wang et al., a study by Dulubova et al. could not confirm that the E2 domain does dimerize in solution (Dulubova et al. 2004). A third dimerization interface is located at the extracellular juxtamembrane/transmembrane (JM/TM) boundary, where APP contains three consecutive glycine-xxx-glycine (GxxxG) motifs (Munter et al. 2007; Gorman et al. 2008; Kienlen-Campard et al. 2008) one embedded within the Aβ sequence. Therefore, this motif was investigated in depth because of its impact on Aβ generation. Structural, combined with mutational studies on the APP JM/TM region, showed that the GxxxG motifs can mediate TM helix homodimerization in lipid bilayers (Munter et al. 2007), by employing a bacterial membrane system, where mutual affinity of short TMS is monitored by transcription activation of a reporter gene (ToxR system) (Munter et al. 2007). As previously shown by Munter and colleagues, Aβ42 generation presumably depends on the dimerization of the α-helical APP transmembrane sequence mediated by a GxxxG motif encompassing Aβ residues G29 and G33 (Munter et al. 2007). They demonstrated that the GxxxG motif within the APP transmembrane (TMS)/Aβ sequence has regulatory impact on the Aβ species produced. In a neuronal cell system, mutations of glycine residues G29 and G33 of the GxxxG motif gradually attenuated the dimerization strength of the TMS, specifically reduce the formation of Aβ42, left the level of Aβ40 unaffected, but increased Aβ38 and shorter Aβ species (Munter et al. 2007). According to the notion that the dimerization strength of the APP TM increases toxic Aβ species, heterodimerization with its homologues APLP1 and APLP2 was shown to decrease overall Aβ formation (Kaden et al. 2009). Other studies however, applied an inducible system where APP was fused to an FK-506 binding protein (FKBP)-domain, and dimerization was rapidly triggered upon addition of a synthetic drug AP20187 (Eggert et al. 2009), binding selectively to an engineered mutant of APP-FKBP. In contrast to previous studies (Munter et al. 2007), induced dimerization of APP chimeras did not cause alterations in the profile of Aβ peptides (Eggert et al. 2009). Thus, dimerization and dissociation of APP might regulate various APP functions, whereas the physiological significance and subcellular localization of its generation remain elusive. Therefore, oligomerization state of the ectodomain is still under debate.

1.10 The secretory pathway – overview

The secretory pathway consists of several functionally and structurally different membrane compartments and is responsible for delivery of a variety of proteins to their proper subcellular location and is essential for cellular function and development. The structural and functional organization includes the ER, ER-Golgi intermediate compartment (ERGIC) or vesicular transport cluster (VTC), *cis*-Golgi network (CGN), the Golgi stacks and *trans*-Golgi network (TGN) (Bannykh and Balch 1997). Proteins destined for the secretory pathway contain an N-terminal sequence that is recognized by the signal recognition particle (SRP). This sequence directs the nascent chain complex to the rough ER and the proteins enter the ER co-translationally. Three kinds of transport vesicles have been functionally characterized at a molecular level and can be defined by both their

membrane origin and their coat proteins (Kirchhausen 2000). Clathrin-coated vesicles are formed from both the plasma membrane and the *trans*-Golgi network (TGN) and mediate vesicular trafficking within the endosomal membrane system (Goodson et al. 1997; Haucke 2003).

Figure 6

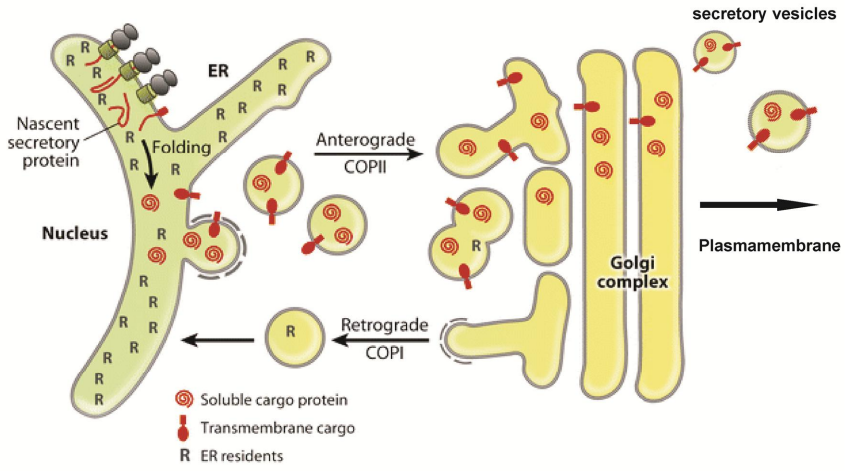

Fig. 6: Schematic depiction of secretory membrane traffic pathways

Model depicting bidirectional transport between the endoplasmic reticulum (ER) and Golgi compartments. After translation and folding of nascent secretory proteins, cargo is exported from the ER in coat protein complex II (COPII)-formed transport vesicles (anterograde). At the *trans*–Golgi network, cargo leaves the Golgi and is transported to the plasmamembrane. Proteins can be transported back to the ER using COPI-coated vesicles (retrograde) which recycle components and retrieve resident proteins (R) that have escaped the ER (illustration adapted from Dancourt and Barlowe 2010). For details see text.

Coat Protein I (COPI) -coated vesicles and Coat Protein II (COPII) -coated vesicles are transport intermediates of the secretory pathway (Otte and Barlowe 2004) (Fig. 6). COPII vesicles emerge from the ER in order to export newly synthesized secretory proteins towards the Golgi (Barlowe 1998). COPI vesicles instead appear to be involved in both biosynthetic (anterograde) and retrograde transport within the Golgi complex (Orci et al. 1997), as well as mediating the recycling of proteins from the *cis*-Golgi to the ER (Cosson and Letourneur 1994; Letourneur et al. 1994; Sonnichsen et al. 1996). These coat proteins perform the dual, essential tasks of selecting appropriate cargo proteins and deforming the lipid bilayer of appropriate donor membranes into buds and vesicles. Secretory proteins contain sorting elements that are recognized by the intracellular transport machinery at multiple stages to route proteins to their proper location. For membrane-bound compartments, COP-complexes are major components of this machinery that decode protein sorting signals presented on the surface of distinct membrane compartments. However, in certain instances, adaptor proteins or transmembrane receptors are needed for efficient linkage of cargo to a coat protein complex. This principle enables the eukaryotic cell to actively sort proteins and lipids at every level of this route, in both the anterograde and the retrograde direction (Dancourt and Barlowe 2010).

1.11 Protein targeting and retrieval to the ER is mediated by specific dilysine motifs

The endoplasmic reticulum (ER) is the starting site of newly synthesized proteins to their sub-cellular destinations, for instance the plasma membrane (Rothman and Wieland 1996). Within the integral membrane-spanning class, type I or type II topologies are established during translocation and face the N-terminus in or out of the ER lumen, respectively. For soluble secretory proteins, an N-terminal signal sequence targets polypeptides to the ER and is cleaved upon translocation into the ER lumen. Forward transport of folded secretory proteins in COPII vesicles is also balanced by a retrograde transport pathway that relies on COPI to recycle vesicle components and retrieve escaped ER resident proteins. A simplified view of bidirectional transport in the early secretory pathway is provided in Figure 6.

Figure 7

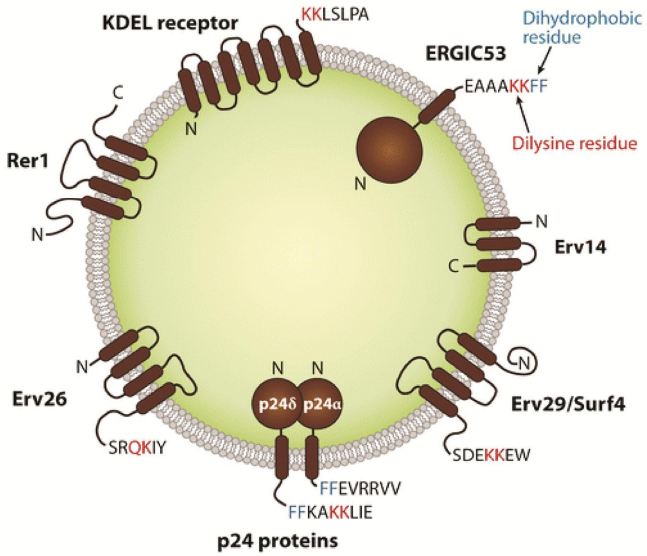

Fig.7: Structures and membrane topologies of sorting receptors in the early secretory pathway

Sorting receptors cycle between ER and Golgi compartments in vesicle intermediates formed by both, coat protein complexes I and II (COPI and COPII). The N-terminus and C-terminus are indicated. ERGIC-53, Erv14p, Erv29p, Erv26p, and the p24 proteins act in anterograde transport of secretory proteins from the endoplasmic reticulum (ER). The KDEL receptor and Rer1p act in retrograde transport of proteins from Golgi compartments to the ER. The C-terminal amino acid sequences from human proteins are shown for cargo receptors, where sorting signals have been identified. Dilysine residues are implicated in COPI-dependent retrograde transport, whereas dihydrophobic residues are implicated in COPII-dependent export from the ER. (illustration adapted from Dancourt and Barlowe 2010.

Proteins resident in the ER contain structural motifs, responsible for their correct subcellular localization. Many soluble ER proteins, such as the chaperone binding immunoglobulin protein (BiP) or *protein disulfide Isomerase*, (PDI) carry a C-terminal tetrapeptide -KDEL (lysine - aspartic acid - glutamic acid - leucine) motif for localization in the ER (Munro and Pelham 1987; Pelham 1988; Mazzarella et al. 1990) (Fig. 7). They are recognized in the *cis*-Golgi by a multi-spanning

transmembrane protein, the KDEL-receptor and are targeted into COPI vesicles as a receptor/ligand complex (Sonnichsen et al. 1996; Aoe et al. 1997). However, for the ER localization of type I membrane proteins in mammals and yeast, a C-terminal, cytosolic dilysine motif is essential (Nilsson et al. 1989; Jackson et al. 1990) (Fig. 7). The two lysine residues need to be in either the -3, -4 (KKXX) or -3,-5 (KXKXX) positions relative to the C terminus (with X = any amino acid), and no other basic amino acid can be substituted (Nilsson et al. 1989; Jackson et al. 1990, 1993). It has been shown that mutation of lysine residues lead to the expression of a reporter protein on the cell surface in mammals (Nilsson et al. 1989; Jackson et al. 1990). Many type I membrane proteins carry a dilysine signal in their cytosolic domain that confers localization to the ER (Teasdale and Jackson 1996). Chimeric proteins bearing a dilysine signal are localized to the ER but can acquire Golgi-specific carbohydrate modifications, suggesting that ER localization involves retrieval from the Golgi (Duden et al. 1991; Jackson et al. 1993). Further biochemical evidence implicated COPI in the recognition and binding of the dilysine signals in vitro (Cosson and Letourneur 1994) and the first interaction described between COPI and potential transmembrane proteins was the binding of coatomer (specifically subcomplex α, β´, ε, COPI) to C-terminal KKXX motifs (Jackson et al. 1990; Cosson and Letourneur 1994).

1.12 The endoplasmic reticulum and disulfide bond formation

Proteins destined to the extracellular space are synthesized on ER-bound ribosomes (rough endoplasmic reticulum (rER)), and are cotranslationally translocated into the ER lumen where they attain their native conformation, before being transported to the Golgi and downstream compartments. In the ER lumen, the proteins fold and oligomerize, disulfide bonds are formed, and *N*-linked oligosaccharides are added. *N*-linked glycosylation is used to indicate the extent of protein folding, so that proteins leave the ER only when they are properly folded. Translocation of soluble proteins into the ER depends on the *N*-terminal signal peptide. Integral membrane proteins may also be synthesized with an N-terminal signal peptide, but their orientation within the ER membrane and the translocation are determined by the corresponding membrane-spanning domains. The N-terminal signal peptide is removed co-translationally by a signal peptidase on the luminal side of the ER membrane, while the nascent polypeptide is emerging into the ER lumen (Senkevich et al. 2002; Giovacchini et al. 2007). Upon cotranslational translocation, nascent secretory proteins enter the crowded environment of the ER lumen and soon begin folding into more stable, lower energy conformation (Dobson 2004). Proteins that do not fold or oligomerize correctly are translocated back into the cytosol, where they are deglycosylated, ubiquitylated, and degraded in proteasomes. If misfolded proteins accumulate excessively in the ER, they trigger an unfolded protein response (UPR), which activates appropriate genes in the nucleus to help the ER to cope. Protein folding in the ER is often associated with the formation of native disulfide bonds, which function to stabilize the tertiary and/or quaternary structures of proteins (Freedman et al. 1984; Hillson et al. 1984) and may be intra-protein (i.e., stabilizing the folding of a single polypeptide chain) or inter-protein (i.e., covalently liked dimers, multi-subunit proteins such as antibodies or the A and B chains of insulin). For a disulfide bond to form, the redox environment must be oxidizing (Hwang et al. 1992). The

cytoplasmic redox potential and the high GSH/GSSG ratio in the cytosol is not favorable to the formation and existence of disulfide bridges (Pigiet and Schuster 1986; Arner and Holmgren 2000). The ER in eukaryotes however, is more oxidizing than the surrounding cytosol, which is maintained by the high ratio of oxidized glutathione to reduced glutathione (GSSG/GSH). Therefore, the formation of disulfide bonds within secreted- and integral membrane proteins, proceeds in the lumen of the ER, where protein oxidation initiates upon the translocation of the nascent peptide chain into the ER (Braakman et al. 1991). The formation of disulfide bonds is a reversible reaction in which the thiol groups in two cysteine residues are oxidized to form a covalently linked disulfide bond. The greater the number of disulfide bonds, the less susceptible the protein to denaturation by other forces such as detergents or heat. One important ER resident enzyme is the *protein disulfide* i*somerase* (PDI), which catalyzes the oxidation of free sulfhydryl (-SH) groups on cysteines to form covalent disulfide (S-S) bonds (Hatahet and Ruddock 2009). The PDI is a 55 kDa protein, constitutively expressed in most tissues and organs, and is retained in the ER by its C-terminal –KDEL ER retention signal. PDI is one of the most abundant proteins in the ER, containing an independent active site with two cysteines in the sequence -CGHC- (thioredoxin-like motifs), which mediate PDI's activities (Hayano et al. 1993). These two cysteines can either form an intramolecular disulfide (oxidized PDI) or then exist in the dithiol form (reduced PDI). Protein disulfide isomerases can create, cleave and isomerize the disulfide bonds depending on the state of the substrate and the redox equilibrium.

2 Aims of the current study

Homo- and heterodimerization of the APP protein family as well as the influence on processing and function of APP are still under debate. Several independent studies have shown that APP can form homodimers within the cell, whereby the exact molecular mechanism and the origin of dimer formation remains elusive. At least three regions of APP, including the extracellular E1 domain, the centrally located, conserved E2 domain, as well as transmembrane GxxxG motifs, have been proposed to contribute to APP-APP homodimerization. Structural analysis has revealed that APP and APLPs can form antiparallel homo- and heterodimers through their ectodomains (Soba et al. 2005; Wang and Ha 2004), or that full-length APP may also dimerize upon interacting with heparin at the cell surface (Gralle et al. 2006). Indeed, in addition to monomeric proteins, dimeric and tetrameric forms have been isolated for both, single domains and full length APP (Gralle et al. 2006; Scheuermann et al. 2001; Wang and Ha, 2004). Recently, several pieces of data have suggested that APP processing and function is thought to be influenced by homodimerization and the oligomerization state of APP could play a role in the pathology of AD, by regulating Aβ production (Scheuermann et al. 2001; Munter et al. 2007; Eggert et al. 2009; Khalifa et al. 2010). Moreover, it has been reported that cell-bound APP could form dimers in *trans*-regulating cell–cell adhesion (Soba et al. 2005; Kaden et al. 2009). However, the exact consequence of APP homodimerization on processing and function is not fully understood and remains a controversial topic. Additionally, the precise mode of dimerization remained somewhat elusive. Interestingly, few studies showed that e.g. C99 (Kienlen-Campard et al. 2008) or myc and GFP-tagged APP migrates as a dimer on SDS-polyacrylamide gels (Scheuermann et al. 2001), suggesting that stronger interactions, other than hydrophobic associations might play a role in APP dimer formation.

The main focus of the current study was to analyze a putative dimerization potential of APP in different cellular compartments, and if possible to elucidate a mechanism by which APP oligomerization might be achieved in a cellular context. Therefore, a cell culture model system in CHO-K1 cells was elaborated, stably overexpressing APP chimeric proteins, tagged with C-terminal doublelysine retention motifs. The application of various biochemical methods, including SDS-PAGE under reducing and non-reducing conditions, surface biotinylation and co-immunoprecipitation experiments, should provide insight into the subcellular localization of potential APP-APP interactions within early secretory compartments, i.e. endoplasmic reticulum (ER) or Golgi-compartments. In particular, this *in-vitro* model should exemplify APP dimerization as it might occur under cellular conditions and different redox states, possibly influencing monomer-dimer equilibrium. Furthermore, a Bimolecular Fluorescence Complementation approach (BiFC), using split GFP constructs, should asses the subcellular localization of wildtype APP homodimers witin the cell.

The three major isoforms of human APP, APP695 and APP751 and APP770 differ by the presence of a Kunitz-type protease inhibitor (KPI) domain in the extracellular region. Therefore, we aimed to analyze the dimerization capacities of all three major APP isoforms, regarding intracellular *cis*-directed, and intercellular *trans*-directed dimer formation, likely influencing cell adhesion properties. The *trans*-directed dimerization of APP isoforms at the surface of different cells should be investigated by the application of an aggregation assay in *Drosophila Schneider* (S2)-cells. Finally, we set out to characterize putative dimerization mechanism between APP and one of its homologues, APLP1 in our cell culture model.

3 Materials and Methods

3.1 Chemicals

30% Acrylamide 37.5 : 1, Bis-Acrylamide	National Diagnostics, USA
Acrylamide, 99.9%	Biorad, Munich
Agar	Roth, Karlsruhe
Agarose-A-Beads	Thermo Fisher, USA
Ammoniumpersulfate (APS)	Sigma, Deisenhofen
ß-Mercaptoethanol	Roth, Karlsruhe
BIS	Biorad, Munich
Bis-Tris	Calbiochem, Darmstadt
Brefeldin A (BFA)	Sigma-Aldrich, Taufkirchen
Bromphenolblue	Roth, Karlsruhe
Bovine Serum Albumin (BSA)	Sigma-Aldrich, Taufkirchen
Chlorpromazine	Sigma-Aldrich, Taufkirchen
Coppersulfate ($CuSO_4$)	Sigma-Aldrich, Taufkirchen
Desoxynucleotide-tri-phosphate (dNTP)	New England Biolabs
DAPT	Sigma-Aldrich, Taufkirchen
Dimethylsulfoxide (DMSO)	Sigma-Aldrich, Taufkirchen
Dithiothreiotol (DTT)	Sigma-Aldrich, Taufkirchen
DMEM	Invitrogen, Karlsruhe
Dry-milk (fat-free)	VONS, USA
Ethanol	Roth, Karlsruhe
Ethidiumbromide	Sigma-Aldrich, Taufkirchen
Ethylendiaminetetraacetic acid (EDTA)	Roth, Karlsruhe
EXPRE ^{35}S Protein Labeling Mix,14mCi (518MBq)	Perkin Elmer, Boston
Fetal Calf Serum (FCS)	Invitrogen, Karlsruhe
Glacial Acetic Acid	Merck, Darmstadt
Glycerine	Roth, Karlsruhe
Glycine	Roth, Karlsruhe
HEPES	Serva, Heidelberg
Hydrochloric acid (HCl)	Sigma-Aldrich, Taufkirchen
Igepal (NP-40)	Sigma-Aldrich, Taufkirchen
Immobilion™ Western HRP Substrate Reagents	Millipore, USA
Isopropanol	Roth, Karlsruhe
Magnesium-chloride ($MgCl_2$)	Roth, Karlsruhe
Methanol	Roth, Karlsruhe
N-ethylmaleimide (NEM)	Sigma-Aldrich, Taufkirchen
NeutrAvidin-Agarose beads	Thermo Fisher, USA
Nitrocellulose membrane	Hartenstein, Würzburg

Opti-MEM	Invitrogen, Karlsruhe
Ponceau S	Sigma-Aldrich, Taufkirchen
Potassium chloride (KCl)	Sigma-Aldrich, Taufkirchen
Potassium di-hydrogen phosphate (KH_2PO_4)	Roth, Karlsruhe
Protease inhibitor cocktail tablets, EDTA-free	Roche, Mannheim
Roti-Load (4 x Protein loading buffer)	Roth, Karlsruhe
Seakem LE Agarose	Cambrex, USA
Sodium azide (NaN_3)	Merck, Darmstadt
Sodium chloride (NaCl)	Roth, Karlsruhe
Sodium di-hydrogen phosphate (NaH_2PO_4)	Merck, Darmstadt
Sodium dodecyl sulfate (SDS)	BioRad, Munich
Sodium hydroxide (NaOH)	Merck, Darmstadt
Sodium pyruvate	Invitrogen, Karlsruhe
Sulfo-NHS-LC-LC-Biotin	Pierce, Rockford, USA
TEMED (N,N,N+,N+-Tetramethylendiamine)	BioRad, Munich
Tris-Hydrochloride (HCl)	Roth, Karlsruhe
Tris-Base	Roth, Karlsruhe
Triton X-100	Sigma-Aldrich, Taufkirchen
Trypsin/EDTA	Invitrogen, Karlsruhe
Tryptone	Roth, Karlsruhe
Tween-20	Roth, Karlsruhe
Yeast Extract	Roth, Karlsruhe

3.2 Antibiotics

Ampicillin	Sigma-Aldrich, Taufkirchen
Blasticidin	Sigma-Aldrich, Taufkirchen
Hygromycin	Invitrogen, Karlsruhe
Penicillin/Streptomycin	Invitrogen, Karlsruhe

3.3 Kits

BCA Protein Assay Kit	Pierce, Bonn
NucleoSpin® Extract II-PCR clean-up /Gel extraction kit	Macherey-Nagel
NucleoBond® Xtra Midi kit	Macherey-Nagel
High Pure Plasmid Isolation Kit (Mini)	Roche, Mannheim
JetStar Plasmid Maxi-Prep Kit	Genomed, Germany

3.4 Laboratory hardware and appliances

Agarose gel electrophoresis system	Biometra, Göttingen
Agarose gel documentation imager	INTAS, Göttingen
BioPhotometer plus UV/vis	Eppendorf, Hamburg
Centrifuge Eppendorf 5415D	Eppendorf, Hamburg
Centrifuge Hettich Universal 32	Hettich, Tuttlingen
Centrifuge Hereus Fresco	Kendro, Langenselbold
Centrifuge Sorvall RC5B	Kendro, Langenselbold
CO_2 incubators	New Brunswick, USA
Cryo Freezing Container	Nunc, Wiesbaden
Flat bed shaker Infors	Bolmingen, Switzerland
Freezer -20 C	Liebherr, Germany
Freezer -80°C	Heraeus, Hanau
Fridge + 4°C	Privileg, Germany
Confocal laser scanning microscope LSM 700	Zeiss, Germany
GelAir dryer	Biorad, Munich
Glassware	Schott, Mainz
Heating block	Grant, Berlin
Incubator for bacteria	Binder, Tuttlingen
Laminar flow	Nunc, Wiesbaden
LAS 3000 FujiFilm	Fuji, Japan
Light-optical microscope	Wilovert, Wetzlar
Light-optical microscope	OLYMPUS, Hamburg
Mini Protean III, Western Blotting System	BioRad, Munich
Magnetic stirrer	Heidolph, Kehlheim
Microwave	Micromaxx
Pasteur pipettes	Roth, Karlsruhe
pH-Meter	inoLab, Weinheim
Pipettes 0.1 µl – 1000 µl	Eppendorf, Hamburg
Pipettor AccuJet	VWR, Darmstadt
Scale Mettler P1200	Mettler-Toledo, Giessen
Spectrophotometer	Beckmann, Krefeld
T3 Thermocycler	Biometra, Göttingen
Vortex-Genie 2™	Bender & Hobein AG, Zurich
Waterbath GFL1086	GFL, Burgwedel
Xcell II Surelock™ Mini-cell electrophoresis system	Invitrogen, Karlsruhe
X-ray film developer	Fuji, Japan

3.5 Software

Adobe Photoshop CS5
Corel Draw X14
EndNote X4
Finch TV 1.4, Geospiza
GraphPad Prism 5
ImageJ 1.44, NIH
Microsoft Office 2007
SECentral 7.0/ Clonemanager

3.6 Biochemical protein methods

3.6.1 Harvesting and lysis of cultured cells

NP-40 lysis-buffer:
500 mM Tris, pH 7.4
150 mM NaCl
5 mM EDTA
1% Nonidet P-40
0.02% Sodium Azide
Complete Protease Inhibitor Cocktail (Roche)

To investigate intracellular proteins, cells were lysed in NP40-buffer. Lysates were stored at –20°C, or directly subjected to SDS-PAGE and Western Blot. First, the cell culture dishes were removed from the incubator and placed on ice, then the supernatants were aspirated and cells were carefully washed once with cold 1 x PBS. To detach adherent cells from the plates a cell scraper was used then, cells were srcaped off in 1 ml 1 x PBS and transferred into 1.5 ml microcentrifuge tubes and pelleted for 3 min at 5000 x *g*. The supernatant was discarded and pellets were lysed in an appropriate amount of NP40 lysis-buffer supplemented with 1 x Protease Inhibitor Cocktail (Roche Diagnostics) for 20 min on ice and vortexed every 5 minutes. Optional, lysates were supplemented with 40 mM *N*-ethylmaleimide (NEM), to prevent post lysis disulfide bond formation. Cellular debris were pelleted by centrifugation at 20.000 × *g* for 20 min and cleared lysates were transferred into fresh tubes. Total protein content was determined by the BCA assay (Pierce).

3.6.2 Bicinchoninic acid protein assay (BCA)

To load equal amount of protein on gels or use equal amounts of protein for experiments, such as immunoprecipitations, the concentration of the samples was determined by the bicinchoninic acid (BCA) Protein Assay (Smith et al. 1985), a colorimetric detection and quantitation of total protein. The BCA Protein Assay combines the protein-induced biuret reaction with the selective colorimetric

detection of the resulting cuprous cation (Cu^{1+}) by bicinchoninic acid. Protein concentrations were measured using the BCA Protein Assay Kit (Pierce) according to the manufacturer's protocol. As a reference protein BSA was used at 1 mg/ml for the standard curve, which was prepared as follows:

Final concentration [µg/ml]	Volume NP-40 lysisbuffer [µl]	Volume BSA-standard 1mg/ml [µl]
0	50	0
100	45	5
200	40	10
300	35	15
400	30	20
500	25	25

Table 1: BSA standard dilutions

All protein samples were diluted 1/10 with NP-40 buffer into fresh 1.5 ml tubes. The BCA Reagents A and B were mixed in a 50:1 ratio and 1 ml of BCA reagent mix was added to each sample and standard, followed by incubation for 30 min at 60°C. Subsequently, all samples and standard were loaded in duplicates onto a clear 96-well microtiterplate. The purple colored reaction product is formed by the chelation of two molecules of BCA with one cuprous ion and the OD of the complex was measured at a wavelength of 560 nm.

3.6.3 SDS-Polyacrylamide gelelectrophoresis (SDS-PAGE)

<u>20 x MES SDS Elektrophoresis buffer for NuPage Bis-Tris-Gels:</u>

1 M (2-(N-morpholino)ethanesulfonic acid) MES

1 M Tris Base

69,3 mM SDS

20,5 mM EDTA

H_2Odd

SDS-Polyacrylamide gelelectrophoresis allows the separation of denatured proteins according to their molecular weight. The loading buffer for the proteins contains SDS, which results in an overall negative charge of the protein therefore their separation is not influenced by any intrinsic charges. In this study separation of proteins was carried out, using Bis-Tris-HCl polyacrylamide gels, which were either handmade according to the following recipe, alternatively, pre-cast 4-12% NuPAGE gels (Invitrogen) were used to separate proteins reproducibly, especially when APP dimers were detected. All Bis-Tris gels were run in 1 x MES buffer.

Resolving Gel	10%	12%	14%
30% Acrylamide 37.5 : 1	2.20 ml	2.64 ml	2.30 ml
1.6 M Bis Tris pH 6.4	1.65 ml	1.65 ml	1.65 ml
H_2Odd	2.70 ml	2.26 ml	3.88 ml
10% APS stock	20 µl	20 µl	20 µl
TEMED	5 µl	5 µl	5 µl

Comb Gel	4%
30% Acrylamide 37.5 : 1	2.20 ml
1.6 M Bis Tris pH 6.4	1.65 ml
H_2Odd	2.70 ml
10% APS stock	20 µl
TEMED	5 µl

Table 2: Preparation of Bis-Tris resolving- and comb gels

3.6.4 Western Blotting (Wet-Blot)

Transfer buffer:

192 mM Glycin,

25 mM Tris-Base

20% Methanol

H_2Odd

Following SDS-PAGE proteins were transferred to nitrocellulose or PVDF membranes in transfer buffer containing 20% (v/v) methanol for 1.5 hours at constant 70 V, using the wet-blot based Mini Trans-Blot electrophoretic transfer cell system (BioRad). The gel and the membrane were embedded between soaked pieces of sponge pads, Whatman paper, and gel-cassette plates as follows:

Anode (+)

- Sponge pad
- 1 Whatman sheet - 1 mm
- Nitrocellulose- or PVDF membrane
- SDS gel
- 1 Whatman sheet - 1mm
- Sponge pad

Cathode (-)

The transfer was performed in a blotting tank (Biorad) for 1.5 at 250 mA at room temperature. Thereafter, protein transfer was checked by reversible staining of proteins on membranes with Ponceau-S solution. Blocking of unspecific binding-sites on the nitrocellulose membrane was carried out in TBST containing 5% (w/v) non-fat dry milk powder for 60 min. at room temperature. For immunodetection, blots were incubated with primary antibody in TBST supplemented with 5% (w/v) non-fat dry milk overnight at 4°C in an appropriate dilution (Table 3). Subsequently, membranes were washed three times, for 10 min with TBST under vigorous shaking, to remove unspecific bound primary antibodies and blots were then incubated with HRP-conjugated secondary antibodies in TBST + 5% non-fat dry milk for 1 h. After three final washes with TBST, each time 10 min, membrane-bound secondary antibodies were detected by chemiluminescence using Immobilon (Millipore) substrates and visualized with the Fuji LAS-3000 intelligent dark box (Fujifilm). Antibodies and corresponding dilutions used throughout this study are listed in Table 3 and 4.

Antigen	Species	Dilution	Reference/Supplier
α-Tubulin	mouse/monoclonal	1:3000 (WB)	Sigma-Aldrich
26D6 (Aβ aa 1-12)	mouse/monoclonal	1:3000 (WB)	(Soriano et al. 2001)
anti HA/clone 3F10	rat/polyclonal	1:1000 (WB)	Roche
anti c-myc/clone 9E10	mouse/monoclonal	1:300 (WB) 1:20 (IP)	Hybridoma cell-line
anti-APP CT15 (last 15 aa)	rabbit/polyclonal	1:10.000 (WB)	(Sisodia et al. 1993)
anti-APLP1 (aa 643-653)	rabbit /polyclonal	1:5000 (WB) 1:300 (IP)	Calbiochem
anti-APP 22C11 (aa 66-81)	mouse/monoclonal	1:1000 (WB)	Millipore
anti-APP CT, clone Y188 (APP NpXY-motiv)	rabbit/polyclonal	1:1000 (WB)	Epitomics
anti-GFP	mouse/monoclonal	1:1000 (WB)	Santa Cruz
anti-APP CT20 (last 20 aa)	rabbit/polyclonal	1:1000 (IC)	Calbiochem
anti-HA HA.11	mouse/monoclonal	1.1000 (IC)	Covance
anti Bip/Grp78	rabbit/polyclonal	1:500 (IC)	Stressgen
anti Bip/Grp78	mouse/monoclonal	1:1000 (WB)	BD Biosciences

Table 3: Primary antibodies (WB: western blot; IP immunoprecipitation; IC immunocytochemistry)

Antigen	Conjugate	Dilution	Reference/Supplier
Goat-anti mouse IgG	HRP	1:5000 (WB)	Sigma-Aldrich
Goat-anti rabbit IgG	HRP	1:5000 (WB)	Sigma-Aldrich
Goat-anti rat IgG	HRP	1:2000 (WB)	Sigma-Aldrich
Goat-anti rabbit IgG	Alexa-Fluor594	1:500 (IC)	Invitrogen
Goat-anti rabbit IgG	Alexa-Fluor488	1:500 (IC)	Invitrogen

Table 4: Secondary antibodies (WB: western blot; IC immunocytochemistry)

3.6.5 Ponceau S-staining

Ponceau S-solution:

0.2% (w/v) Ponceau-S red,
3% (w/v) sulfonic acid
0.1% (v/v) glacial acid
H_2Odd

After transfer PVDF or nitrocellulose membranes were rinsed twice with ddH_2O to remove residual SDS and immobilized proteins were visualised by staining with Ponceau S and subsequent rinsing with ddH_2O.

3.6.6 Cell surface biotinylation

1 x PBS

Sulfo-NHS-SS-Biotin

1M NH_4Cl

Biotinylation describes a biochemical method where biotin is covalently attached to a protein, which is exposed to the cell surface. Biotin itself binds to avidin or NeutrAvidin with high affinity which can be exploited to isolate biotinylated molecules of interest by pull down assays with NeutrAvidin coated agarose beads. Therefore Sulfo-NHS-SS-Biotin, which is a water soluble, non cell permeable, thiol-cleavable amine-binding reagent, was used. The reactive Sulfo-NHS ester on this reagent reacts rapidly with primary amines of lysine residues to produce a stable product. To analyze surface levels of APP or APLPs, CHO-K1 cells overexpressing the respective cDNA constructs were grown in 60 mm dishes, and transiently co-transfected with APLP1 or vector control, using Lipofectamine 2000 (Invitrogen). 24 h after transfections, when cells had reached a confluency of 90%, culture dishes were placed directly on ice to block further protein endocytosis. Cells were then washed three times with ice-cold phosphate-buffered saline and subsequently biotinylated with 0.5 mg/ml Sulfo-NHS-LC-LC-Biotin (Pierce) in ice-cold PBS for 40 min at 4°C. The biotin solution was exchanged once after 20 min. To quench any unconjugated biotin, cells were washed four times with ice-cold PBS containing 50 mM NH_4Cl. Subsequently, the cells were harvested and lysed in 500 µl NP-40 buffer and protein concentration was determined via BCA assay. Equal amounts (250 µg) of total protein lysates were incubated with 40 µl of NeutrAvidin Agarose resin beads (Pierce) at 4°C, overnight on a rotating wheel. The next day, biotinylated surface proteins were purified by washing NeutrAvidin beads three times with NP-40 buffer and one time with 1 x PBS to remove nonspecifically bound proteins. The NeutrAvidin Agarose bead-bound fraction, representing plasma membrane proteins, was recovered in equivalent volumes of 2 x SDS loading buffer (100 mM Tris-HCl, pH 6.8, 2% SDS (w/v), 20% glycerol (v/v), and 2% β-mercaptoethanol), boiled for 5 min and size-fractionated by SDS-PAGE on 4-12% precast Novex gels (Invitrogen). Subsequently proteins were transferred to nitrocellulose membranes and incubated with antibodies against APP or APLP1. Each time, blots were reprobed with a monoclonal anti-Tubulin antibody, to verify the absence of endomembrane contaminants from the biotinylation.

3.6.7 Co-immunoprecipitations of APP and APLP1

CHO-K1 cells, stably overexpressing APP constructs, were cultivated in alpha-MEM (Lonza) supplemented with 10% FCS (v/v) (Biochrom) according to standard cell culture techniques. Cells were transiently co-transfected with pLBCX-APLP1, or empty vector using Lipofectamine 2000 (Invitrogen) according to the manufacturer's protocol. 24 h post transfections, CHO-K1 cells were washed with cold 1 x PBS, scraped of culture dishes and lysed in NP-40 lysis buffer (500 mM Tris, pH 7.4, 150 mM NaCl, 5 mM EDTA, 1% Nonidet P-40 (v/v), 0.02% Sodium Azide (v/v)), plus Complete Protease Inhibitor Cocktail (Roche) for 20 min on ice. Debris were pelleted by centrifugation at 20.000 × *g* for 20 min at 4°C in a microcentrifuge, subsequently cleared lysates were transferred to a

clean microcentrifuge tube. Protein content was determined by BCA assay, and 20 µg of total cell lysates were kept as input control. For coimmunoprecipitations, equal amounts of total lysates (250 µg) were incubated with 30 µl of protein A agarose beads (50% (v/v) slurry) (Invitrogen), and either monoclonal 9E10 antibody for myc-tagged APP at 1:50 dilution, or polyclonal antibody 171615 for APLP1 (Calbiochem), at 1:300 dilution. The total sample volume was adjusted to 500 µl with NP-40 buffer plus Protease Inhibitor mix. Then samples were incubated at 4°C with constant rotation, over night. The next day, beads were precipitated by low speed centrifugation and washed three times with NP-40 lysis buffer. Finally, bound proteins were eluted from the beads at 95 °C with 30 µl 2 x SDS sample buffer containing β-mercaptoethanol (BME). Cell lysates that served as input and transfection controls (20 µg) were mixed with SDS sample loading buffer (+BME) and not heat denatured. All samples were electrophoresed on 4-12% NuPage (Novex, Invitrogen) gradient gels and transferred onto nitrocellulose membranes (Millipore, Bedford, MA, USA). Immunoreactive bands were visualized using an ECL enhanced chemiluminescence system (Millipore), after immunoblotting for myc-tagged APP or APLP1, with specific primary and secondary antibodies, as listed in table 3.

3.6.8 Crude membrane preparation and AICD generation assay

CHO-K1 cells overexpressing different APP constructs were grown in 60 mm culture dishes to nearly confluency. Cells were collected and resuspended in 500 µl hypotonic buffer (10 mM Mops, pH 7, 10 mM KCl) containing 1 × Complete Protease Inhibitor Cocktail (Roche) and passed through a 30 gauge neelde, twenty times. To prepare a postnuclear supernatant, the homogenate was centrifuged at 1000 × g for 15 min at 4°C. The membranes were then isolated from the supernatant by centrifugation at 20 000 ×g for 60 min at 4°C. The membranes were resuspended and incubated in 50 µl sodium citrate buffer at 37°C for 1 h to generate AICD, supplemented with 5 mM ortho-phenanthroline to block AICD degradation. Reaction was terminated on ice and membranes were isolated again by centrifugation at 4°C for 2 h. Supernatants were denatured with 4 x SDS sample buffer containing BME and separated on 16% BisTris gels. Proteins were transferred to polyvinylidenfluorid (PVDF) membranes (Millipore). For AICD detecten membranes were boiled for 5 min (after transfer) in PBS and incubated with monoclonal 9E10 antibody.

3.6.9 Detection of Aβ and APPs in cell culture supernatants

To detect APPs and secreted Aβ, the medium was changed 24-48 h after seeding and collected for additional 24 h, while it was concentrated to 1 ml total volume per 6 well. Culture dishes were placed on ice and 500 µl of medium was transferred into clean microcentrifuge tubes and supplemented with Protease Inhibitor mix (Roche) and 5 mM orthophenanthroline, to inhibit Aβ degradation. Samples were centrifuged for 10 min at 4°C to remove particulate material and kept on ice. Meanwhile, cells were washed with cold 1 x PBS, harvested and lysed in an appropriate volume of NP-40 lysis buffer. Equal amounts of total protein, determined by using the BCA Protein Assay (Pierce Chemicals, Rockford, IL, USA), were used for lysate analysis, while media samples were normalized to total protein content in the corresponding cell extract and separated on 14% BisTris acrylamide gels.

Proteins were blotted on PVDF membranes which were boiled for 5 minutes in 1 x PBS, prior to blocking in skimmed milk. APPs was separated on 10% BisTris acrylamide gels and transferred on nitrocellulose membranes. Corresponding cell lysates (20 µg) of CHO-K1 cells stably overexpressing APP constructs were incubated with SDS sample loading buffer, containing β-mercaptoethanol (BME) and directly subjected to SDS PAGE without boiling, or optional heat denatured at 95°C. All lysate aliquots were separated on 4-12% NuPage (Novex) gradient gels and transferred onto nitrocellulose membranes. Aβ was immmunoblotted using antibodies 26D6, whereas APPs total was detected with 22C11.

3.7 Cell biological methods

3.7.1 Metabolic labeling and immunoprecipitation of APP

CHO-K1 cells, stable overexpressing APP695 wt or APP695 KKAA were seeded in six-well culture dishes. 24 h later, cultures were starved for 1 hour in DMEM deprived of Methionine/Cysteine (-Met/Cys, Gibco) and subsequently pulse-labeled for 15 min at 37°C with 1 ml Methionine/Cysteine-free DMEM containing 150 µCi of [^{35}S]-Methionine/Cysteine (EasyTag™ EXPRESS^{35}S Protein Labeling Mix, Perkin Elmer, Boston) and 20 mM 4-(2-hydroxyethyl)-1-piperazineethanesulfonic acid (HEPES; Lonza). Cells were lysed immediately after the pulse (time 0), or chased for 15 min – 48 h in alpha-MEM complete growth medium supplemented with 20 mM HEPES, to determine the turnover of APP. All cell pellets were lysed in 500 µl of NP-40 lysis buffer (50 mM Tris, pH 7.4, 150 mM NaCl, 5 mM EDTA, 1% Nonidet P-40 (v/v), 0.02% Sodium Azide (v/v)), plus Complete Protease Inhibitors (Roche). Lysates were cleared by centrifugation at 20.000 x *g* for 20 min. Post nuclear supernatants were incubated over night at 4°C with monoclonal anti myc antibody 9E10 (dilution 1:20) and 30 µl protein A-agarose beads (50% (v/v) slurry). Immunocomplexes were washed three times with NP-40 buffer, one time with PBS, and eluted from the beads by boiling for 10 min in 30 µl of 2 x SDS-Page sample buffer. Proteins were separated on 4-12% Novex gradient gels, followed by autoradiography on an X-ray film for a minimum of 12 h.

3.7.2 Autoradiography of gels containing [^{35}S]-labeled samples

Fixation solution: 30% (v/v) Methanol
60% (v/v) dd H_2O
10% (v/v) Acetic acid

After gel electrophoresis, the proteins were immobilized by incubating the gel in fixation buffer on a horizontal shaker for 30 min. One sheet of Whatman paper was soaked with ddH_2O and the gel was put on top of the Whatman papers and covered with cling film. The gel was dried on a vacuum gel dryer for 1.5 h at 70°C and later analyzed by autoradiography with [^{35}S]-Methionine sensitive BioMax-MR-films (Kodak) in a lightproof film cassette, at – 80 °C for a minimum of 12 h.

3.7.3 Drug treatments

To inhibit anterograde transport from ER to Golgi compartments, cells were treated with the fungal metabolite brefeldin A, BFA (Sigma), ranging from 5 µg/ml to 30 µg/ml. Stock solutions were prepared in 100% ethanol with 5mg/ml and stored at – 20°C. 24 h after seeding, the medium from cells was replaced with fresh medium containing indicated concentrations of BFA or vehicle alone and treated from 1 h - 4 h.

To inhibit clathrin-mediated endocytosis, cell cultures were treated with 10 µM chlorpromazine (CPZ) (Sigma) for 30 min. Chlorpromazine was dissolved in DMSO and stored as stock solutions (50 mM) at -20 °C.

For γ-*secretase* inhibition, (to block Aβ- and AICD generation), medium from cells was removed and replaced with fresh media containing either vehicle (DMSO) or 10 µM DAPT (Sigma) and incubated for a further 16 hours. After drug treatments, cells were collected in cold PBS and lysed in NP-40 buffer. 20 µg of lysates were incubated with 2 x sample loading buffer, containing BME without boiling, and separated on 4-12% Novex gels. Subsequently, gels were blotted on nitrocellulose or PVDF membranes and incubated with antibody 9E10, for myc-tagged APP variants (dilution 1:300), or 26D6 (1:1000), for detection of Aβ in the medium.

To prevent formation of disulfide bonds in newly synthesized proteins, cell cultures of CHO-K1 cells, stably overexpressing APP KKAA (APP ER) were treated with 1 mM dithiothreitol (DTT) ranging from 30 min-24 h.

Endoplasmic reticulum stress (ER-stress) was induced by tunicamycin (TM). Cell cultures were treated for 12 h with 1 µM or 2 µM tunicamycin, prior to lysis.

3.8 Cell culture methods

3.8.1 General tissue culture

Routine cell culture was performed under sterile working conditions in S1 or S2 qualified laboratories. Cell culture glassware was kept separately which included separate washing and autoclaving. Pipettes, dishes, plates, filter tips, 15 ml, 50 ml, and 1.5 ml tubes, syringes and sterile filters were single-use plastic items and cell culture qualified. All solutions and media were stored at 4°C, unless otherwise indicated by the manufacturer. Media were pre-warmed before use in a 37°C waterbath. Cell growth and morphology was checked on a daily basis and mycoplasm tests performed twice a year.

3.8.2 Cultivation of stably transfected CHO-K1 cell lines

Culture medium for CHO-K1 cell-lines:

Alpha-MEM (4500 mg/l Glucose; 0.11 g/l sodium pyruvate)
1% (v/v) Penicillin/Streptomycin (10.000 U Penicillin, 10 mg Streptomycin/ml in 0.9% NaCl)
10% (v/v) FCS

For stably transfected CHO-K1 cells, overexpressing different myc-tagged APP constructs, Hygromycin B or Blasticindin was used once a week at final concentrations of 300 µg/ml (Hygromycin B) or 6 µg/ml (Blasticidin), to selectively inhibit growth of non-transfected cell clones. The cells were cultivated in 10 cm^2 cell culture dishes (TPP, Trasadingen, Switzerland) and passaged with Trypsin-EDTA at 90-100% confluency. Therefore, cells were washed with sterile 1 x PBS once, and trypsinized with 1.5 ml of Trypsin-EDTA for 3-5 min at 37°C. The detached cells were resuspended in an appropriate volume of fresh growth medium until a single cell suspension was obtained. Aliquots of

the resuspended cells were plated in dishes containing 10 ml fresh medium and equally distributed with gentle shaking. Cells were cultivated at 37°C and 5% CO_2.

3.8.3 Cultivation of semi-adherent *Schneider* (S2) cells

Culture Medium for *Schneider* (S2) cells:

Schneider´s Medium (Invitrogen)
1% (v/v) Penicillin/Streptomycin (10.000 U Penicillin, 10 mg Streptomycin/ml in 0.9% NaCl)
10% (v/v) FCS

The cells were cultivated in T-75 cell culture flasks (Costar) with 20 ml growth medium. S2 cells stayed adherent until 80-90% confluency was reached, after which they detached and proliferated in suspension. At this time point, cells were passaged by resuspending until a single cell suspension was present. An aliquot (1/40-1/20) of the resuspended cells was transferred into a new flask containing 20 ml fresh medium, and equally distributed with gentle shaking. Cells were cultivated at 25°C under a normal atmosphere.

3.8.4 Cultivation of HEK-293T cells and HEK-GP2 cells

Culture medium for HEK cells:

DMEM (4500 mg/l Glucose; 0.11 g/l sodium pyruvate)
1% (v/v) Penicillin/Streptomycin (10.000 U Penicillin, 10 mg Streptomycin/ml in 0.9% NaCl)
10% (v/v) FCS

➔ Cells were cultivated and passaged equivalent to CHO-K1 cells (section 3.8.2)

3.8.5 Freezing of cells for long term storage

Freezing medium:

10% (v/v) DMSO in growth medium with 10% (v/v) FCS and antibiotics

When cells had reached 70-90% confluency (in l*og*-phase) they were used for freezing. Cells were washed and trypsinized from a 10 cm^2 dish as described. After the addition of 10 ml of fresh growth medium, the suspension was transferred into 15 ml sterile tubes and cells were sedimented at 1200 rpm x g for 5 min and resuspended in freezing medium. 1.5 ml aliquots were transferred into cryovials (Nunc), and incubated on ice for 30 min. The vials were then stored at -80°C over night, and then transferred into a liquid nitrogen tank for long term storage. Alternatively, vials were directly incubated in a cryobox (Nunc) containing isopropanol at -80°C over night, and afterwards transferred into a liquid nitrogen tank.

3.8.6 Thawing of frozen cells

Cells frozen in liquid nitrogen were quickly thawed at 37°C in a water bath. Subsequently, cells were transferred into a 10 cm^2 dish with 10 ml fresh growth medium and equally distributed with gentle shaking. The medium was replaced the next day to remove residual DMSO and cells were passaged if necessary.

3.8.7 Transfections

3.8.7.1 Transient transfection of Drosophila Schneider cells with Effectene

S2 cells were plated in 12 well dishes at 30-50% confluency the day before transfection. 2-3 h before transfection, the growth medium was replaced with 800 µl fresh medium, and cells were double transfected with Effectene (Qiagen) according to the manufacturer´s protocol as follows:

0.5 µg pMT-Gal4 (obtained from P. Soba)
0.5 µg pUAST-DNA (obtained from P. Soba)
add 100 µl enhancer buffer
8 µl enhancer

The mixture was vortexed for 1 s and incubated for 3-5 min at room temperature. Effectene (12.5 µl) was added by pippeting up and down five times and incubated for 10 min at room temperature. Afterwards, 290 µl S2 growth medium were added by pippeting up and down twice. The mixture was directly added dropwise to the cells and incubated for 48 h at 25°C. Expression was induced by adding $CuSO_4$ (0.5 M stock in dd H_2O) to a final concentration of 500 µM. Cells were generally analyzed 16 h later.

3.8.7.2 Transient transfection of CHO-K1 cells with Lipofectamine 2000

OptiMEM serum-free (Invitrogen)
Lipofectamine 2000 (Invitrogen)

Generally, 6-well dishes with cells at 80-90% confluency were transfected. In one Eppendorf tube, 2 µg DNA were mixed with 250 µl OptiMEM and in a second tube 6 µl Lipofectamine 2000 (Invitrogen) were mixed with 250 µl OptiMEM and incubated for 5 min at room temperature. After incubation, the DNA- and Lipofectamine containing tubes were mixed by pipetting up and down several times and incubated for another 15 min at room temperature. Meanwhile, cells were washed with OptiMEM once and 2 ml OptiMEM was added to each well. Finally the Lipofectamine/DNA mixture was added dropwise to the cells and incubated for 3-4 h at 37 °C and 5% CO_2. Afterwards, the reagent was removed and fresh growth medim, containing serum was added. After 24 h, the cells were harvested and lysed in NP-40 buffer, as described under 3.6.1.

3.8.8 Generation of CHO-K1 cell lines, stably overexpressing APP constructs

3.8.8.1 Transient transfection of HEK-GP2 cells and generating of retroviral particles

The GP2-293 Packaging Cell Line is a HEK-293-based cell line that carries the viral *gag* and *pol* genes, whereas the viral *env* gene must be cotransfected with a retroviral expression construct. Upon transient transfection of the *env* gene, located on the plasmid pVSV-G, the GP2 cell line expresses an envelope glycoprotein from the vesicular stomatitis virus (VSV) that mediates viral entry through lipid binding and plasma membrane fusion. As a result high levels of infectious viral particles can be produced, providing a highly efficient way of transferring genes into target cell populations. Because the gene of interest integrates by a retroviral 5' LTR into the host cell genome, retroviral transduction produces heritable expression which is used to generate mass cell cultures, permanently overexpressing different APP constructs.

Initially, HEK GP2 cells were transfected with a retroviral expression plasmid (pLBCX), encoding for the specific APP variants and containing a selection marker (Blasticidin) to screen for stable transfected clones, after infection of target CHO-K1 cells. Additionally the pVSV-G plasmid was cotransfected, encoding for the viral envelope glycoprotein. Therefore, GP2 cells were seeded on 10 cm^2 culture dishes, at a confluency of 40-50%, 24 h prior to transfection. For transfection the calcium phosphate precipitation method ($CaPO_4$) was used.

The following mix was prepared for one 10 cm^2 dish in the same order:

856 µl sterile H_20
124 µl 2 M $CaCl_2$
20 µg DNA (10 µg of desired plasmid e.g APP wt in pLBCX + 10 µg pVSV-G)

This was followed by the addition (drop-wise) of 1 ml of 2 x HEPES buffer while air bubbeling the mix, using a 1000 µl pipet and incubated for 15 minutes at room temperature. Subsequently, the mixture was dispersed gently onto the culture dish in a drop wise fashion and the dish was placed back in the incubator. After 6 hours of incubation the medium was replaced with 5 ml of fresh complete DMEM and incubated another 48 hours at 37°C to produce viral particles which are accumulating in the medium.

3.8.8.2 Infection of target cells with retroviral particles

To produce cell lines with stable expression of transgenes, cells were infected with retroviral particles and then subjected to selection with the appropriate antibiotic depending on the resistance gene, encoded on the plasmid. Therefore, the target cells were seeded 24 hours prior to infection on 6-well plates. The cell density should be adjusted individually, so that cell lines reach confluency about 48 – 72 h later. CHO-K1 cells were plated at 300.000 cells/well on a 6-well plate. On the second day, medium was removed from target cells and 1 ml fresh medium and 2 µl polybrene stock solution (5 mg/ml) was added. Polybrene is a cationic polymer used to facilitate adsorption of retroviral particles to eukaryotic cells. Finally, 1 ml of retroviral particle containing medium was added, and

incubated for another 24 h. On the third day, infected cells were transferred into selection medium. Therefore, medium containing retroviral particles was removed and each well was washed with one ml 1 x PBS and cells were trypsinized off culture dishes. Finally, cells from each 6 well were suspended in fresh medium containing 6 µg/ml blasticidin as selection antibiotic and dispersed on a 10 cm^2 culture plate. The selection medium was changed every 2 – 3 days until stable cell clones appeared and the expression of the transgene was analyzed by western blot analysis.

3.9 *Drosophila Schneider* (S2) cell aggregation assay

Culture Medium for *Schneider* (S2) cells:
Schneider´s Medium (Invitrogen)
1% (v/v) Penicillin/Streptomycin (10000 U Penicillin, 10 mg Streptomycin/ml in 0.9% NaCl)
10% (v/v) FCS

Semi-adherent S2 cells were cultivated at 25°C with growth medium. Cells stayed adherent until 70-80% confluency was reached, after which they detached and proliferated in suspension. At this time point, cells were passaged (1/40-1/20) after resuspending to single cell suspension. S2 cells were transiently co-transfected with pMT-Gal4 and the corresponding pUAST constructs containing APP695, APP751, APP770 using Effectene (Qiagen), and subjected to the cell aggregation assay as described previously (Soba et al. 2005). Briefly, expression was induced 48 h post-transfection by addition of $CuSO_4$ (500 µM) for 16 h. In all experiments, comparable transfection efficiencies of about 10% for all analyzed constructs were achieved. For analysis $4x10^5$ cells (single cell suspension) were incubated in a total volume of 1 ml fresh growth medium for 2 h at 90 rpm on a horizontal shaker. Afterwards, cells were transferred to poly-L-lysine coated cover slips using an abscised 1 ml Gilson pipette tip. Cells were allowed to attach to the cover slip for 2-3 h and subjected to immocytochemical analysis as described before (Soba et al. 2005), using anti-APP antibody (CT-20, Calbiochem) in 5% normal goat serum in PBS (1:1000) and anti-rabbit AlexaFluor488 (Invitrogen) as secondary antibody. For quantification of aggregated cells, clusters of three or more transfected cells were scored as positive. In total, 900-1100 transfected cells from at least three independent experiments were counted for each experimental setup in a blinded fashion. Statistical significance was tested with a student´s *t*-test. Representative images of clustered cells were taken on a Leica laser scanning confocal microscope with a 63x water immersion objective.

3.10 Bimolecular Fluorescence Complementation (BiFC) technique with APP split GFP constructs

A GFP tagging system was employed (experiment in cooperation with S. Eggert, Kaiserslautern) for the intracellular detection of APP695, which is based on the auto-assembly capacity of two nonfluorescent portions of GFP, termed GFP 1-10 and GFP 11. When brought together by the association of two interacting partner proteins, individually fused to the fragments, they restore a fully fluorescent GFP, termed Bimolecular Fluorescence Complementation (BiFC) (Feinberg et al. 2008). Thus, monitoring APP-APP interactions and their subcellular localization under physiological conditions (Feinberg et al. 2008). Therefore, two complementary GFP fragments were separately fused to the C-termini of HA-APP695 (Soba et al. 2005) and both constructs expressed in the neuroblastoma N2a cell line. N2a cells were grown on poly-L-lysine (Sigma) coated coverslips in 24-well plates (Falcon) and transiently transfected (Lipofectamine 2000) with NT HA APP695 CT 1-10 and NT HA APP695 CT 11. Fixation of the cells followed 17 h later for ten minutes with 4% paraformaldehyde + 4% sucrose in 1 x PBS at 37°C. Subsequently, fixed cells were permeabilized with 0.1% NP-40 in 1 x PBS. The cells were blocked with 5% (v/v) goat serum (Sigma) in 1 x PBS for 1 h and the primary antibody (ER marker Grp78, rabbit polyclonal) (StressGen), or monoclonal mouse HA.11 antibody (Covance) was incubated over night at 4°C. The secondary antibody, AlexaFlour594 conjugated goat anti rabbit (Invitrogen), was incubated for 1 hour at room temperature. The coverslips were embedded in Mowiol and analyzed by fluorescence microscopy (63x objective, Axio Observer Z.1, Zeiss).

3.11 Densitometry and statistics

All Western blots were quantified using the free image processing and analysis software ImageJ 1.44 (National Institute of Health; Bethesda, MD). Statistical analysis was performed using the statistics package GraphPad Prism 4® software (La Jolla, CA, USA).). Data were analysed by one-way analysis of variance (ANOVA) coupled to Newman-Keuls post test for multiple comparison or *t*-test. $p < 0.05$ was considered as statistically significant.

3.12 Molecular Biology

3.12.1 Generation of chemically competent *E. coli* with the RbCl-method

RFI buffer:

100 mM RbCl

50 mM $MnCl_2$ x 4 H_2O

30 mM Potassium acetate

10 mM $CaCl_2$ x 2 H_2O

15% (w/v) Glycerol

The pH value was adjusted to 5.8 with acidic acid. The buffer was sterile filtered, and 50 ml aliquots were stored at -20 °C.

RFII buffer:
10 mM MOPS (3-(N-Morpholino)-propanesulfonic acid)
10 mM RbCl
75 mM $CaCl_2$ x 2 H_2O
15% (w/v) Glycerol
The pH value was adjusted to 6.8 with NaOH. The buffer was sterile filtered, and 15 ml aliquots were stored at -20 °C.

The components were dissolved and 10 ml of a 250 mM KCl solution were added. The pH value was adjusted to 7.0 with NaOH and the water was added to a final volume of 1 litre. A single colony (*E. coli* DH5α) was inoculated into 2 ml LB-medium without antibiotics and incubated for 2 h at 37°C under vigorous shaking. Afterwards, 500 µl were inoculated into 50 ml LB medium and incubated at 37°C, until an OD (600 nm) ~0.5-0.6 was reached. The following steps were performed at 4°C with pre-cooled equipment. The culture was transferred to 50 ml Falcon tubes and incubated for 15 min at 4°C, and centrifuged at 3000 rpm/4°C (Heraeus centrifuge) for 10 min. The sedimented cells were resuspended in 17 ml RFI buffer and incubated on ice for 30 min. The cells were again centrifuged at 3000 rpm/4 °C (Heraeus centrifuge) for 10 min, resuspended in 4 ml RFII buffer, and incubated on ice for 15 min. Aliquots of 100 µl were transferred into chilled Eppendorf tubes and shock frozen in liquid nitrogen. Competent DH5α were stored at -80°C.

3.12.2 Transformation of chemically competent *E. coli*

LB-(Luria-Bertani) Medium:
0,5% (w/v) NaCl
1% (w/v) Bacto-Tryptone
0.5% (w/v) yeast extract
20 mM Tris/HCl pH 7.5
The pH value was adjusted to 7.0 with NaOH

- Chemo-competent DH5α
- Bacterial agar plates (1 l LB-media + 15 g (w/v) Bacto Agar)

Chemo-competent *E.coli* cells (DH5α) were thawed on ice, and plasmid DNA (5-200 ng) was added to a 100 µl aliquot, and incubated for 15 min on ice. Subsequently, cells were heat shocked for 45 sec at 42°C, and cooled on ice for 2 min. 900 µl LB medium was added and cells were incubated for 45-60 min at 37°C on a thermoshaker at 1.000 rpm. Afterwards, 100 µl aliquots (or less) were plated on bacterial agar plates, containing the appropriate antibiotic and incubated over night at 37°C.

3.12.3 Preparation of bacterial agar plates

Solutions:

LB-(Luria-Bertani) Medium: 0,5% (w/v) NaCl
1% (w/v) Bacto-Tryptone
0.5% (w/v) yeast extract
20 mM Tris/HCl pH 7.5
The pH value was adjusted to 7.0 with NaOH
Bacto-Agar
Ampicillin final conc. (100 µg/ml)
Kanamycin final conc. (50 µg/ml)

For agar plates, 7.5 g bacto-agar was added to 500 ml LB medium and autoclaved. After cooling to 60°C, the appropriate antibiotic was added to a final concentration of 100 µg/ml for Ampicillin or 50 µg/ml for Kanamycin, respectively. The liquid medium was poured into 10 cm culture dishes and allowed to cool to room temperature. The agar plates were stored upside down at 4°C and covered from light and humidity.

3.12.4 Liquid cultures of bacteria

Small scale liquid cultures:

A single colony was inoculated into 3-5 ml LB medium supplemented with the appropriate antibiotic, and incubated over night at 37 °C under vigorous shaking. The bacterial culture was used for small scale DNA preparation (Mini-Prep).

Large scale liquid cultures:

For large scale DNA preparation (Maxi-Prep), 250 µl of a 1 ml pre-culture was inoculated into 250 ml LB-medium supplemented with the appropriate antibiotic, and incubated over night at 37°C under vigorous shaking.

3.12.5 Plasmid preparation from bacteria (Mini-/ Maxi-Prep)

Plasmid DNA from bacteria was isolated using a combination of alkaline lysis and ion-exchange columns which are the basis for almost all commercially available DNA extraction kits. For large scale DNA extraction from 250 ml bacterial cultures either the JETstar® plasmid purification system form Genomed, or the NucleoBond® Xtra Midi kit from Macherey Nagel. For small quantities of purified plasmid DNA (Mini-Prep from 3-5 ml of bacterial culture), the High Pure Plasmid Isolation Kit (Roche) was used. Both kits contained all the necessary buffers and solutions and the DNA extraction was performed according to the manufacturers´ protocol.

3.12.6 Photometric analysis of DNA concentrations

The concentrations of plasmid DNA were measured with a spectral photometer (SmartSpec 3000, Biorad) at a wavelength of 260 nm. In general, the DNA was diluted to 1:100 in ddH_2O for measurement.

dsDNA: A260nm (1cm)= 1 c ~50 µg/ml. The purity of the DNA samples was determined by measuring the A280nm and A310nm, which correspond to the absorption maxima of proteins and polysaccharides. For pure DNA, the A260 nm/A280 nm ratio is supposed to be between 1.8 and 2.0, with no absorption at A310 nm.

3.12.7 Restriction digest of DNA

Digestion of DNA with restriction enzymes leads to formation of either sticky or blunt ended DNA. Sticky ends have single stranded base overlaps that can anneal to sticky ends of a different DNA fragment, which was digested with the same enzyme(s). The recognition sequences of restriction enzymes are palindromic stretches of DNA of four-, six-, or eight base pairs length. For an analytic digest, 1 µg DNA was digested in a final volume of 30 µl with either one or two enzymes at the same time. The analytic digests were incubated at 37°C, or the respective optimal temperature for the enzyme, for 2 h. Preparative digests in the case of PCR-products or vector linearisations were carried out over night at 37°C.

Usually, cleaving of DNA with two restriction enzymes simultaneously (double digestion) was performed. For analytic purposes approximately 2 µg of plasmid DNA was digested at 37°C for 2-3 h Reactions were carried out as follows in t toatal volume of 30 µl:

Plasmid DNA	1-2 µg of Midi prep DNA or ~5 µl Mini prep DNA
Restriction buffer NEB (10x)	3 µl
BSA (100 x)	0.3 µl
Enzyme each (10 U/**µ**l)	0.5 µl
Nuclease free water	Fill to 30 µl

Table 5: Analytical restriction digest

For preparative purposes 2-5 µg of plasmid DNA were digested at 37°C for 90 minutes as follows:

Plasmid DNA	2-5 µg
Restriction buffer NEB (10 x)	5 µl
BSA (100 x)	0.5 µl
Enzyme each (10U/µl)	1 µl
Nuclease-free water	Fill to 50 µl

Table 6: Preparative restriction digest

Restriction enzymes and supplied buffers (NEB 1 - 4, optimal for each enzyme) were purchased from New England Biolabs (NEB) and double digests were performed as recommended by the company's online software: http://www.neb.com/nebecomm/DoubleDigestCalculator.asp
Digested DNA fragments were analysed or purified by agarose gel electrophoresis.

3.12.8 Ligation of DNA fragments

Insert DNA and plasmid vector were individually cut to yield complementary ends, then both were added to a ligation reaction to be circularized by DNA T4-*Ligase*, which closes nicks in the phosphodiester backbone of the DNA, generated during restriction. The ligation of cohesive or blunt ended DNA was performed in a total volume of 30 µl. The vector backbone and insert DNA were digested with appropriate enzymes and purified as described in 3.12.7 and 3.12.10. The concentration of the fragments was estimated from their signal on an agarose gel, and ligations were carried out at molar ratios of 1 (vector) to 3-5 (insert) using T4 *DNA-Ligase* (NEB) with incubation at ~16°C over night.
A typical reaction for ligation of cohesive (sticky) ends 30 µl total volume:

10 X T4 DNA Ligase Buffer	3 µl
Vector DNA (3kb)	50 ng (0.025 pmol)
Insert DNA (1kb)	50 ng (0.076 pmol)
Nuclease-free water	fill up to 30 µl
T4 DNA-*Ligase*	1 µl

Table 7: Ligation Mix

3.12.9 Agarose gel electrophoresis

1 x TAE buffer:

40 mM Tris-acetate

1 mM EDTA pH 8.0

Ethidiumbromide stock: 10 mg/ml (final conc. 0.5-1 µg/ml)

DNA fragments were separated by agarose gel electrophoresis. Agarose (0.8-1.5% w/v) was dissolved by boiling in TAE buffer. Ethidiumbromide (0.5µg/ml) was added to the cooled (~60°C) agarose solution and poured into a horizontal gel chamber. DNA samples were combined with a 6 x loading dye solution (Fermentas), and electrophoresis was performed at 100-200 V. As size reference, 5 µl of 1kb DNA ladder (Fermentas) was loaded. Subsequently, the gels were photographed and printed with a gel documentation device. For preparative purposes, the DNA fragments were cut out from the gel under weaker UV light (254 nm) to avoid DNA damage, and transferred into a sterile Eppendorf tube for gel extraction.

3.12.10 DNA extraction from agarose gels

DNA fragments, resulting from restriction digestions or PCR reactions, were excised and extracted from agarose gels using the "NucleoSpin® Extract II"-PCR clean-up and gel extraction kit from Macherey Nagel, according to the manufacturer's instructions. This procedure was necessary to remove primes, buffers and enzymes which may disturb downstream applications, for example ligation reactions.

3.12.11 Polymerase Chain Reaction (PCR)

The PCR strategy facilitates in vitro amplification of specific DNA sequences using a thermostable DNA polymerase. During the PCR the DNA becomes thermally denatured and hybridizes with short oligonucleotides that are subsequently elongated by a DNA polymerase (Mullis and Faloona, 1987). These steps, denaturation, hybridization/annealing and elongation are repeated several times and result in amplification of the DNA stretch that was flanked by the specific primer sequences. PCR protocols vary, depending on the template DNA, the oligonucleotide sequence, the polymerase, and the length of the amplified DNA fragment. For all cloning experiments, the Phusion™ High-Fidelity DNA Polymerase (Finnzymes) with 5´→ 3´ DNA polymerase activity and 3´→ 5´ exonuclease ("proof reading") activity was used.

A typical 50 µl PCR reaction was prepared as follows:

DNA template	50-200 ng
Phusion™ Polymerase 2U/µl (Finnzymes)	0.5 µl
5x Phusion HF Buffer	10 µl
10 mM dNTPs Mix: (dATP, dTTP, dGTP, dCTP)	1.5 µl
sense-Primer (10 pM)	1 µl
antisense-Primer (10 pM)	1 µl
Nuclease-free water	fill up to 50 µl

Table 8: PCR-reaction-mix for Phusion Polymerase

PCR parameters were adjusted to the appropriate conditions. Generally, 25-35 cycles were applied for amplification. A standard PCR program, using Phusion™ Polymerase was conducted as follows:

Cycle Step	Temperature	Time	Cycles
Initial Denaturation	98°C	30 sec	1
Denaturation	98°C	5-10 sec	25-35
Annealing	60°C	30 sec	
Extension	72°C	30 sec/1 kb	
Final Extension	72°C	10 min	1
Hold	4°C	∞	____

Table 9: PCR standard program for Phusion Polymerase

3.12.12 Cloning of cDNA constructs

3.12.12.1 Cloning of myc- or HA-tagged APP/C99 retention constructs

The plasmids pLHCX-APP695 wt, pLHCX-APP770 wt and pcDNA3.1-APP751 wt described in (Jager et al. 2009), were used as PCR templates to subclone APP sequences into the pLBCX vector backbone with a *5´HindIII* and a *3´ClaI* restriction site, containing an additional 3´myc-epitope. The same plasmids were used to add the -KKAA (APP ER) or -KKFF (APP Golgi) retention motifs to the very C-terminus of APP, following the myc-tag. To attach an HA-epitope to the C-terminus of all three different APP isoforms, the aforementioned cDNAs were used as templates for standard PCR

techniques, using specific primers, listed in table 10. The N-terminal truncated APP695ΔE1 in pcDNA3 was described previously (Kaden et al. 2009). This cDNA was also subcloned into pLBCX and amplified by standard PCR techniques, either to attach a myc-epitope alone, or followed by a KKAA retention motif. The pLHCX vector encoding the myc-tagged C99 expression construct (Jager et al. 2009) was used as template to introduce the KKAA motif to the very C-terminus, using the primers as listed in table 10. All PCR products were digested with *HindIII* x *ClaI* and ligated into pLBCX retroviral expression vector.

3.12.12.2 Cloning of APP Cysteine-/Serine-mutants using Overlap Extension PCR strategy

The cysteine mutants APP695 K28C and APP770 K28C, contain a cysteine residue instead a lysine at position 28, corresponding to Aβ numbering. Furthermore, a C-terminal myc-epitope was attached to detect exclusively overexpressed APP variants. As templates for PCRs, APP695 wt in pLBCX and APP770wt in pLBCX were used, and the mutation was introduced by an Overlap Extension PCR strategy, or four-oligo method (Lee et al. 2010). This method allows selective introduction of base pair exchanges into DNA fragments. Therefore, two sets of DNA oligonucleotides/primers were used. One pair was set at the outer end of the DNA fragment, containing each a restriction cleavage site (5´HindIII and 3´ClaI), and one pair was complementary to the mutagenesis-site. For the design of the two inner primers, it was essential that the base pair exchange and the resultant mismatch were located in the middle of the primer, and that at least 15 matching bases were present on both sides of the mutant site. The first two PCRs were performed in separate reactions with each oligonucleotide pair consisting of one outer and one inner primer. These PCRs resulted in two products, which overlapped in the middle, both containing the respective mutation. In a third PCR, both halves of the construct which are partly complementarity and prime off each other, were mixed and the outer primer pair alone was used for amplification. Finally, this resulted in a PCR product, encompassing the full length construct, comprising the desired mutation. The APP695 ER 98-105_{ser} mutant was generated with the same method as described. For all mutagenesis cloning experiments the Phusion™ High-Fidelity DNA Polymerase (Finnzymes) was used. All final PCR products were ligated into a HindIII x ClaI digested pLBCX-vector.

3.12.12.3 Subcloning of APLP1 in pLBCX

The human APLP1 cDNA in the peak8 expression vector was kindly provided by Stefan F. Lichtenthaler (Munich, Germany). The coding sequence was amplified by standard PCR to add the *HindIII* and *ClaI* restriction sites, using primers listed in table 10. The PCR product was ligated into a *HindIII* x *ClaI* digested pLBCX-vector.

3.12.12.4 Cloning of NT HA APP695 CT Split GFP constructs 1-10 and 11

Generation of plasmid NT HA APP695 CT Split GFP 1-10: for the first PCR, template APP695 NT HA in pcDNA3.1 (Soba et al. 2005) was amplified with sense primer sAPP-3 (starts at position 1681 in the APP695 ORF) and antisense primer, introducing a *MluI* restriction site. The resulting PCR product was digested with *EcoRI* and *MluI* to obtain a 293 bp fragment. For the second PCR, template GFP 1-10 (Feinberg et al. 2008) was amplified with forward primer containing a *MluI* site and reverse primer including an *XhoI* site. The resulting PCR product was digested with *MluI* and *XhoI.* The two PCR fragments were ligated into vector pcDNA3.1+, containing the 3' UTR cassette of APP (*XhoI/XbaI*) (described in Eggert et al. 2009), using the recognition sites for *EcoRI* and *XhoI*. To add in the 5' end of the APP fragment, the plasmid APP695 NT HA (Soba et al. 2005) was digested with *EcoRI*. The resulting 1900 bp fragment, including the HA tag, was ligated in the above mentioned new plasmid. Cloning of NT HA APP695 CT Split GFP 11 was performed in analogy to NT HA APP695 CT Split GFP 1-10. Only the second PCR product was generated differently: Template Split GFP 11 was amplified with the forward primer, encompassing a *MluI* site, and the reverse primer introducing an *XhoI* site. The resulting 100 bp PCR product was digested *MluI/XhoI.*

3.12.12.5 Oligonucleotides

Primer name	Sequence 5´ → 3´	Enzyme site
APP universal fwd all isoforms	CCCAAGCTTATGCTGCCCGGTTTGGCACTGCTC	*Hind III*
APP myc rev universal all isoforms and C99, APP695ΔE1	CCATCGATTTAATGGTGATGGTGATGATGACCGGTATGCATATTCAGATCCTCTTCTGAGATGAGTTTTTGTTCGAAGGGCCCTCTAGAGTTCTGCATC	*ClaI*
APP KKAA rev	CCATCGATTTAGGCGGCCTTCTTATGGTGATGGTGATGATGACCGGTATGCATATT	*ClaI*
APP KKFF rev	CCATCGATTTAGAAGAACTTCTTATGGTGATGGTGATGATGACCGGTATGCATATT	*ClaI*
APP K28C fwd	GTGGGTTCAAACTGTGGTGCAATCATTG	___
APP K28C rev	CAATGATTGCACCACAGTTTGAACCCAC	___
APP 98/105 serine fwd	CCAGTGACCATCCAGAACTGGTCCAAGCGGGGCCGCAAGCAGTCCAAGACCCATCCCCACTTTGT	___
APP 98/105 serine rev	ACAAAGTGGGGATGGGTCTTGGACTGCTTGCGGCCCCGCTTGGACCAGTTCTGGATGGTCACTGG	___

APP KKAA HA rev	CCATCGATTTAAGCGTAATCTGGAACATCGTATGGGTAGTTCTGC ATCTGCTCAAAGAACTTGTAGGTTGGATT	*ClaI*
APP HA rev	CCATCGATAGCGTAATCTGGAACATCGTATGGGTAGTTCTGCATC TGCTCAAAGAACTTGTAGGTTGGATT	*ClaI*
APLP1 fwd	CCCAAGCTTTAATGGGGCCCGCCAGCCCCGCTGCTC	*HindIII*
APLP1 rev	CCATCGATTTAGGGTCGTTCCTCCAGGAAGCGGTAA	*ClaI*
sAPP-3 fwd split GFP 1-10	GAAGTTGAGCCTGTTGATGCC	___
sAPP-3 rev split GFP 1-10	GCTATGACGCGTGTTCTGCATCTGCTC	*MluI*
2nd PCR fwd GFP 1-10	GCGATGACGCGTGGTGGTTCGGGTGGTATGTCCAAAGGAGAAG	*MluI*
2nd PCR rev GFP 1-10	GCCCGCCTCGAGTCATGTTCCTTTTTCATTTGG	*XhoI*
2nd PCR fwd GFP 11	CTATGACGCGTTCGGGTGGTGGTGGTTCGGGTGGTGGTGGT	*MluI*
2nd PCR rev GFP 11	CTATGCTCGAGTTAGGTGATGCCGGGGCGTTC	*XhoI*

Table 10: Oligonucleotides for generation of expression constructs

3.12.12.6 DNA-Sequencing

All cDNA constructs were sequenced at SEQ.IT GmbH & Co. KG in Kaiserlsautern.

4 Results

In previous studies it has been shown that APP can form cellular *cis*-dimers (Scheuermann et al. 2001), reminiscent of a classical receptor dimerization described for the EGF receptor (Schlessinger 2002), as well as *trans*-dimers at the cell surface with itself or APLPs (Soba et al. 2005). To date, at least three domains have been reported to promote APP dimerization: the E1 domain containing the N-terminal growth factor like domain (GFLD) and copper binding domain (CuBD) (Soba et al. 2005), which is mainly responsible for full length APP dimerization (Kaden et al. 2009). The second region is the E2 ectodomain, containing the carbohydrate sites, which has been shown to dimerize in solution in an antiparallel orientation (Wang and Ha 2004). A third dimerization interface is located at the extracellular juxtamembrane/transmembrane (JM/TM) boundary, where APP contains three consecutive glycine-xxx-glycine (GxxxG) motifs (Munter et al. 2007; Gormann et al. 2008). Structural-, combined with mutational studies on the APP JM/ TM region, using a bacterial membrane system, showed that the GxxxG motifs can mediate TM helix homodimerization in lipid bilayers (Munter et al. 2007). Other studies forced APP dimerization artificially, either by fusing APP to FKBP-domains that dimerized rapidly upon addition of a synthetic drug (Eggert et al. 2009), or via a constitutive disulfide bond upon cysteine introduction at the juxtamembrane region (Scheuermann et al. 2001). Recent studies were designed to dissect single domains involved in homo-and heterointeraction of APP and (Soba et al. 2005; Kaden et al. 2009), identifying the E1 domain of APP and APLPs to be essential for cellular *cis*-and *trans*-interactions (Soba et al. 2005; Kaden et al. 2009), Although many potential physiological functions of APP dimers have been proposed, the subcellular localization of their generation remains elusive. To address the compartment where APP dimerization might originate, we fused double-lysine retention motifs to the C-terminus of different APP isoforms (KKAA for endoplasmatic reticulum, ER; KKFF for the Golgi-compartment), inhibiting trafficking to the plasma membrane and retaining APP in intracellular compartments. It has been demonstrated that proteins harboring the KK*XX* sequences bind to specific recycling receptors in the membranes of these compartments and are selectively transported back to the ER (Teasdale and Jackson 1996; Norkin et al. 2002; Wang et al. 2002). In this study we clearly show that retention of APP695 in the ER induces formation of SDS-stable homodimers, which can be recovered from cell lysates and dissociate upon strong reducing conditions. Therefore, we propose that APP dimerization is initiated in the ER and sustained via intermolecular disulfide linkage, mediated by the cysteine-rich APP-E1 ectodomain. Additionally we demonstrate different dimerization properties of KPI- versus non-KPI-APP regarding both, *cis*-and *trans*-interactions. Finally we show that heterodimerization between APP and APLP1 is also initiated in the ER and that APP can retain APLP1 intracellularly, thus decreasing its surface expression.

4.1 Retention of APP in the ER leads to the formation of SDS-stable homodimers

Although many aspects of APP dimerization have been studied, the precise cellular localization of its generation remains unclear. In order to identify the cellular compartment where APP dimerization is initiated, we generated chimeric proteins using APP isoform 695, harboring C-terminal dilysine retention signals. Therefore, the APP695 wt cDNA was used as a template to add a C-terminal myc tag followed by either a -Lys-Lys-Ala-Ala (KKAA) or -Lys-Lys-Phe-Phe (KKFF) dilysine motif – designated as APP ER or APP Golgi, illustrated in Figure 8A. All APP constructs were subcloned into the retroviral expression vector pLBCX, containing a blasticidin resistance gene for selection in eukaryotic cells, the correctness of the constructs was verified by sequencing. It has been reported previously that the sequence context of the dilysine signals designates the efficiency of ER retention, acting as an ER exit determinant, which was shown for CD4-receptor chimeras fused to either retention motif (Andersson et al. 1999). In this case, the KKAA chimeras were strictly localized to the ER, unlike KKFF constructs which had access to post-ER compartments, such as the *cis*-Golgi (Pelham 1989; Teasdale et al. 1996; Andersson et al. 1999). As a first step to analyze APP dimerization, depending on its cellular destination, mass cultures of CHO-K1 cells, stably overexpressing the respective APP695 retention or APP695 wt constructs (Fig. 8B) were generated, using a viral transduction system. After selecting the stable clones with 6µg/ml of blasticidin for two weeks, the expression levels of mass cultures was tested via SDS-PAGE and western blot analysis (Fig. 8B). APP constructs were detected using the monoclonal 9E10 antibody, specifically recognizing the attached myc epitope, thus it was possible to discriminate between endogenous APP and solely overexpressed retention constructs in our cell lines. Indeed, stable CHO-K1 cell cultures displayed comparable expression ratios of the respective APP trafficking mutants. Surprisingly, in the lysate controls we detected two bands for the APP695 ER construct (Fig. 8B, left panel), migrating at ~110 kDa and ~220 kDa. The faster migrating band (~110 kDa) represents immature APP (before *cis*-Golgi-specific carbohydrate modifications), which is in accordance with a permanent ER retention. Furthermore the intracellular retention of APP KKXX chimeras was confirmed by the absence of C-terminal fragments (CTFs), since they are generated later in the secretory pathway, whereas only wt APP revealed CTFs. Most interestingly, the explicit slower migrating band detected for APP695 ER, co-migrated at the apparent molecular weight of a putative APP dimer, as expected around ~220 kDa. In contrast, APP Golgi (containing the "leaky" KKFF motif) did not display a higher molecular weight band around 220 kDa, compared to APP ER. However, APP695 wt migrated as a set of two bands with the slower form (~130 kDa) representing the mature protein that has undergone complex *O*-glycosylation in the *medial-late*-Golgi compartment and the faster migrating form at ~110 kDa indicating immature, mostly ER glycosylated APP. In our experimental conditions we treated all lysate samples with loading buffer, containing SDS (2% v/v final concentration in sample) and β-mercaptoethanol (BME, 5% v/v final concentration in sample) prior to electrophoresis, but most importantly, the samples were not heat denatured at the same time (Fig. 8B, left panel, + BME/-95°C). Consequently, the high molecular weight band that we detected for APP695 ER was highly resistant to SDS treatment, which suggested that stronger interactions than hydrophobic associations of two APP molecules must be

involved, such as intermolecular covalent disulfide bonds. To cleave putative disulfides, potentially linking APP monomers, the same lysates were treated with the reducing agent BME and heat-denatured at 95°C, prior to SDS-PAGE, indeed resulting in the disappearance of the upper band around ~220 kDa (Fig. 8B, right blot).

Figure 8

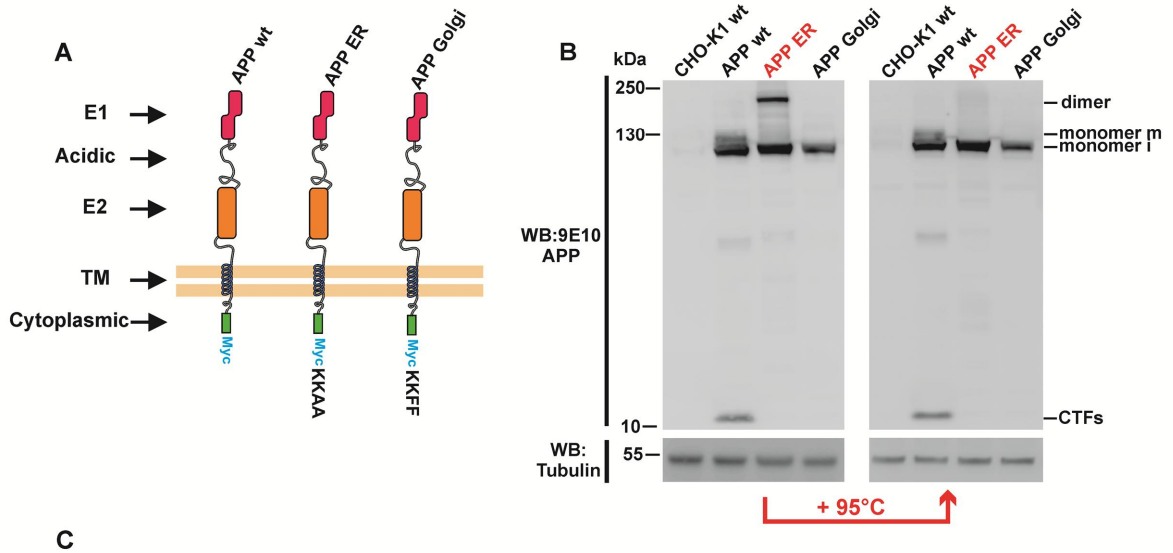

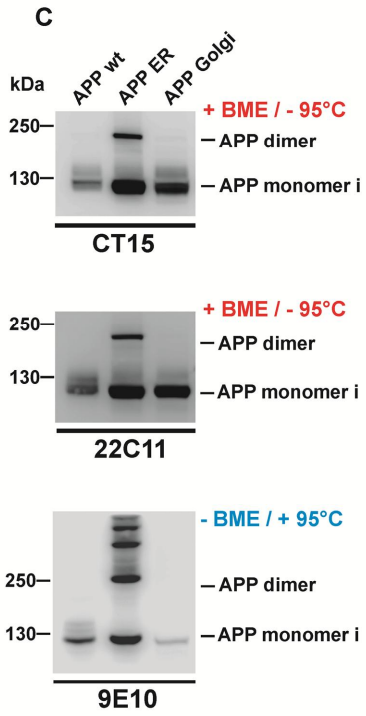

Fig. 8: Retention of APP in the ER by addition of a dilysine -KKAA- motif leads to the formation of SDS-stable homodimers

(A) Schematic illustration of the APP domain structure and the used dilysine retention constructs. APP isoform 695 (APP695) was fused to a C-terminal myc-tag, followed by either a KKAA ER retention motif, or a "leaky" KKFF motif allowing trafficking to the *cis*-Golgi compartment, designated as APP ER or APP Golgi, respectively. The E1 domain, acidic domain, E2 domain, transmembrane domain (TM), and the intracellular domain are indicated. **(B)** CHO-K1 cells stably overexpressing either APP695 wt or the dilysine retention constructs were analyzed by SDS-PAGE and western blot analysis. As negative control CHO-K1 cells were transfected with empty vector, indicated as mock. 20 µg of cell lysates were mixed with sample buffer containing β-mercaptoethanol and either directly seperated on a 4-12% SDS gel (left blot), or 5 min heat denatured at 95°C, prior to electrophoresis (right blot). APP was probed with 9E10 antibody and α-Tubulin antibody served as a loading control. Note that the explicit upper band (dimer), migrating at ~220 kDa, was disrupted after heat denaturing at 95°C. The absence of C-terminal fragments (CTFs), and fully glycosylated APP indicates intracellular retention. **(C)** The same lysates as under (B) were analyzed again on SDS-PAGE (20 µg), using either the same conditions (+BME/-95°C), or without β-mercaptoethanol (-BME/+95°C). Blots were incubated either with polyclonal CT15, raised against the last 15 aa of APP, or the monoclonal antibody 22C11, detecting the very N-terminus of APP. The bottom blot was incubated with monoclonal 9E10 antibody, after the samples were heat denatured without addition of reducing agents. Note that appilcation of high temperatures without BME does not disrupt APP dimers, even higher oligomers appear. APPfl m/i: mature (glycosylated) and immature species of full-length APP.

These observations implicated that retention of APP695 in the ER lumen might be sufficient to induce S-S bridged intermolecular homodimers between some of the 12 cysteine residues, exclusively located in the E1 ectodomain, of APP695. In fact, the ER provides a sufficiently oxidizing environment for disulfide formation as well as an enzyme, *protein disulfide isomerase* (PDI), to promote the

formation of disulfide bonds (Hatahet et al. 2009). Interestingly, APP Golgi did not reveal a high molecular weight-band, even though it migrated predominantly as a single band around ~110 kDa, representing immature APP, indicating that trafficking beyond ER compartments does not strictly promote APP dimerization.To confirm the specificity of the slower migrating band, representing a putative APP homodimer, we used the same lysates of CHO cells overexpressing APP retention mutants and applied two additional antibodies, reacting either with the N-or C-terminal epitope of APP (Fig. 8C). Correspondingly, we employed either polyclonal antibody CT15, raised against the last 15 C-terminal amino acids of APP, or the monoclonal 22C11 antibody, recognizing the very N-terminus of APP. Indeed, we were able to detect the APP homodimer for the ER retention mutant with a C-terminal and N-terminal-directed antibody, respectively (Fig. 8C). Subsequently we reversed the experimental conditions and heat denatured lysate samples, without adding BME to the SDS-sample buffer. After separating the proteins on SDS-PAGE, we applied the 9E10 antibody to detect solely overexpressed APP (Fig. 8C, bottom blot). Interestingly we found even higher molecular weight bands for APP ER, migrating slower than the APP dimer, probably representing APP multimers. So far, these results provide evidence that APP dimerization is driven by covalent cysteine bonds, supposably generated by oxidation in the ER.

4.2 Retention of APP within early secretory compartments inhibits its trafficking to the cell surface and limits its metabolism

To further assess the intracellular retention of the APP KK*XX* chimeras and to ensure that only APP wt was capable of reaching the cell surface, we performed cell surface biotinylation experiments (Fig. 9A). Additionally, we transiently co-expressed a dominant negative mutant of Adapter Protein 180 (AP180 D/N) (Fig. 9A) in APP695 wt cells to retain APP at the plasmamembrane, thus increasing its surface expression. This dominant-negative form of AP180 has been shown to inhibit the uptake of epidermal growth factor and transferrin through disrupting the formation of clathrin-coated pits (Kusano et al. 2001; Kolset et al. 2002). Because it has been recently proposed that APP can form heparin induced dimers at the cell surface (Gralle et al. 2006), we aimed to include the plasmamembrane as a putative source of dimerization by exposing APP prolonged at the cell surface. Consequently, clathrin-mediated endocytosis was selectively blocked by overexpressing a D/N AP180 construct (65 kDa) (Zhao et al. 2001), whereby efficient transient transfection of AP180 D/N into the CHO cells was confirmed by western blot analysis using a 9E10 antibody against the myc tag on the C-terminus of the protein (Fig. 9A, left blot, lane four). To label surface proteins, confluent monolayers of CHO cells, overexpressing the APP wt or retention constructs were incubated with a cleavable biotinylation reagent (Sulfo-NHS-SS-Biotin), reacting with exposed primary amines of proteins on the surface of adherent cells. Treated cells were then harvested, lysed, and the labeled surface proteins were purified using Neutravidin agarose beads, which selectively captured biotin. Since the biotinylation only represents surface bound proteins, no APP full length for either APP Golgi- or APP ER retention mutant was detected at the surface, confirming intracellular retention by the double-lysine motifs (Fig. 9A, right blot). However, solely the fully mature form of APP wt appeared at the plasma membrane (APPfl mature), indicating that it has undergone Golgi-specific carbohydrate

modifications, thus verifying its passage through the secretory route. However, the coexpression of AP180 D/N led to a strong increase in surface exposed mature APP, as well as in the lysate controls, due to inhibited endocytosis (Fig. 9A, right blot, lane four).

Figure 9

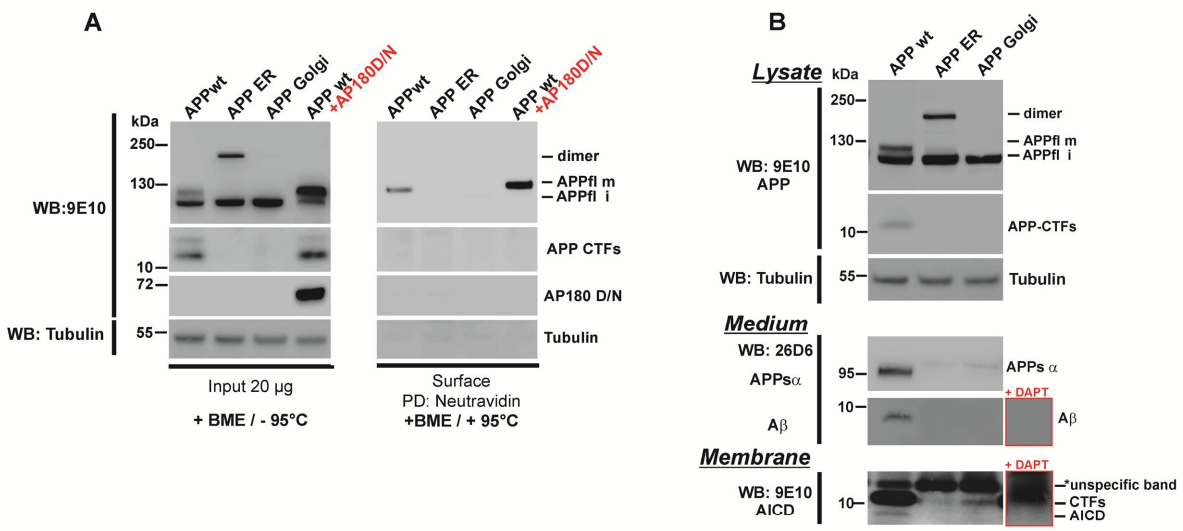

Fig.9: Retention of APP within early secretory compartments inhibits trafficking to the cell surface and limits its metabolism

(A) CHO-K1 cells stably overexpressing the respective APP695 wt or APP695 retention constructs were subjected to cell surface biotinylation. To inhibit endocytosis from the cell surface, AP180 D/N (lane four) was transiently coexpressed. Cell surface proteins were labeled with sulfo-NHS-biotin prior to lysis. Biotinylated samples were precipitated with neutravidin agarose beads and analysed by SDS-PAGE and western blot (PD: neutravidin; right panel). 20 µg of total cell lysates were used as input controls (Input; left panel). APP full length, CTFs and AP180 D/N were probed with 9E10 antibody. α-Tubulin antibody served as a loading control and to verify the absence of endomembrane contaminants in the biotinylation. For the input control, all samples were treated with SDS sample loading buffer, containing β-mercaptoethanol (BME) without heat denaturing, prior to SDS gel electrophoresis. To elute surface proteins from neutravidin beads, samples were denatured for 5 min at 95°C with BME, and separated on 4-12% SDS gels. Note that APP ER migrates as two distinct bands in lysate controls, with the slower migrating band (~220 kDa) likely representing an SDS stable homodimer. APP ER and APP Golgi are completely absent from the cell surface, confirming intracellular retention, whereas AP180 D/N selectively increases mature APP at the surface. **(B)** APP metabolism is severly limited upon ER retention. APP cleavage products are monitored in CHO-K1 cells, stably overexpressing the respective APP constructs by western blot analysis of total cell lysates, conditioned media, or crude membrane preparations. For detection of APP full-length and C-terminal fragments, equal amounts of cell lysates were separated by SDS gel electrophoresis and probed with monoclonal 9E10 antibody. Blots were reprobed with anti-Tubulin antibody as a loading control. For APPsα and Aβ, conditioned media was collected 24 h and adjusted to total protein content. Detection was carried out using the monoclonal antibody 26D6, recognizing the aa 1-12 of Aβ. AICD fragments were obtained after in vitro γ-secretase assay of crude membrane preparations in sodium citrate assay buffer at 37°C, to liberate AICD from membrane-bound stubs. As negative control, APP695 wt cells were incubated with 5 µM of γ-secretase inhibitor DAPT to prevent AICD- and Aβ generation. Fractions were separated on 16% BisTris gels, and western blots were incubated with monoclonal 9E10 antibody. Note that no CTFs, AICD, or Aβ were generated when APP was intracellulary retained.

Moreover, the absence of Tubulin in the biotinylation verified the lack of endomembrane contaminants, indicative of its cleanness. Considering the input controls (Fig. 9A, left blot), APP wt migrated as a set of two bands, as seen previously (compare Fig. 8B), whereas APP ER migrated as one band, revealing that lack of the slower migrating, i.e. upper band, was due to the altered glycosylation pattern caused by ER retention of APP KKAA. However, consistently with previous results (compare Fig. 8B) a slower migrating band was detected for APP ER in lysate controls (Fig 9A, left panel), most likely generated in the ER. However, for APP Golgi no dimer band appeared although it displayed a similar glycosylation pattern to that of the APP ER construct, resulting in

exclusive immature APP. This indicated that the KKFF motif (Golgi) provided indeed some leakiness, resulting in ER-exit of APP and transport to the *cis*-Golgi compartment, whereas the absence of a complex *O*-glycosylation pattern suggested that the construct did not reach beyond *cis*-Golgi. This notion was supported by the absence of APP Golgi from the cell surface biotinylation. Although AP180 D/N led to a strong increase of mature APP at the cell surface, we did not detect a dimer band in our system. Thus, it cannot be excluded that dimerization properties differ between cellular compartments therefore weaker interactions could possibly keep up APP dimerization at the plasmamembrane. Furthermore we analyzed the levels of *secretase*-derived APP metabolites in cell lines, overexpressing the different constructs. Since it has been shown previously that ER retention of BACE-cleaved APP stubs (C99) led to a dramatic decreased secretion of Aβ and APPsα/β into the culture medium (Wang et al. 2001), we were interested whether we observe the same for the full length protein. To do so, we subjected nearly confluent cultures of CHO cells, stably overexpressing APP wt or the respective retention chimeras, to a crude membrane preparation, followed by an in vitro-γ-*secretase* assay to facilitate generation of APP intracellular domain i.e. AICD (Fig. 9B, membrane). In parallel, the conditioned medium was collected over 24 hours and analyzed for the generation of secreted, soluble fragments i.e. Aβ and APPsα (Fig. 9B, medium). Finally, the corresponding cells were harvested and lysed, to adjust the media samples to total protein content (Figure 9B, lysate). As negative control, APP695 wt cells were incubated with 5 µM of γ-*secretase* inhibitor DAPT (N-[N-(3,5-difluorophenacetyl)-L-alanyl]-S-phenylglycine-t-butyl-ester) to prevent APP cleavage by γ-*secretase* complex, thus precluding AICD- and Aβ-formation. In agreement with our previous results, CTFs were only generated from cells expressing APP wt, as seen in lysate controls and membrane preparations. Accordingly, AICD was not produced in APP ER- or APP Golgi expressing cells, since CTFs constitute a direct substrate for intramembranous γ-*secretase* cleavage. However, regarding the membrane preparation and in vitro γ-*secretase* assay (Fig. 9B, bottom panel), a minor amount of CTFs was generated from APP Golgi cells, revealing that APP processing by α- or β-*secretase* occurs downstream of the ER, e.g. α-*secretase* has been shown to be most active at the cell surface (Parvathy et al. 1999). Nevertheless, generated CTFs for APP Golgi were below detection limit to visualize them in regular lysate controls (Fig. 9B, top part), whereas the membrane preparation selectively increased CTF fragments in an accumulative fashion, enabling visualization of minimal amounts under these circumstances. Moreover, we observed a strong decline in shedded fragments for both APP retention constructs, compared to APP wt (Fig. 9B, medium). In fact, Aβ or APPsα fragments were almost undetectable in media samples from cells expressing APP ER or APP Golgi, using the monoclonal antibody 26D6, which reacts with the ectodomain of APP (aa 1-12 of Aβ). However, minimal levels of APPsα in cells expressing the retention constructs were due to endogenous APP751, marginally expressed in CHO-K1 cells which were also recognized by antibody 26D6. In conclusion, retention of APP within early secretory compartments prevented it from being processed by *secretases,* thereby precluding the formation of catabolites, such as Aβ, AICD and APPs). Furthermore, these results indicate that APP dimerization occurs before *secretase* cleavage and full maturation, shown by the absence of fully glycosylated APP (Fig. 9A and B, lysate).

4.3 APP dimer formation is promoted by oxidizing conditions and not caused by post-lysis aggregation or the KKAA retention motif

To verify that the formation of APP dimers is not somewhat influenced by the C-terminal KKAA-motif, we employed another established transmembrane protein, the well-characterized C-terminal part of LRP1 (Low density lipoprotein receptor related Protein 1), described previously (Pietrzik et al. 2002; Waldron et al. 2008). The C-terminal part was used, due to the molecular weight of LRP1 as a 600-kDa receptor, which makes it very difficult to transfect cell cultures with a construct of that size. We therefore employed a truncated version (described in Pietrzik et al. 2002) and analyzed whether the addition of a KKAA motif to the C-terminal part of LRP1 was sufficient to trigger dimerization, reminiscent of APP. Native CHO-K1 cells were transiently transfected with myc-tagged constructs encoding either the wt LRP-CT, or LRP-CT KKAA, designated as LRP-CT ER (see schematic representation Fig. 10B).

Figure 10

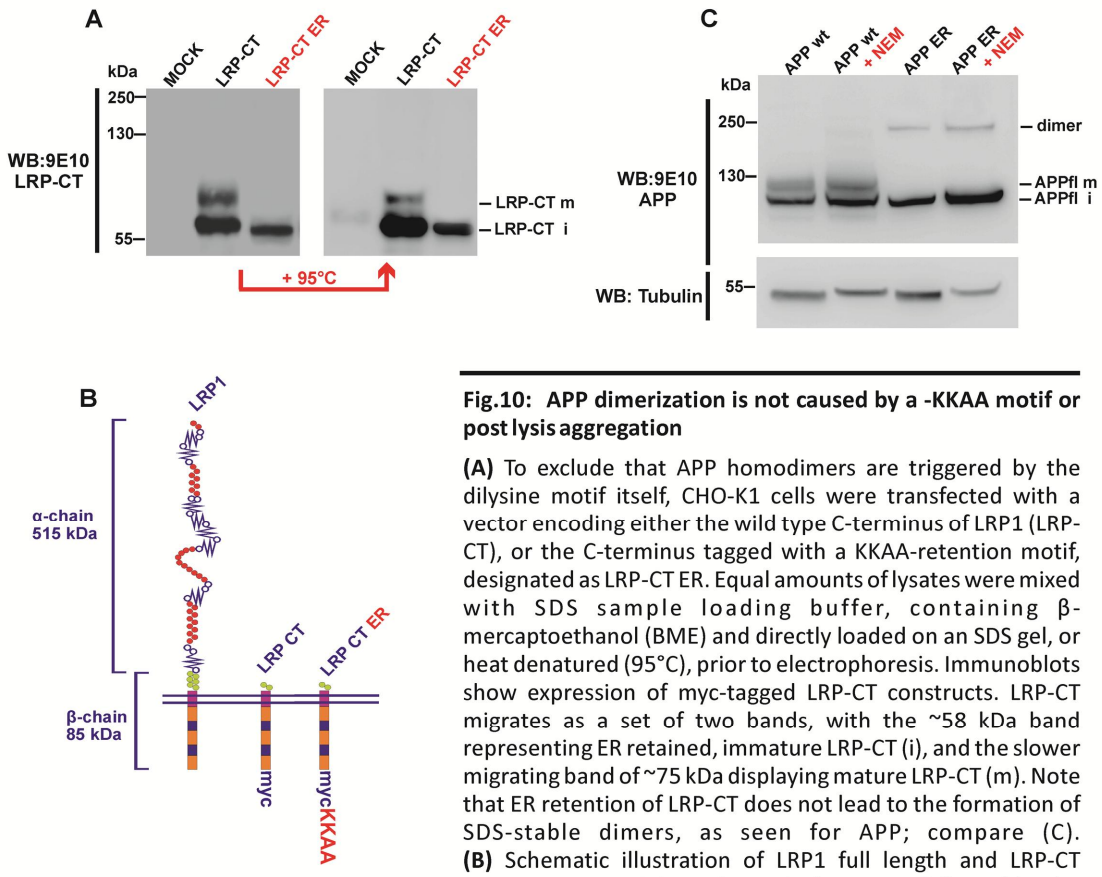

Fig.10: APP dimerization is not caused by a -KKAA motif or post lysis aggregation

(A) To exclude that APP homodimers are triggered by the dilysine motif itself, CHO-K1 cells were transfected with a vector encoding either the wild type C-terminus of LRP1 (LRP-CT), or the C-terminus tagged with a KKAA-retention motif, designated as LRP-CT ER. Equal amounts of lysates were mixed with SDS sample loading buffer, containing β-mercaptoethanol (BME) and directly loaded on an SDS gel, or heat denatured (95°C), prior to electrophoresis. Immunoblots show expression of myc-tagged LRP-CT constructs. LRP-CT migrates as a set of two bands, with the ~58 kDa band representing ER retained, immature LRP-CT (i), and the slower migrating band of ~75 kDa displaying mature LRP-CT (m). Note that ER retention of LRP-CT does not lead to the formation of SDS-stable dimers, as seen for APP; compare (C). **(B)** Schematic illustration of LRP1 full length and LRP-CT constructs, containing a C-terminal myc tag, followed by the dilysine ER retention motif -KKAA. **(C)** CHO-K1 cells stably overexpressing APP695 wt or APP695 ER retention construct were lysed in NP40 buffer, containing 40 mM *N*-Ethylmaleimide (NEM) to prevent sulfhydryls (i.e., reduced cysteines) from post lysis disulfide bond formation. For control, cells were lysed in regular NP40 buffer containing ethanol as vehicle. 20 µg of cell lysates were treated with SDS sample loading buffer, containing BME without heat denaturing, prior to SDS-PAGE and western blot analysis. APP was probed with 9E10 antibody and α-Tubulin antibody served as a loading control. Note that APP dimerization is not due to post lysis aggregation, since the upper band (~220 kDa) does not disappear upon NEM treatment.

As expected, the LRP-CT construct migrated as a set of two bands, with the faster migrating band around ~57 kDa, representing the unglycosylated form and the slower migrating band around ~75 kDa, reflecting maturation, typical for ER to Golgi transport (Malo et al. 2000). LRP-CT ER however migrated exclusively as one band at ~57 kDa, indicating that it is retained as an immature glycoprotein on intracellular membranes (ER), comparable to APP (e.g. see Fig. 9A). Nevertheless, immunoblotting with 9E10 antibody did not reveal a distinct higher molecular weight band as previously seen for APP ER (compare Figs 8 and 9), expectedly co-migrating ~110 kDa in the case of LRP-CT ER, despite samples were treated virtually as APP ER samples before. This outcome so far corroborated that not the KKAA motif per se is responsible for dimerization, rather than the protein it is attached to. Correspondingly, APP dimerization is likely triggered by disulfide bond formation due to its contact with a sufficient oxidative milieu, provided by the ER. Next we set out to verify that APP dimerization was not caused by spontaneous post-lysis aggregation between APP molecules, but generated between molecules while inserted within the same membranous compartment, also designated as *cis*-dimerization (Soba et al. 2005). In order to prevent putative post lysis disulfide formation between APP molecules we applied N-ethylmaleimide (NEM), an alkene that reacts irreversibly and permanently with thiols (i.e. reduced cysteines) to block further rearrangement of disulfide bonds, preferably in the pH range of 6.5-7.5 (Akabas et al. 1992). Therefore, the PBS (pH 7.4) and the NP-40 cell lysis buffer (pH 7.4) were supplemented with 40 mM of the alkylating agent NEM to block free sulfhydryl groups, thus preventing folding intermediates or unspecific oxidation of APP molecules during cell harvesting and lysis procedure. Indeed, we observed no difference in dimer formation for APP ER when cells were lysed in NP-40 containing 40 mM NEM or vehicle (ethanol) only (Fig. 10C). Consequently, the high molecular weight band around ~220 kDa did not disappear, indicating that dimers were generated prior to lysis. Taken together, these results implied that disulfide pairing between APP molecules was originated in the ER during the folding process, likely catalyzed by *protein disulfide isomerase (PDI)* in an oxidizing surrounding (Hatahet et al 2009).

4.4 The high molecular weight band represents APP homodimers with differential tagged APP variants

Having established that APP homodimers are not generated via unspecific disulfide arrangement during cell lysis, we next set out to ascertain that the ~220 kDa band indeed represented an APP homodimer and not any heterodimer of APP with another protein of the same putative molecular mass. Therefore we generated an additional APP695 construct with a C-terminal HA tag and co-expressed APP695 HA wt or its ER retained counterpart (APP695 HA ER) in CHO cells, stably overexpressing APP695 myc ER (Fig. 11). The overexpressed APP-myc and APP-HA fusion proteins were probed with mouse anti-myc or rat anti-HA primary antibody vice versa on different immunoblots. In fact, we confirmed that the high molecular weight band represents APP homodimers, since western blots with either myc-or HA-antibody independently revealed a band at ~220 kDa in cells co-expressing HA-tagged and myc-tagged APP species. Individually, the APP HA and APP myc proteins migrate as distinct and separable bands under either reducing or non-reducing conditions (Fig. 11). However, in the presence of reducing and denaturing conditions (+95°C) dimers

were converted to monomers, which increased simultaneously (Fig. 11, right blots). Moreover, co-transfection of APP HA wt into cells, already expressing APP myc ER, revealed a slightly weaker band around ~220 kDa with HA antibody (Fig. 11 bottom blot, third lane), additional to the doublet representing both maturation states of APP. This band most likely represented a dimer composed of APP myc ER and APP HA wt, suggesting that APP695 ER could retain a portion of wt APP within the ER, due to homodimer formation. The simplest interpretation of our approach is that these high molecular weight bands represent APP myc/APP HA "heterodimers", indicating that APP forms homodimers within the same cellular compartment (*cis*-dimers). Finally, these findings also minimized the possibility that APP happens to "heterodimerize" with any other unrelated protein of the same molecular weight.

Figure 11

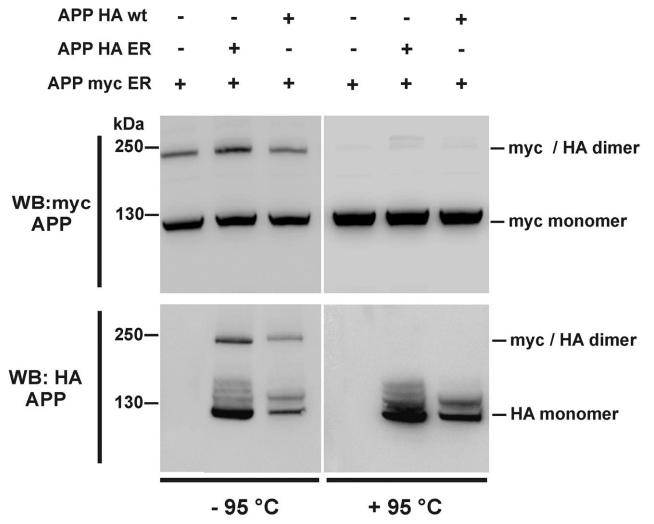

Fig.11: Specificity of APP homodimerization using myc-and HA-tagged APP variants

CHO-K1 cells stably overexpressing myc-tagged APP695 ER, were transiently co-transfected with HA-tagged APP constructs, APP695 HA ER or APP 695 HA wt. Immunoblotting with myc or HA antibody revealed dimers (~220 kDa myc-/HA-APP) under non-reducing conditions, when separated on 4–12% acrylamide gradient gels. In the presence of β-mercaptoethnol (BME) and 95°C APP dimers were converted to monomers, which increase at the same time (myc-monomers). Note that dimers were detected with both antibodies independently, whereas myc dimers increased upon APP HA ER co-expression (top blot, second lane). Additionally, a weaker dimer band appeared when APP HA wt was coexpressed in APP myc ER cells (bottom blot, third lane), indicating that APP myc ER retained a portion of APP HA wt in the ER, leading to the formation of APP myc and APP HA „heterodimers".

4.5 APP dimers are highly stable, but sensitive to strong reducing and denaturing conditions

Our previous results demonstrated that APP dimers disappeared when cell lysates of APP ER expressing cells were supplemented with β-mercaptoethanol (BME), followed by heat denaturing at 95°C (see Fig. 8B and 11). Next we questioned, up to which temperature these dimers remain stable under the application of BME. To establish a temperature curve, equal amounts of lysates from APP ER overexpressing cells were mixed with identical amounts of BME-containing SDS sample buffer (BME 5% v/v final conc. in samples).

Figure 12

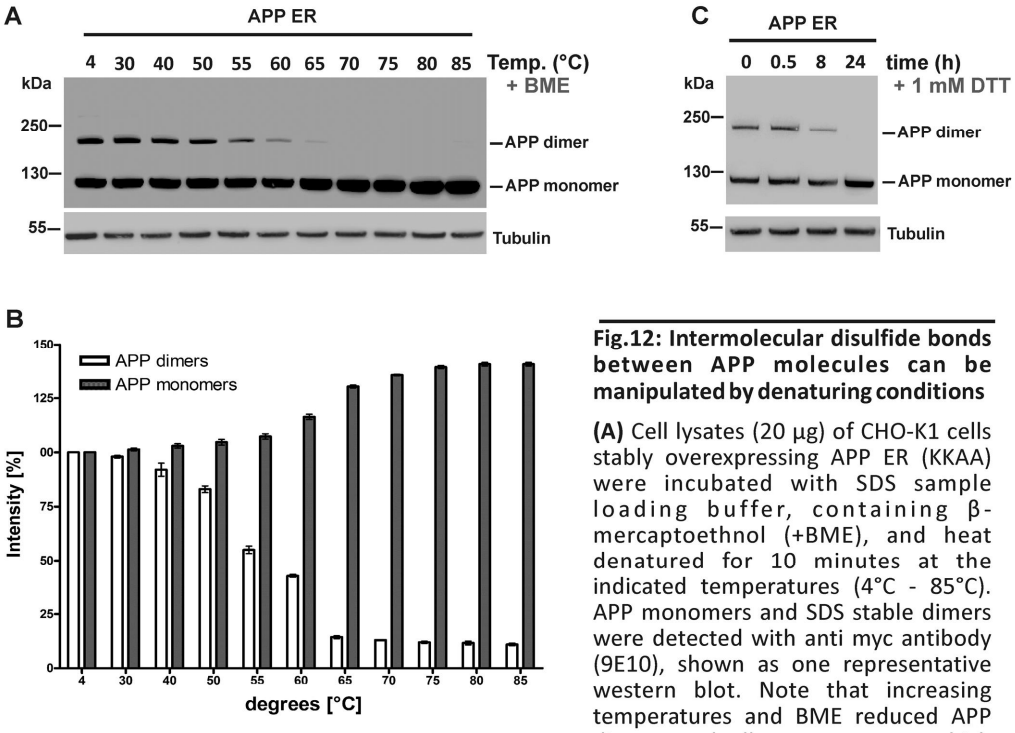

Fig.12: Intermolecular disulfide bonds between APP molecules can be manipulated by denaturing conditions

(A) Cell lysates (20 µg) of CHO-K1 cells stably overexpressing APP ER (KKAA) were incubated with SDS sample loading buffer, containing β-mercaptoethnol (+BME), and heat denatured for 10 minutes at the indicated temperatures (4°C - 85°C). APP monomers and SDS stable dimers were detected with anti myc antibody (9E10), shown as one representative western blot. Note that increasing temperatures and BME reduced APP dimers gradually to monomers, which increased vice versa. **(B)** APP dimers and monomers were quantified by densitometric analysis of western blots, as the one representative shown in (A). In each case, intensities at 4°C were set as 100 %. Diagram shows relative intensity (%) of APP monomers and dimers, plottet against different temperatures. Data are ($n \geq 3$) ± SEM, one way ANOVA. APP monomers gradually increased by 50% with declining dimers, vice versa. **(C)** Cultures of CHO-K1 cells stably expressing APP ER were treated with 1 mM of the reducing agent dithiotreitol (DTT) for the indicated time (0h -24h), to prevent interchain disulfide bonds between newly synthesized APP molecules. Note that 24h of DTT exposure precluded APP dimer formation, indicating that reducing conditions interfered with arrangement of disulfide bonds between APP molecules.

Subsequently, the samples were heated for 10 minutes at the indicated temperatures (4°C-85°C), prior to electrophoresis on a 4-12% SDS gel (Fig. 12A). Immunoblotting with 9E10 antibody revealed that dimers persisted up to 50°C, whereas higher temperatures led to a severe drop, and temperatures over 60°C dissolved dimers completely. Quantification of immunoblots clearly showed a corresponding increase of ~50% in monomers (Fig. 12B). These results indicated that under standard detergent lysis conditions, interchain APP dimers remain stably associated. However, full reduction was achieved when the samples were boiled to denature the protein, hence, APP migrated

exclusively as monomers (compare Fig. 8A). In addition, we analyzed whether it was possible to reduce newly synthesized APP dimers, or to prevent the formation of new homodimers in the ER of living cells. Therefore, we added a final concentration of 1 mM of dithithreitol (DTT) to the growth medium of cultures expressing APP ER and incubated them up to 24 h at 37°C (Fig. 12C). Subsequently, cells were lysed in NP-40 buffer, containing 40 mM NEM (preventing putative post lysis disulfide arrangement) and equal aliquots were supplemented with SDS loading buffer (containing BME). Analysis of non-heated samples by SDS-PAGE and immunoblotting with 9E10 antibody showed that more than 8 h of 1 mM DTT exposure was needed to reduce APP dimers in the ER, whereas 24 h treatment resulted in efficient reduction of oxidized APP dimers, and prevented further generation of newly synthesized dimers. At the same time, an increase in immature APP monomers was monitored (Fig. 12C, 24 h), thus indicating that intermolecular disulfide bonds once generated, remain stable for a long time, and are not sensitive to moderate concentrations of reducing agent DTT (Kochhar et al. 1992). Interestingly, DTT treatment between 8h and 24h prevented the formation of new APP *cis*-dimers, but did not inhibit synthesis of APP molecules itself (revealed by increased monomers). This is in line with previously published data that DTT (up to 5 mM) does not affect translation, translocation, or glycosylation of newly synthesized proteins in the secretory pathway (Lodish and Kong 1993). Taken together, the aforementioned results demonstrated that reducing agents, either added to the culture medium of living cells (i.e. DTT), or boiling lysates in the presence of BME, can manipulate the monomer-dimer equilibrium of APP. Nevertheless, DTT treatment mainly prevented formation of disulfides in newly synthesized proteins within the ER (Lodish and Kong 1993), instead of reducing preexisting APP dimers. Therefore the effect of DTT became visible after an extended incubation time (24 h).

4.6 Dimer formation of wildtype APP695 without a C-terminal KKAA motif can be induced by inhibition of ER export with Brefeldin A

Our next objective was, to find out whether it is possible to induce the dimerization of unmodified wildtype APP695 (APP695 wt) without adding a C-terminal retention signal. To test this, we chose brefeldin A (BFA), a fungal macrocyclic lactone antibiotic, inhibiting protein secretion at an early step in the secretory pathway (Pelham 1991). It has been shown that BFA leads to rapid redistribution of the Golgi apparatus into the ER, inhibiting the anterograde movement of membrane traffic beyond the mixed ER/Golgi system, thereby retaining secretory and membrane proteins in the ER (Lippincott-Schwartz et al. 1989; Klausner et al. 1992). Cell cultures, overexpressing APP ER or APP wt were treated with 5 µg/ml BFA for different time periods (0h-8h) at 37°C, to block ER export. Subsequently cells were harvested, lysed and separated on a non-reducing SDS-PAGE, followed by immunoblotting with APP specific polyclonal antibody CT15. Indeed, we found that addition of BFA to cell cultures caused the dimerization of APP wildtype (unmodified APP), already visible after 1 h treatment (Fig. 13A, longer exposure and Fig. 13B), with further increase after 8 h drug treatment. Moreover, the difference between mature and immature APP becomes indistinct, indicating the accumulation of immature APP was due to reduced membrane traffic out of the ER. In fact, we found the same effect for already pre-existing dimers of the KKAA mutant (APP ER), revealing a two-fold

increased stability after 1h of BFA treatment (Fig. 13A and B). However, the increase in monomers for APP ER was due to the employed antibody (CT15), recognizing the last fifteen amino acids of APP, thereby also detecting the fraction of endogenous APP from CHO cells. The above results already suggested that APP dimerization can be elevated when ER exit was further inhibited by the application of BFA. Since we have used only one concentration of BFA (5 µg/ml) over different time points, we were now interested if higher concentrations of the drug necessarily result in intensified dimer formation.

Figure 13

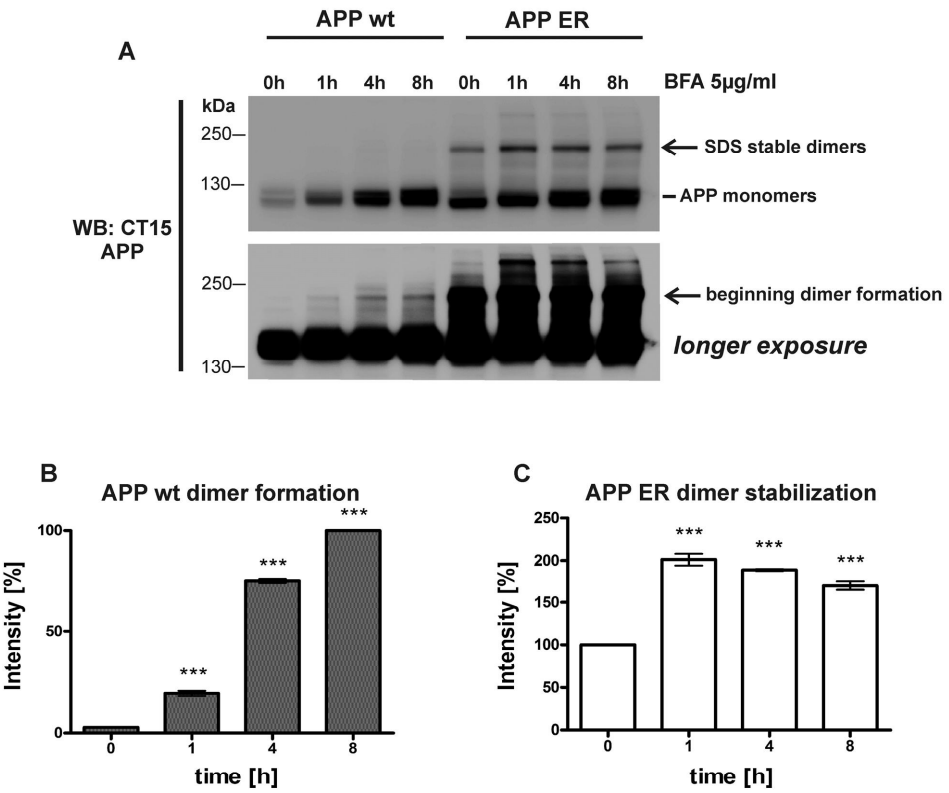

Fig.13: Homodimerization of APP wt can be visualized by inhibition of ER export with brefeldin A

(A) CHO-K1 cells stably overexpressing either APP695 wt or APP695 fused to the ER retention motif KKAA (APP695 ER) were treated with 5µg/ml brefeldin A (BFA) for the indicated time points (0h – 8h). Aliquots of cell lysates were mixed with SDS sample buffer, without heat denaturing the samples, priot to gel electrophoresis. APP was detected with C-terminal APP antibody CT15, shown on one representative western blot. The bottom panel shows a longer exposure time, indicating dimer formation of APP695 wt when export of the ER is blocked by the BFA. **(B)** Diagram shows the ratio of APP wt dimer formation during BFA treatment, plotted against time, with ±SEM of three independent experiments, statistical significance: ***p<0.001, one way ANOVA. **(C)** Diagram depicts increasing stabilization of APP ER preexisting dimers during BFA treatment, plotted against time. Data represent ±SEM (n≥3), statistical significance: ***p<0.001, one way ANOVA.

Therefore, cell cultures overexpressing APP ER were treated with increasing concentrations of BFA (10-, 20-, 30 µg/ml) or vehicle only (ethanol) for one hour, because the effect was already visible after that time point (compare Fig. 13A and B). This time, 9E10 antibody was applied to visualize exclusively overexpressed APP. Immunoblotting of lysates revealed an inverted monomer/dimer equilibrium (Fig. 14A-C) with a ~50% decline in monomers, accompanied by a ~two-fold increase in dimers, consistent with our previous data (compare Fig. 13A and B). However, the reduction in

monomers was not seen before because endogenous APP levels likely obscured this effect (compare Fig. 13A), likewise detected by CT15 antibody. Nevertheless, this effect was highly reproducible and seemed not concentration dependent. Taken together, these results implicated that not all APP molecules retained in the ER, have necessarily transformed into a dimeric state so far. Thus, extended exposure of APP to an oxidative surrounding had a considerable influence on the monomer/dimer balance, favoring dimerization.

Figure 14

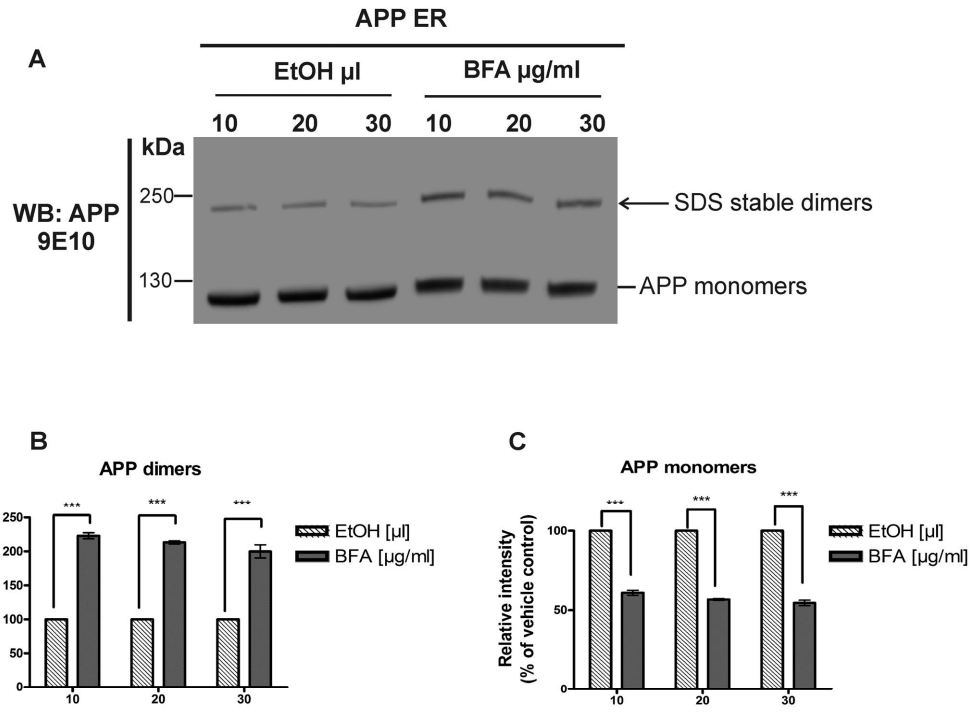

Fig. 14: APP monomer-dimer equilibrium is influenced in the ER

(A) Cell cultures of CHO-K1 overexpressing APP ER were treated for 1h with increasing concentrations (10-30 µg) of BFA, or with vehicle (100% ethanol) alone. Aliquots of cell lysates (20 µg) were mixed with SDS sample buffer, containing BME, without heat denaturing, and separated on a 4-12% SDS-PAGE. APP was detected with monoclonal 9E10 antibody, shown as one representative western blot. **(B**) Diagram shows relative increase of APP ER dimers with higher BFA concentrations, quantified as percentage over vehicle control. Data represent ±SEM as indicated (n≥3). Statistical significance: ***p<0.001, t-test. **(C)** Diagram shows simultaneous reduction of APP monomers with increasing BFA concentrations, depicted as percentage of vehicle control. Data represent ±SEM as indicated (n≥ 3). Statistical significance: ***p<0.001, t-test.

4.7 Overxpression of APP ER is not associated with increased ER stress

Finally we attempt to ensure that retention of APP within the ER does not cause abnormal ER stress. Since we selectively increased the amount of APP within the ER lumen, which otherwise would be destined for the secretory route, flux out of the ER is somewhat modified.

Figure 15

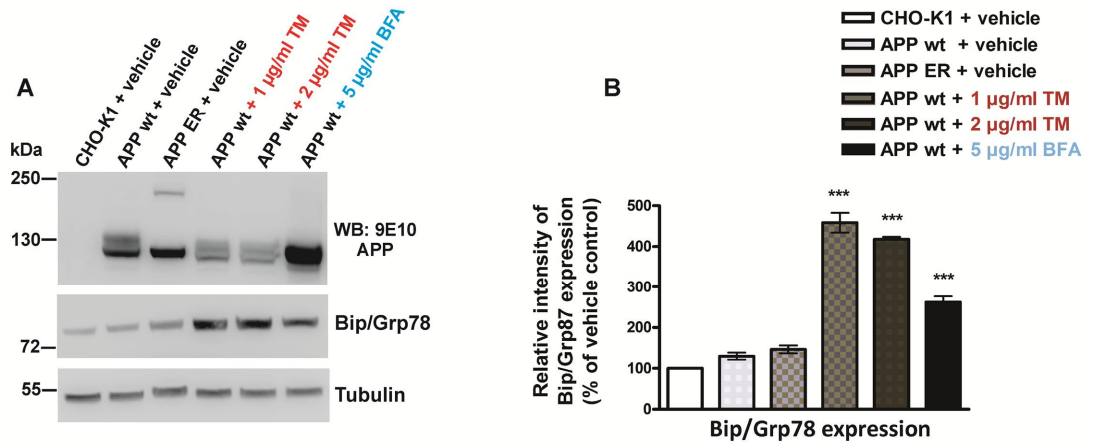

Fig.15: Overexpression of APP ER does not correlate with increased ER stress

(A) Analysis of BiP/Grp78 protein levels after induction of ER stress with tunicamycin and brefeldin A. Cell cultures overexpressing APP695 wt were treated for 12h with 1 and 2 µg/ml of tunicamycin (TM), or 5 µg/ml brefeldin A (BFA) and subjected to western blotting with an anti-BiP/Grp78 antibody. Tubulin served as a loading control. Control cultures were treated with vehicle (DMSO) for 12h. Note that exposure to tunicamycin and BFA strongly induced expression of the chaperone Bip/Grp78, as a biochemical marker for increased ER stress. Alternatively, Bip/Grp78 was insignificantly upregulated in cultures, expressing APP wt or APP ER, compared to vehicle treated CHO-K1 cells. **(B)** Diagram depicts quantification of Bip/Grp78, normalized to tubulin levels. Data represent ±SEM (n≥3), statistical significance: ***p<0.001, one way ANOVA.

It has been shown that accumulation of unfolded or malfolded proteins in the ER lumen, widely designated as “ER stress” (Schroder and Kaufman 2005; Wu and Kaufman 2006), triggers an adaptive stress response by the ER, termed the unfolded protein response (UPR). Several signaling pathways have evolved to detect the accumulation of misfolded proteins in the ER and activate a cellular response that attempts to maintain homeostasis and a normal flux of proteins in the ER. This ensures that only correctly folded proteins transit to the Golgi and unfolded or misfolded proteins are retained and subsequently degraded. Therefore, we investigated whether overexpression of APP ER is somewhat associated with alterations in ER stress-induced activation of one of the UPR target genes, such as the anti-apoptotic molecular chaperone Bip/Grp78 (Bertolotti et al. 2000; Bailey and O'Hare 2007). Based on that, we analyzed the expression level of Bip/Grp78 in our cell culture models, stably expressing either APP wt, or APP ER. As a baseline we used native CHO-K1 cells, not overexpressing any external protein. In order to obtain appropriate positive controls, ER stress was induced by exposure to tunicamycin (TM) and brefeldin A (BFA), control cells were treated with vehicle (DMSO). Tunicamycin is a nucleoside antibiotic that inhibits *N*-glycosylation in the luminal domains of proteins (Ling et al. 2009), whereas BFA blocks the translocation of proteins from the ER to the Golgi apparatus by causing disassembly of the Golgi complex (Lippincott-Schwartz et al. 1989),

resulting in up-regulation of certain target genes of the unfolded protein response (Schroder and Kaufman 2005; Wu and Kaufman 2006). Analysis of Bip/Grp78 expression after induction of ER stress was performed by Immunoblotting with a monoclonal anti Bip/Grp78 antibody (Fig. 15A). Treatment of APP wt cells with 1- or 2 µg/ml TM for 12 h significantly upregulated Bip/Grp78 levels, whereas a slightly weaker effect was observed when ER stress was induced with 5 µg/ml BFA for 12 h, compared to vehicle treated controls. However, only a minor increase in Bip/Grp78 was monitored in APP wt and APP ER expressing cells (Fig. 15A and B), not reaching statistical significance, when quantified and normalized to tubulin levels (Fig. 15B). This suggested that exogenous protein overexpression itself might stimulate the ER folding machinery, since all newly synthesized proteins must pass through the ER causing a temporary overload, varying slightly from basal conditions. Moreover, protein levels of APP after TM treatment showed a reduced glycosylation pattern, since it acts as an inhibitor of *N*-glycosylation. In BFA treated cells however, immature APP accumulated due to its intracellular retention, thus preventing terminal glycosylation.

4.8 Bimolecular Fluorescence Complementation technique with APP695 wt suggests APP dimerization in the ER

We demonstrated above that retention of APP695 in the ER, either by a C-terminal retention motif or by blocking its export using BFA, led to the formation of SDS stable homodimers (compare Figs. 8 and 13). To verify that APP dimerization occurred early in the secretory pathway, we aimed to use a different approach. Therefore, we applied a GFP (green fluorescent protein) tagging system for the intracellular detection of APP695, which is based on the auto-assembly capacity of two nonfluorescent portions of GFP, termed GFP 1-10 and GFP 11 (Cabantous and Waldo 2006). The smaller GFP fragment, GFP 11, comprises the last 15 amino acids and the larger fragment GFP 1-10, encompasses the first 214 N-terminal amino acids. The individual GFP portions are themselves inactive, but when brought together by the association of two interacting partner proteins, individually fused to the fragments, they restore a fully fluorescent GFP, termed Bimolecular Fluorescence Complementation (BiFC) (Kerppola 2006; Feinberg et al. 2008). This provides information on both, the interaction of APP-APP and its subcellular location under physiological conditions (Hu et al. 2005). Therefore the two complementary GFP fragments were separately fused to the C-termini of HA-APP695 (previously described in Soba et al. 2005) and coexpressed in neuroblastoma N2a cells (Fig. 16A), which was analyzed by confocal microscopy. The green fluorescence in cells co-expressing the spilt-GFP constructs clearly indicated an interaction between APP molecules under physiological conditions (APP BiFC). APP was distributed throughout punctate vesicular structures, possibly resembling Golgi or endosomal compartments. However, incubation with the antibody against ER marker Bip/Grp78 (Fig. 16A, red), showed the typical reticular structure of the ER (see magnified sections), whereas individual stainings and the merged picture, as well as detailed areas (insets), displayed a co-localization of APP dimers in the ER (overlay). In contrast, no specific GFP fluorescence was detected when single halves of GFP fused to APP (APP-GFP 1-10 and APP-GFP 11) were individually expressed in N2a cells (Fig. 16B). To rule out that the non-detectable GFP signals in the negative controls might result from no expression of transfected plasmids,

immunostainings of APP were performed, using an HA antibody (Fig. 16B, right part). The stainings clearly showed the presence of the APP fusion proteins, also confirming that the split GFP does not perturb the true APP localization in the cell, since expression patterns of negative controls (HA-APP) were comparable to those of APP BiFC in the positive controls (Fig. 16A).

Figure 16

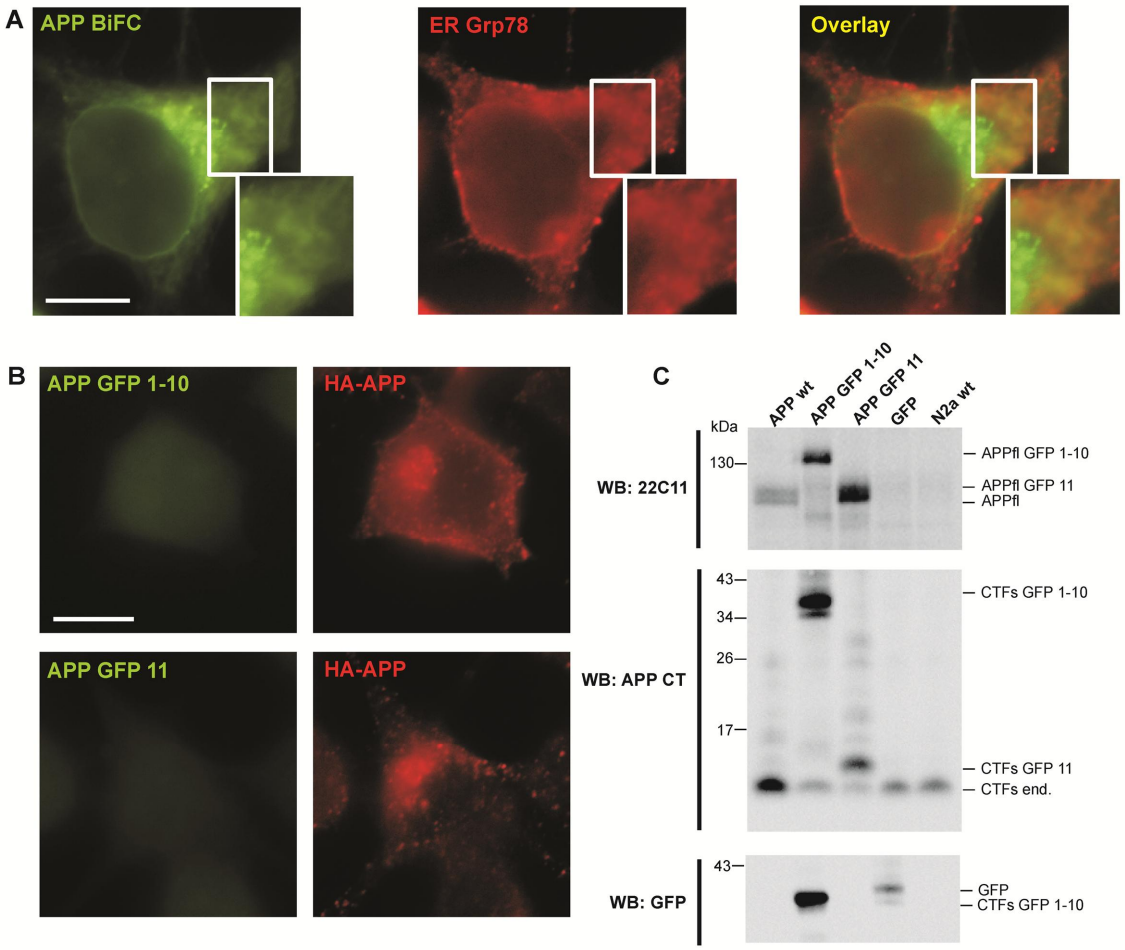

Fig. 16: APP wt homodimers are initially formed in the ER

(A) N2a cells were transiently co-transfected with NT HA APP695 CT Split GFP 1-10 and NT HA APP695 CT Split GFP 11. The cells were fixed with paraformaldehyde and immunostained with ER marker Grp78, followed by incubation with AlexaFlour594 conjugated secondary antibody. The green fluorescence is representing the APP dimer, induced by Bimolecular fluorescence complementation (BiFC). Co-staining with Grp78 revealed colocalization of the APP dimer (inset) with the ER. **(B)** Single transfections of N2a cells with either NT HA APP695 CT Split GFP 1-10 or NT HA APP695 CT Split GFP 11. APP expression was verified with HA antibody, confirming a non perturbed distribution (right panel, red). The green channel does not show any specific fluorescence. Scale bar is 10 µm. **(C)** N2a cells were transiently transfected with NT HA APP695 CT Split GFP 1-10, NT HA APP695 CT Split GFP 11 or GFP only. Cell lysates were analyzed via western blotting for APP full length (top part), APP CTFs (middle part) and GFP, or GFP containing CTFs (bottom part). Note that GFP antibody does not recognize GFP 11 alone. The experiment was performed by Simone Eggert (Laboratory of Prof. Stefan Kins, Kaiserslautern).

Additionally, the expression levels of the APP-GFP fusion proteins in the positive and negative controls were also confirmed by western blotting (Fig. 16C). Collectively, these data corroborated together with our data based on the ER retention signal that APP dimerization originates in the endoplasmic reticulum (ER) before its passage through the Golgi to the cell surface. Due to its rapid travel along the secretory pathway we observed the same outcome on SDS-PAGE, only when we

mediated APP retention in the ER (compare Figs. 8 and 13), because the amount of APP molecules exposed within the ER at a time is probably too less under physiological conditions to capture it on immunoblots. Taken together, these results provided further evidence in support of our hypothesis that APP dimerization initially sarts in the ER. However, it cannot be ruled out that dimers are also formed at later stages of the transport.

4.9 Stable APP695 homodimers are generated in the ER, but can also reach the cell surface

Having established that APP695 wt can form homodimers at an early stage in the secretory pathway, this does not tell us whether these dimers are associated by disulfide bonds or other interactions. We therefore wanted to show that disulfide bridged APP homodimers are in fact generated in the ER, but do also occur within the cell. The APP ER retention construct has proven as a reliable tool to visualize stable dimer formation in the ER, nevertheless since it does not traffic beyond ER, we cannot use this construct to show the existence of disulfide linked APP dimers in other cellular compartments, e.g. at the plasma membrane.

Figure 17

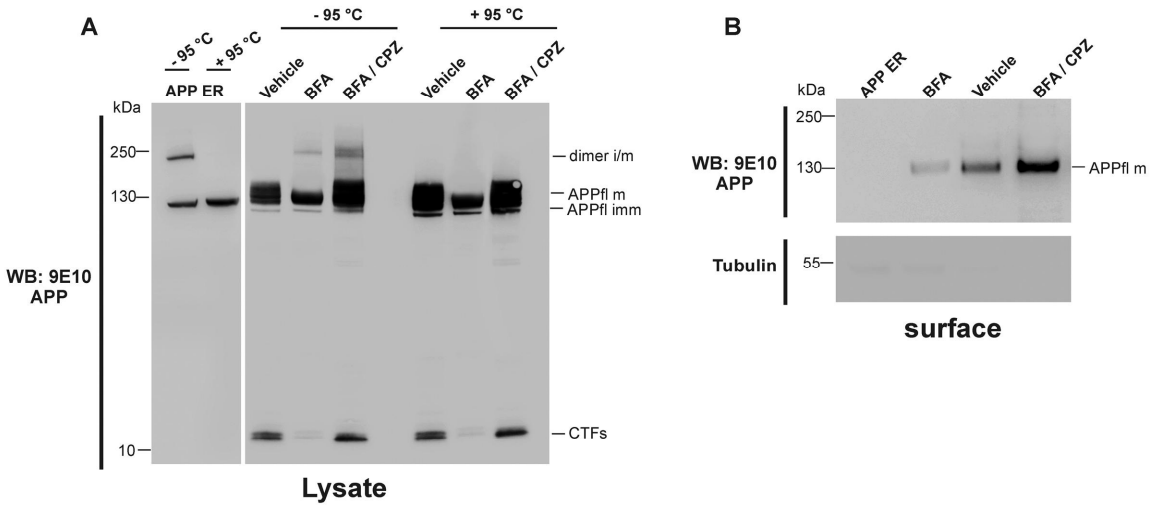

Fig. 17: Stable APP homodimers are trafficked to the cell surface

(A) CHO-K1 cells stably overexpressing APP 695 wt were pretreated for 1h at 37°C in the presence of 10 µg/ml brefeldin A (BFA), or DMSO (vehicle) for 1h, to block protein secretion from the ER. Subsequently, cells were either directly lysed (BFA), or medium containing BFA was removed, and cells were incubated for additional 30 min at 37°C with 10 µM chlorpromazine (BFA/CPZ), allowing transport to the cell surface, but inhibiting further endocytosis. Lysates were analyzed either under non-reducing, or reducing conditions. Note that cells pretreated with BFA, followed by chloropromazine exposure (BFA/CPZ), display two upper SDS-resistant bands migrating with a slight size shift, indicating different glycosylation patterns (dimer i/m). Note that strong denaturing conditions (+95°C) result in the disappearance of the upper migrating bands, suggesting disulfide bond formation. The separating line indicates different exposure times to visualize dimer formation in treated cells, whereas APP ER overexpressing cells served as size reference for dimers. **(B)** Cells were treated as described under (A), and subjected to cell surface biotinylation to confirm drug treatments. APP ER is completely absent from the surface, whereas only moieties of mature APP reach the surface upon BFA treatment. Strikingly, removal of BFA and subsequent incubation with chlorpromazine (BFA/CPZ) strongly increase surface exposed mature APP, compared to vehicle control. Note that in biotinylation no dimers can be recovered, since neutravidin beads were boiled in BME containing sample buffer, to release biotin conjugated proteins.

We employed a different approach to demonstrate that dimers generated in the ER can indeed reach the cell surface. We first slowed down anterograde ER-to-Golgi transport (Fujiwara et al. 1988; Lippincott-Schwartz et al. 1989; Pelham 1991) by pre-treating cells overexpressing APP 695 wt with 10 µg/ml BFA for 1h, to allow efficient dimer formation in the ER (Fig. 17A). Next, cells were either directly lysed, or BFA was washed out and cultures were incubated for additional 30 min at 37°C with medium containing chlorpromazine (CPZ, 10 µM). Chlorpromazine prevents assembly of adaptor protein-2 (AP-2) on clathrin-coated pits and thus causes a loss of endocytosis (Wang et al. 1993). Subsequently, cells were lysed or optionally subjected to a surface biotinylation (Fig. 17B). As expected, upon BFA treatment APP disappeared from the cell surface, verified by biotinylation (Fig. 17B). Furthermore, we were able to trigger APP695 wt dimer formation, as seen previously (compare Fig. 13A). In contrast, removal of BFA rapidly restored protein secretion form the ER to the Golgi and the cell surface (Lippincott-Schwartz et al. 1989), and APP reappeared the plasma membrane, established by CTF generation and fully glycosylated species, both in lysates and biotinylation experiments (Fig. 17A and B). Strikingly, chlorpromazine (CPZ) treatment led to a marked re-establishment of mature APP at the surface, compared to vehicle control (Fig. 17B), and BFA/CPZ-treatment caused the formation of SDS-resistant high molecular weight species, migrating as a doublet (Fig. 17B). We assume that the slight size shift of the upper bands represents different glycosylated APP dimers, indicating transport along the secretory route. However, this higher "mature" dimer was absent in APP ER- or BFA treated APP695 cells, suggesting that dimers were initially generated in the ER, but can be efficiently transported through the secretory pathway, reaching the cell surface. This was particular visible upon blocking endocytosis, thus preventing newly generated dimers from being instantly re-internalized. Note that heating the samples (+ 95°C) with BME resulted in the disappearance of the upper band(s), supporting our proposed model that APP dimers can associate via covalent intermolecular disulfide bonds.

4.10 ER retention does not affect APP biosynthesis but dramatically increases its half-life

Previously we could show that retention of APP in the ER severely restrained its catabolism (compare Fig. 9B), already suggesting a prolonged half-life. To investigate a potential influence of ER retention on the half-life and biosynthesis of APP, we performed a pulse-chase analysis (Fig. 18A). Cultures of APP wt and APP ER overexpressing CHO-K1 cells were pulse-labeled with 150µCi of [^{35}S]-methionine/cysteine, for 15 minutes and then chased for different time points in normal growth medium. Subsequently cells were lysed, and APP was immunoprecipitated with 9E10 antibody. After gel electrophoresis of precipitated proteins, the dried gels were exposed on an X-ray film for 12 hours. Essentially, the biosynthesis of immature APP between APP695 wt and APP695 ER was equal immediately after the pulse (0 h) and APP consisted predominantly of immature N-linked protein glycosylation species in both cell lines. However, fully mature APP (*N*-and *O*-glycosylated), reflecting trafficking through the Golgi compartment, appeared after 15 minutes exclusively in APP695 wt cells and became stabilized after 30 minutes. After 1 h chase period, the APP wt level was dramatically reduced (Fig. 18B, half-life APP wt 45 min), and hardly detectable after 4 h. In contrast, cells

overexpressing the AP ER retention mutant did not generate any *O*-glycosylated, mature APP during the chase period, indicative of its intracellular retention. However, the turnover of APP ER was substantially prolonged and ~ 50% of total APP was detectable even after 5.5 h (Fig. 18B).

Figure 18

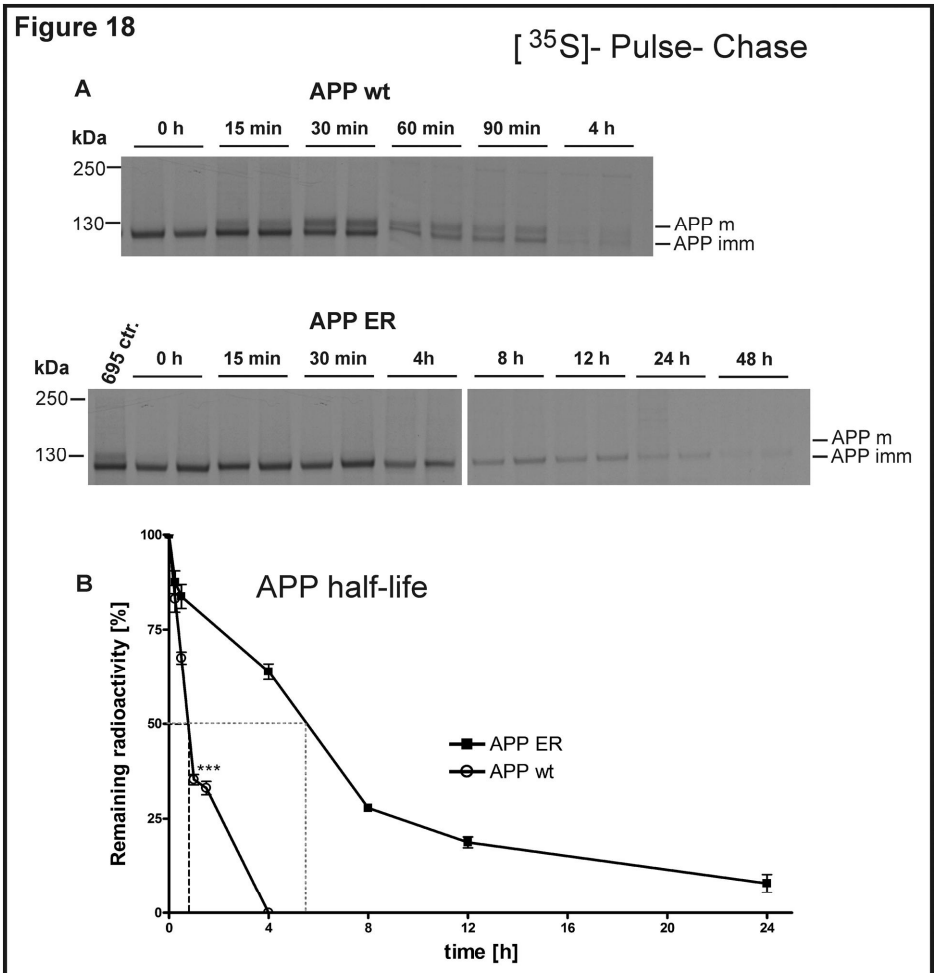

Fig. 18: ER retention hinders APP degradation and extends its half-life

(A) CHO-K1 cell cultures stably overexpressing either APP695 wt or APP695 ER, respectively were pulse-labeled for 15 min with 150 µCi of [^{35}S] methionine/cysteine. Cells were harvested immediately after the pulse (0 min), or chased for the indicated time points with non-radioactive medium. APP was immunoprecipitated with monoclonal 9E10 antibody and subjected to SDS-PAGE followed by autoradiography on an X-ray film for a minimum of 16 h at -80°C. Note, different time points for APP695 ER were chosen, due to its extended half-life. APP mature (APP m) and immature form (APP imm) are indicated. All time points were run in duplicates. For APP ER, samples were run alongside an APP wt control sample, to confirm the difference between immature and mature APP. **(B)** Half-life graph. Data are mean ± SEM of four independent experiments. *** Statistically significant difference ($p < 0.001$; t-test) between APP wt and APP ER is indicated.

Thus, the half-life of APP ER is more than 7-fold longer than in APP695 wt cells. Note that different chase time points for the APP ER mutant were chosen after initial pulse-chase experiments, already suggesting a prolonged half-life (data not shown). Most importantly, no dimers were detected on autoradiographies because immunocomplexes were eluted from agarose beads by heating samples at 95°C, thereby denaturing disulfide bound dimers. Together with our previous findings, these data indicated that APP turnover occurred downstream of the ER (compare Fig. 9B), and was dramatically slowed ($T_{1/2}$ = 5.5 h), as would be expected from interrupted secretion, resulting in reduced catabolism (see Fig. 9B). Additionally, this suggested that ER retention of APP did not trigger the

removal of potentially misfolded proteins by targeting them to the cytoplasmic ubiquitin–proteasome degradation pathways, resulting in prolonged half-life.

4.11 Adapter proteins binding to the C-terminus of APP do not interfere with the formation of homodimers

Our previous results have indicated that APP homodimerization is likely driven by disulfide bond formation between cysteine residues located within the E1 domain, already suggesting a strong involvement of the extracellular part. To further dissect the mechanism by which APP homodimerization is accomplished we employed another approach. We co-expressed well known adapter proteins which interact with the C-terminal, cytosolic part of APP, thus providing a potential sterical hindrance for dimerization, by snatching away or capture APP molecules. On the other hand, binding of proteins to the C-terminus could also induce conformational changes preventing or favoring dimerization. If the hypothesis was right that APP dimerization is driven by its extracellular part, we would expect no influence on dimerization, or at least no decline upon binding of cytosolic interactors.

Figure 19

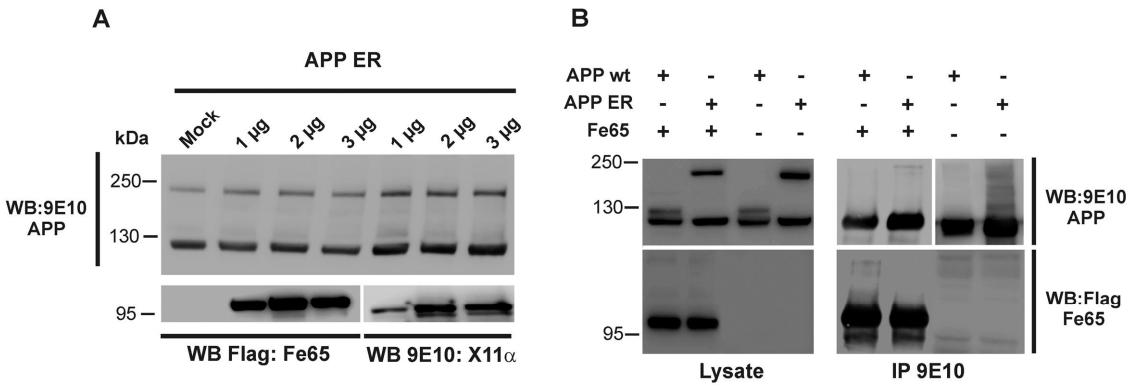

Fig. 19: APP homodimerization is not influenced by C-terminal adapter proteins

(A) CHO-K1 cells stably overexpressing APP695 KKAA (APP ER), were transiently co-transfected with increasing concentrations (1-, 2-, 3 µg) of plasmid-DNA, encoding adaptor proteins Fe65, X11α, or empty vector (mock). The upper western blot shows myc tagged APP ER full length (immature form, lacking Golgi glycosylation pattern) and SDS stable dimers, at a molecular weight of ~220 kDa. The lower blots depict transfection controls, using either flag antibody for Fe65, or 9E10 for X11α. Note that increasing amounts of C-terminal adaptor proteins likewise enhance APP mono- and dimer stability, whereas the effect was more profound for X11α. **(B)** Binding of Fe65 to APP was verified by co-immunoprecipitation. CHO-K1 cells stably overexpressing either APP695 wt or APP695 ER were transiently co-transfected with Flag-Fe65, or vector alone (-). 24h post transfection, 250 µg lysate aliquots were immunoprecipitated with 9E10 antibody against APP myc (IP 9E10, right panel) and immunoblotted for APP (WB: 9E10, upper blots), or Fe65 (WB: Flag, lower blots). Proteins were eluted with 2 x SDS buffer (+BME) and heated at 50°C to sustain disulfide APP dimers. Expression levels of APP and Fe65 were monitored by western blotting using the same antibodies (Lysate, left panel). Samples were treated with 2 x SDS loading buffer, without subsequent heat denaturing.

The intracellular domain of APP contains one so called -GYEYENPTY- motif, a consensus sequence for clathrin-coated pit mediated internalization, which has been shown to interact with the PID/PTB (phosphotyrosine interaction/binding domain) of several cytosolic adaptor proteins, including Fe65,

X11, JIP, Shc, Tip60, and Dab1 (Ando et al. 2001; Tamayev et al. 2009; Beyer et al. 2010). It has been shown that Fe65 interacts through its second PID/PTB with the APP cytodomain (Guenette et al. 1996; Russo et al. 2005) and was isolated within a trimeric complex consisting of Fe65, APP and LRP (Pietrzik et al. 2004), thereby altering APP trafficking, reinternalization and increasing its turnover (Ulery et al. 2000; Pietrzik et al. 2002). Another PID-domain containing adaptor protein, X11, binds to the same -GYENPTY- motif in the C-terminus of APP (Borg et al. 1996). Therefore, we transfected increasing amounts (1-, 2-, and 3 µg plasmid-DNA) of either flag-tagged Fe65 or myc-X11α, exemplary in CHO cells stably overexpressing APP ER (Fig. 19A). Immunoblotting for APP revealed a slight increase in both, APP monomers and dimers, upon the co-expression of Fe65. This effect seemed even more profound for X11α, when compared to vector transfected control cells (Mock). This outcome might be explained by the fact that Fe65 and X11 have been shown to stabilize APP, or its intracellular domain (AICD) (Kimberly et al. 2001), therefore possibly connecting two APP molecules, rather than disrupting them. Moreover, this is in line with findings that X11 decreases APP turnover in cell culture models (Borg et al. 1996; Sastre et al. 1998). Since both adapter proteins are predominantly localized in the cytoplasm, we tried to confirm a direct binding to APP retained within the ER. Therefore, we performed co-immunprecipitation experiments, exemplary using Fe65 (Fig. 19B). Indeed, we successfully co-purified equal amounts of flag-tagged Fe65 with myc-tagged APP wt, and myc tagged APP ER (Fig 19B). These results show that Fe65 can interact efficiently with APP ER via its cytosolic exposed, C-terminal part, while the APP N-terminus remains directed into the ER lumen, where disulfide-bridged dimerization takes place. Furthermore, this suggested that there existed obviously no competitive mechanism between cytosolic adapter proteins and APP molecules, interfering with dimerization.

4.12 APP homodimerization depends on the extracellular, cysteine-rich E1 domain

In previous studies dimerization interfaces in both, the APP transmembrane- and the ectodomain have been suggested (Soba et al. 2005; Munter et al. 2007; Kaden et al. 2008; Kaden et al. 2009). The extracellular part however can be divided into the E1 region, consisting of the growth factor-like domain (GFLD), followed by a copper binding domain (CuBD), which are linked by the so called loop-region. An acidic stretch precedes the E2 domain, containing the *N*-glycosylation sites of the ectodomain (Pahlsson et al. 1992; Yazaki et al. 1996). It has been shown by several groups that the E1 domain is indispensible for APP-homointeraction (Soba et al. 2005; Kaden et al. 2009), although the underlying mechanism remained elusive. Since we propose that disulfide formation is involved in *cis*-dimerization and all 12 cysteine residues of APP695 are located in its N-terminal 187 amino acids, we consequently hypothesized that dimerization of APP ER must be abolished under elimination of the E1 domain. It has been shown by co-immunprecipitations and FRET analysis, that deletion of the E1 domain could impede APP homodimerization (Soba et al. 2005) as well as heterointeraction with APLPs (Soba et al. 2005; Kaden et al. 2009). According to this, we hypothesize that APP, lacking the cysteine-rich E1 domain, is no longer capable of dimer formation in the ER. To analyze this, we generated CHO-K1 cells stably overexpressing the deletion constructs APPΔE1 wt, or APPΔE1 ER,

fused to the KKAA retention motif and compared them to cells expressing the corresponding full length constructs (Fig. 20C). The N-terminal truncated constructs encompassed the APP signal peptide at the N-terminus, directly followed by the acidic stretch (residues aa 190-288) and the E2 domain (see illustration in Fig. 20C), whereas at the C-terminus a myc-epitope was attached. To ensure that the generated constructs work properly and that the KKAA motif verified intracellular retention, we performed cell surface biotinylation experiments (Fig. 20A). Surface exposed proteins were biotinylated and precipitated by NeutrAvidin coated beads.

Figure 20

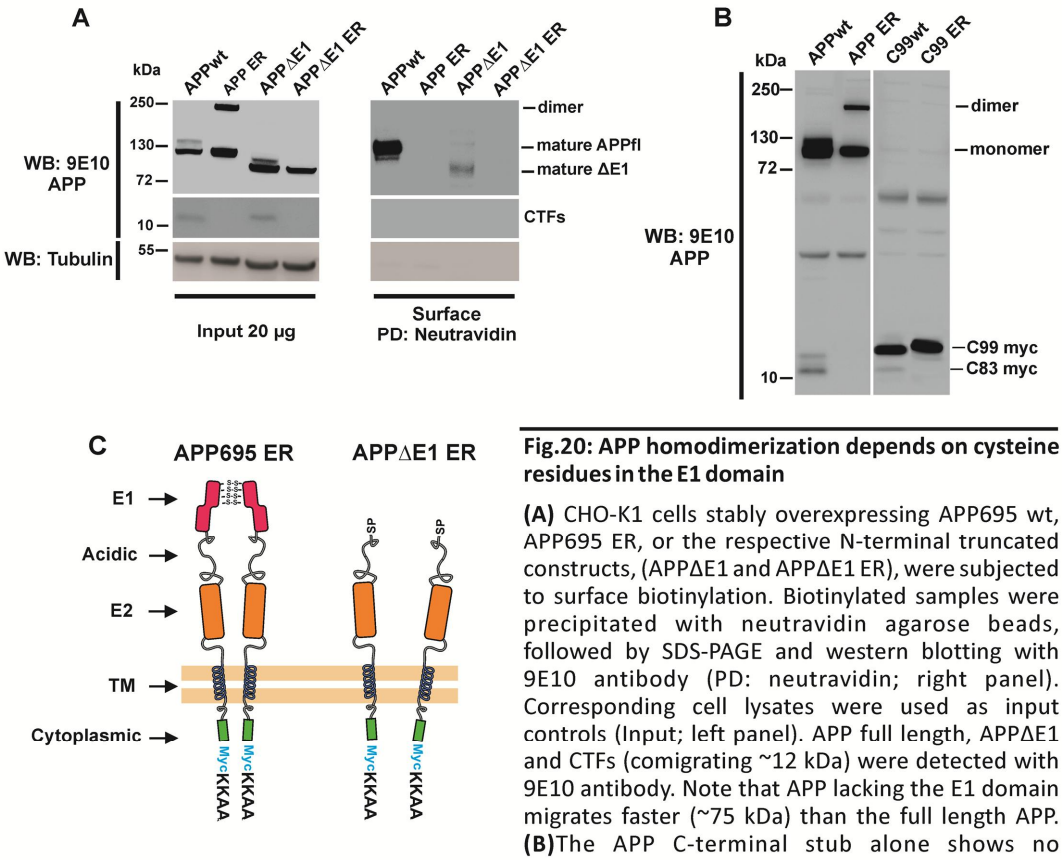

Fig.20: APP homodimerization depends on cysteine residues in the E1 domain

(A) CHO-K1 cells stably overexpressing APP695 wt, APP695 ER, or the respective N-terminal truncated constructs, (APPΔE1 and APPΔE1 ER), were subjected to surface biotinylation. Biotinylated samples were precipitated with neutravidin agarose beads, followed by SDS-PAGE and western blotting with 9E10 antibody (PD: neutravidin; right panel). Corresponding cell lysates were used as input controls (Input; left panel). APP full length, APPΔE1 and CTFs (comigrating ~12 kDa) were detected with 9E10 antibody. Note that APP lacking the E1 domain migrates faster (~75 kDa) than the full length APP. **(B)**The APP C-terminal stub alone shows no dimerization in the ER. CHO-K1 cells stably overexpressing either C99 or C99 KKAA (C99 ER) were analysed by SDS-PAGE, followed by western blot analysis. All APP or C99 constructs were detected with monoclonal 9E10 antibody against the myc epitope. No dimer formation was detected for the C99 constructs, compared to APP695 ER. Note, C99 ER was not further processed to C83, compared to C99 wt, indicative of its intracellular retention. **(C)** Schematic illustration depicting the generated constructs, APP695 ER and the corresponding deletion mutant APPΔE1 ER. For the APP deletion construct, the signal peptide sequence of APP was introduced in frame with the remaining domains, starting with the acidic region (aa 187). Deletion of the entire cysteine-rich E1 domain eliminated APP dimerization because no intermolecular disulfide bonds were formed in the ER as shown under (A). BME, β-mercaptoethanol; SP, signal peptide.

Western blot analysis of the precipitated APP proteins with the 9E10 antibody (Fig. 20A) confirmed that the dilysine-motif actively retained APPΔE1 ER intracellular (Fig. 20A, right panel), since it was absent from biotinylation, comparable to APP ER (Fig. 20A, right panel, lane 2 and 3). Additionally, the APPΔE1 ER mutant appeared as one band in lysates controls, just like the full length protein, indicative of its ER retention, thus preventing Golgi-specific *O*-glycosylation (Fig. 20A, left panel). In contrast, APPΔE1 migrates as a set of two bands around 75 kDa, corresponding to the immature and

fully glycosylated species, indicating normal passage through the secretory pathway, where maturation of the E2 domain can occur. Most interestingly, we did not observe the formation of SDS-stable homodimers for the APPΔE1 ER construct, as we always did for APP695 ER. From these results we conclude that the E1 domain is essentially needed to form covalently linked APP dimers, generated via disulfide bond formation in the redox environment of the ER (see illustration Fig. 20C). Moreover, mature APPΔE1 appeared less at the surface, compared to APP695 wt, possibly because the N-terminal truncation removed several free primary amino groups for biotin attachment. Furthermore it has been published that the TM-domain of APP, containing a so called GxxxG motif, was capable to dimerize in a bacterial membrane surrounding (Munter et al. 2007). Since these conditions do not reflect a natural membrane environment in higher eukaryotic cells, we tested the dimerization potential of an APP membrane anchored stub in our cell system. Therefore, we overexpressed exclusively the membrane bound C-terminal stub, which corresponds to β-*secretase*-cleaved CTF (C99) (Lichtenthaler et al. 1999), lacking the entire extracellular part of APP, including the E1 and E2 domains (Fig. 20B). However, when we subjected lysates to SDS-PAGE without heat denaturing the samples, we failed to detect SDS-stable dimers for C99 wt or the C99 ER retention mutant, confirming the requirement of the E1 domain for APP N-terminal interactions (Fig. 20C). Interestingly, when C99 was retained in the ER it was not further converted to C83 by α-*secretase* (Jager et al. 2009), as seen for unmodified C99 (Fig. 20B), thus confirming the specific retention in the ER.

4.13 Cysteine residues within the E1 domain of APP are critical for dimer-formation

To further unravel the mechanism by which APP *cis*-dimerization was accomplished, we focused in more detail on the cysteine residues within the E1 domain. It has been reported that APP comprises a region within the E1 domain, encompassing residues 99-110, with an active heparin binding capacity (Small et al., 1994) that might form a loop-structure, stabilized by an intramolecular disulfide bond between Cys-98 and Cys-105 (see illustration in Fig. 21A). More recently, Kaden and colleagues demonstrated that the molar surplus of a synthetic peptide (APP residues 91-116) containing the disulfide bridge-stabilized loop moderately inhibited chemical cross-linking of pre-existing SDS-labile APP dimers of an isolated ectodomain fragment (corresponding to aa 18-365 of the E1 and KPI domains of APP 770) (Kaden et al. 2008). However, when they replaced the two cysteines within the loop peptide by serine residues, the mutant peptide could no longer interfere with dimerization of the isolated N-terminal APP fragment. Kaden and colleagues believe that the intact loop peptide, stabilized by an intramolecular disulfide bond, might bind to APP by hydrophobic interactions and change its conformation, thereby inhibiting dimer formation. However, when the intrachain disulfide bond was absent due to the serine residues, dimer formation of the isolated APP N-terminal part was obviously not perturbed (Kaden et al. 2008). Based on the previous findings that a synthetic peptide encompassing the loop residues was able to interfere with APP dimerization (Kaden et al. 2008), we wanted to explore the impact of the respective disulfide bond within the full length APP in a cellular context, since it can only be generated via oxidation in the ER. We therefore generated an ER

retained APP695 loop double mutant, exchanging Cys-98 and Cys-105 for serine residues (APP ER 98-105_{ser}), thereby substituting the sulfhydryl- by hydroxyl-groups (Fig. 21A). If the respective cysteine residues are also crucial for APP-APP intermolecular *cis*-dimerization we should detect less, or no SDS-stable homodimers in our model, potentially formed via oxidation in the ER. We compared cell extracts from CHO-K1 cells, transiently transfected with the serine mutant, to lysates of our stably expressing APP 695 wt and APP ER cells (Fig. 21B).

Figure 21

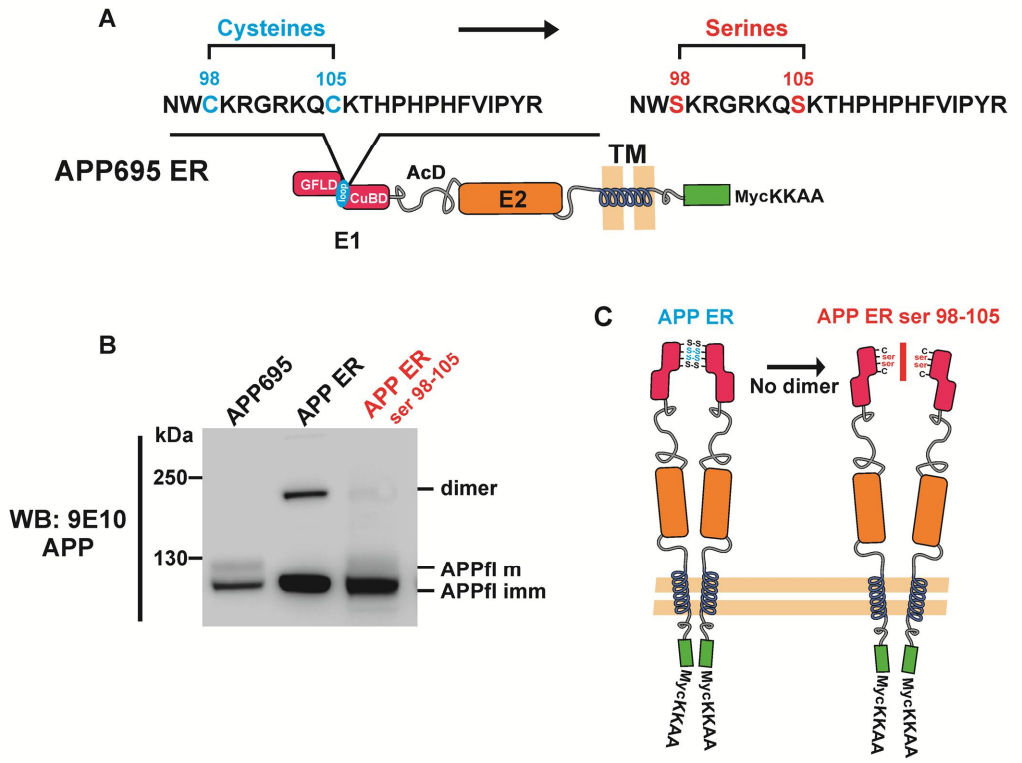

Fig. 21: Cysteine residues at positions Cys-98 and Cys-105 in the APP extracellular (E1) domain are critical for disulfide bridged dimers, generated in the ER

(A) Schematic illustration of the APP 695 ER domain structure. The E1 domain comprises a loop region encompassing residues 96-118, located between the N-terminal growth factor like domain (GFLD) and the copper binding domain (CuBD). The subsequent domains are indicated as AcD: acidic strech; E2 domain; TM: transmembrane domain. The loop region contains two cysteine residues at positions 98 and 105 (highlighted in blue), which are critical for APP homodimerization. The APP retention construct (APP695 ER) was used as a template to substitute cysteine residues Cys98 and Cys105 within the E1 domain, by two hydrophilic serine residues (change of a sulfhydryl group by a hydroxyl group, shown in red). **(B)** Lysates of CHO-K1 cells stably overexpressing APP wt, APP ER, or transiently transfected with APP ER 98-105ser, were analysed on 4-12% gradient SDS gels and immunoblotted with a 9E10 antibody for APP. Effective ER retention of the serine mutant is verified by the absence of the *O*-glycosylated band, compared to APP wt. No APP homodimers are generated in the ER when cysteine residues 98 and 105 are converted to serines, likely precluding the formation of interchain disulfide bonds due to the lack of thiol groups for oxidation. **(C)** Hypothetical illustration depicting a possible mechanism for APP homodimerization, connecting two opposing E1 domains. The cysteine-rich E1 domains might form intermolecular *cis*-dimers between two APP695 molecules (-S-S- stands simplified for a disulfide bond between two cyseine residue, whereas each E1 domain contains 12 cysteine residues). Replacement of Cys98 and Cys105 with serine residues (shown here in red) prevents disulfide bond formation between two E1 domains.

SDS-PAGE without heat denaturing the samples and immunoblots with 9E10 antibody clearly revealed that the APP ER 98-105_{ser} mutant failed to form homodimers in an oxidizing environment,

since no high molecular weight band appeared around 220 kDa, compared to APP ER, which still bears the respective cysteine residues (Fig. 21B).

However, ER retention of the serine mutant was confirmed by the lack of mature, *O*-glycosylated APP, analogous to APP ER. Thus, mutagenesis studies confirmed that alterations of specific cysteines to serines severely impaired the stabilization of APP dimerization in our system, and that oxidation of Cys-98 and Cys-105 might also form interchain disulfide bonds to produce stable, covalently linked protein dimers (Fig. 21C). However, at this point we cannot exclude the possibility that cysteine mutants, other than those analyzed, would have similar effects on APP-APP dimer formation. Collectively, this indicated for the first time that cysteines, located within the E1 domain, might contribute to *cis*-dimerization between two adjacent APP molecules, via intermolecular disulfide bonds, alternatively to intrachain disulfide bonds which sustain folding and stability (see illustration in Fig. 21C).

4.14 The APP-KPI domain impedes intracellular *cis*-dimerization within the endoplasmic reticulum, but not in later cellular compartments

All studies investigating APP dimerization so far, conducted by us and others, have used exclusively the neuronal APP isoform 695 (Soba et al. 2005; Munter et al. 2007; Kaden et al. 2008). However, alternative mRNA splicing of exon 7 can generate APP isoforms containing a 57 amino-acid insert, referred to as the Kunitz protease inhibitor (KPI) domain, one of the main serine protease inhibitors, expressed in most tissues and glial cells (Oltersdorf et al. 1989; Van Nostrand et al. 1991). Accordingly, the non-neuronal APP isoforms comprise either 751- or 770 amino acids, respectively whereby the latter bears an additional 19-residue OX-2 homology domain which is unique to this isoform and is encoded by a single exon 8 that lies adjacent to the KPI domain (see illustration in Figs. 3 and 4). This sequence shows similarities to the immunoregulatory lymphocyte proliferation marker MRC-OX-2 (Weidemann et al. 1989), but has not been further characterized. Structurally, the KPI domain immediately follows the acidic stretch and is located between the E1 and E2 domain of the extracellular part and comprises six further cysteine residues in addition to the twelve already embedded within the E1 domain. Functionally, the KPI domain has been shown to inhibit serine proteases, e.g. trypsin (Godfroid et al. 1990), but its exact purpose in APP function and metabolism remains largely elusive. Therefore, it was of interest whether APP harboring an additional KPI domain in its extracellular part, might show the same dimerization pattern as seen for APP695, lacking the KPI domain. To test the dimerization capacity of KPI-APP, we generated CHO-K1 cells with stably overexpressing APP770 wt and APP770 ER (containing the C-terminal -KKAA ER retention motif), or we transiently overexpressed APP751 in CHO-K1, cells to include all three major human APP isoforms (Fig. 22A). Surprisingly, immunoblotting of cell lysates with 9E10 antibody revealed no high molecular weight band for APP770 ER and APP751 ER, unlike APP695 ER (Fig. 22A and B). In addition to the myc-epitope, we employed APP of all three isoforms with a C-terminal HA tag and transiently overexpressed them in a different cell line (HEK 293T) to corroborate our previous results, idependently (Fig. 22B). Indeed, immunoblotting of lysates with HA antibody revealed a high

molecular weight band exclusively for non-KPI APP 695 when it was retained in the ER, in agreement with our previous data. Again, APP770 ER and APP751 ER migrated as single bands representing immature APP, lacking the *O*-glycosylated species. Moreover, CTFs were only generated in cells expressing the APP wt constructs, indicative of normal passage through the secretory pathway.

In contrast, CTF generation was prevented upon ER retention for all APP isoforms (compare Fig. 22A and B). These findings raised the possibility that the KPI domain might hinder *cis*-directed lateral homodimerization between APP molecules within the same cell. We hypothesized that the KPI domain might somehow provide a sterical obstruction, possibly due to different or delayed intramolecular folding properties.

Figure 22

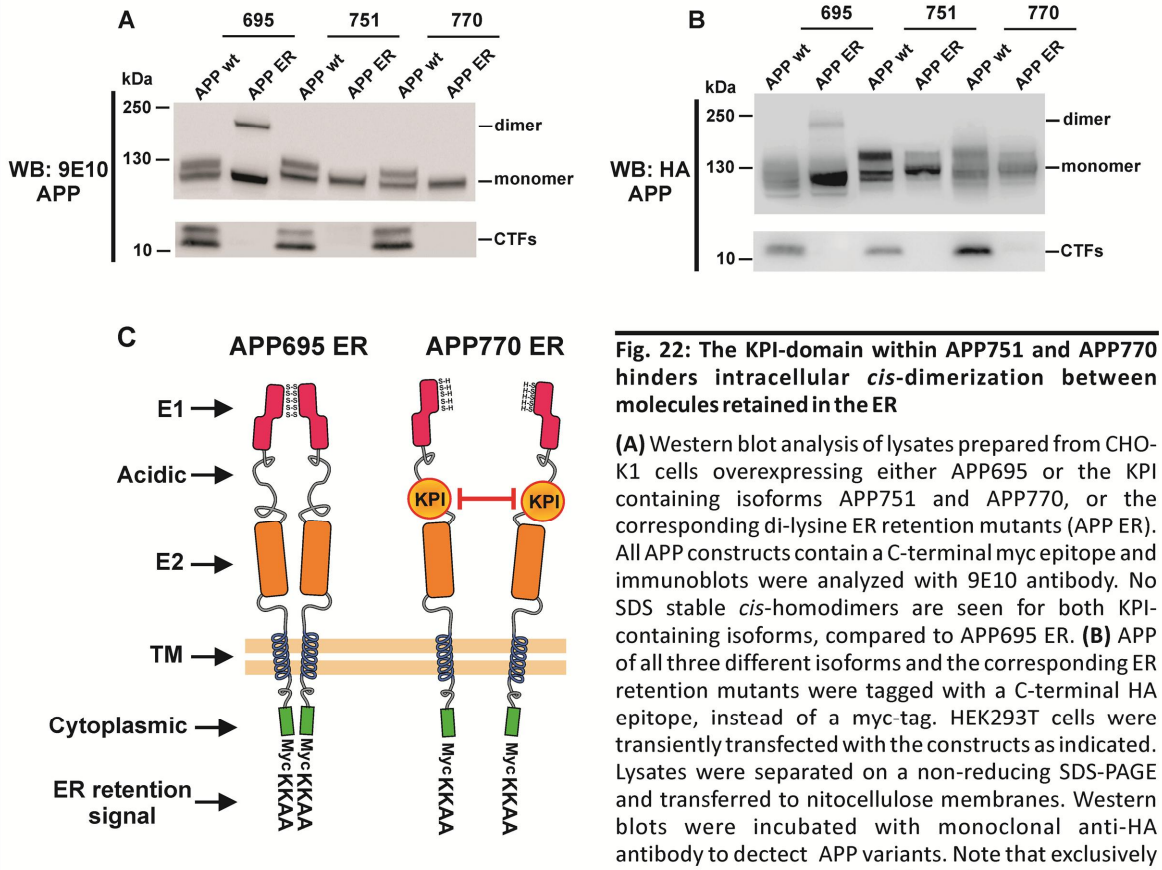

Fig. 22: The KPI-domain within APP751 and APP770 hinders intracellular *cis*-dimerization between molecules retained in the ER

(A) Western blot analysis of lysates prepared from CHO-K1 cells overexpressing either APP695 or the KPI containing isoforms APP751 and APP770, or the corresponding di-lysine ER retention mutants (APP ER). All APP constructs contain a C-terminal myc epitope and immunoblots were analyzed with 9E10 antibody. No SDS stable *cis*-homodimers are seen for both KPI-containing isoforms, compared to APP695 ER. **(B)** APP of all three different isoforms and the corresponding ER retention mutants were tagged with a C-terminal HA epitope, instead of a myc-tag. HEK293T cells were transiently transfected with the constructs as indicated. Lysates were separated on a non-reducing SDS-PAGE and transferred to nitocellulose membranes. Western blots were incubated with monoclonal anti-HA antibody to dectect APP variants. Note that exclusively APP695 ER migrates as an additional upper around 220 kDa, comparable to myc-tagged constructs under (A). The absence of CTFs and fully glycosylated APP verifies ER retention of both, myc and HA-tagged constructs. **(C)** Schematic illustration depicting a putative mechanism for APP dimerization within the ER. APP ER constructs of APP695 and APP770 containing a KPI domain and the respective domains are indicated. The cysteine-rich E1 domains of two adjacent APP695 molecules can form homodimers, possibly via intermolecular disulfide bonds (indicated as -S-S-). KPI-APP does not form homodimers in the ER, likely due to the KPI domain which might provide a sterical obstruction. Therefore, free sulfhydryl groups (-SH) of cysteines do not associate into covalent S-S bonds.

In fact it has been described that the KPI domain might represent an independent folding unit, lateral emerging from the full length construct (Gralle and Ferreira 2007). Correspondingly, the cysteine residues within the KPI domain would display an inhibitory effect on dimer formation, since a bulky-

like intramolecular KPI-structure could prevent the E1 domains from associating into dimers (see illustration in Fig. 22C for a hypothetical model).

To further dissect the dimerization state of the different APP isoforms, and to test whether KPI-APP can oligomerize at all (e.g. when it is not retained within the ER), we performed co-immunoprecipitation experiments, employing the various tagged APP variants, described above. Therefore, we transiently co-expressed APP695 HA plus APP695 myc or APP770 HA plus APP770 myc (wt constructs), or the corresponding myc tagged ER retention constructs (Fig. 23). The expression of APP constructs was assessed by western blotting in total cell lysates with the anti-HA or anti-myc (9E10), antibodies (input, direct lysates). In agreement with our previous results, only APP695 myc ER revealed an additional, discrete SDS-stable band at the expected molecular weight around ~220 kDa, whereas APP770 myc ER migrated exclusively as one band, representing immature APP, indicative of its intracellular retention (compare Fig. 22A and B).

Figure 23

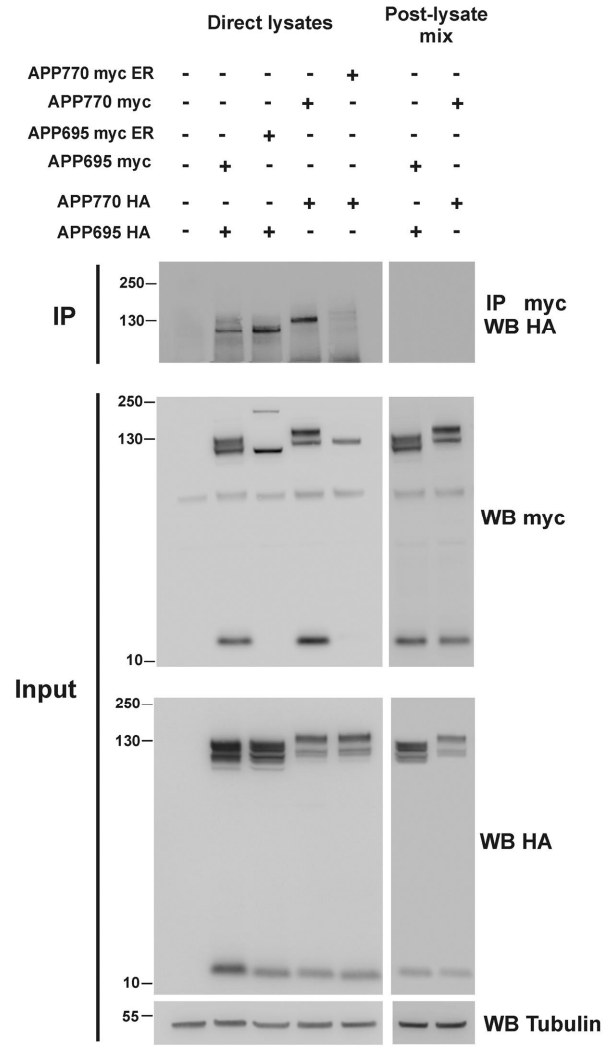

Fig.23: KPI-APP (770) can interact within the same cell, but not in the ER

CHO-K1 cells were transiently co-transfected with C-terminally myc-or HA-tagged APP isoforms, or the corresponding ER retention constructs, as indicated. Equal amounts of direct lysates (200 µg) were pulled down with 9E10 antibody against the myc epitope, using protein A agarose beads, followed by probing with HA antibody. The expression of APP was measured by western blotting with the anti-HA or 9E10 antibody in cell lysates (Input, direct lysates). As controls, extracts from cells expressing separately the APP-HA and APP-myc variants were mixed and analyzed by western blotting (Input, post-lysate mix), or immunoprecipitated with 9E10 antibody and probed with anti-HA antibody (IP, post lysate mix). Note that APP was only immunoprecipitated with 9E10 antibody from cell lysates co-expressing APP-HA and APP-myc constructs, and not when single transfected lysates were mixed. Therefore, interaction between APP molecules did not result from post-lysate aggregation of HA-and myc-tagged proteins. Note that only APP 695 migrated as a distinct high molecular weight band and not APP770 (Input, direct lysates, WB myc). APP770 HA did not co-precipitate with myc-tagged APP770 ER. In contrast, APP 695 HA showed stronger interaction when it was pulled down with APP695 myc ER.

In fact, APP770 was only co-immunoprecipitated when wildtype constructs were co-expressed, whereas APP770 HA was not co-purified whith APP770 myc ER (IP myc, WB HA). Vice versa, higher levels of APP695 HA were immunoprecipitated in cells co-expressing APP 695 myc ER (IP, direct

lysates), compared to the respective wildtype construct. However, APP770 HA was not recovered with APP770 myc ER, indicating that the KPI domain might exhibit a particular interface, possibly inhibiting dimerization of the longer isoforms in the ER. On the other hand, this experiment clearly showed that APP770 was capable of interacting with other APP770 molecules per se, because high levels of wt APP770 HA were co-purified with the myc-tagged counterpart (IP, direct lysates). Srikingly, only the mature form of APP 770 HA was precipitated with another APP770 myc (wt), indicating that KPI-APP interacts later in the secretory pathway, after full glycoslylation has been accomplished. Taken together, these results confirmed that dimerization of non-KPI APP (695) was initiated in the ER, but the longer isoforms likely interact in downstream cellular compartments. Furthermore, we excluded that the interaction of APP molecules might result from post lysate aggregation of HA- and myc-tagged proteins by mixing extracts from cells expressing separately the HA-APP and myc-APP constructs (IP, post lysate mix). When lysates were mixed and analyzed by western blotting with either antibody (Input, Post-lysate mix), the respective APP variants were detected. However, when cell lysates were further immunoprecipitated using the anti-myc antibody, immunoblotting with HA antibody revealed no signal, compared to immunoprecipitates of co-expressing cells (IP, direct lysates, WB HA).

4.15 Intracellular *cis*-dimerization of APP770 can be induced by a constitutive cysteine bond at the transmembrane domain

The results described above indicated that *cis*-dimerization of KPI-containing APP isoforms was sterically restricted, possibly due to intramolecular folding abilities of a KPI domain itself within the ER. We next wanted to investigate whether it is possible to force or trigger lateral *cis*-dimerization of APP770 in our cellular system. Based on the findings, described by Scheuermann and colleagues, replacement of the basic lysine at position 28 (corresponding to Aβ numbering) with a cysteine residue (K28C) triggered an effective dimerization of APP695 (Scheuermann et al. 2001), by engineering a constitutive disulfide bond. We therefore wanted to assess the effect of a cysteine mutation on dimerization using the KPI- isoform APP770. To test this, we generated APP K28C mutants of both APP695 and APP770, respectively, tagged with a C-terminal myc-epitope. After transient transfection of CHO-K1 cells with the cysteine mutants we detected a slower migrating band at ~220 kDa for APP695 K28C and around ~250 kDa for APP770 K28C, under non-reducing conditions (Fig. 24A). These high molecular weight species co-migrated with dimers generated from APP695 ER and disappeared after boiling the samples with BME (Fig. 24A, +BME, +95°C), thus revealing the same stability towards SDS treatment, as seen for dimers generated by APP695 ER. Consistent with our model, these findings provided further evidence that dimerization of APP was initially generated in the ER, since the covalent association of two cysteine residues could only be mediated by oxidation of thiol groups in the ER. Consequently, we demonstrated that introduction of a single cysteine at the APP juxtamembrane region was sufficient to engineer an intermolecular disulfide bond (Scheuermann et al. 2001), triggering lateral *cis*-dimerization of KPI-APP770. This indicated that the K28C mutation was potent enough to overcome a putative conformational restraint of the KPI domain, by cross-linking two apposed transmembrane domains of APP770,

resulting in covalently stabilized dimers (see illustration in Fig. 24C). Next, we questioned whether the artificial disulfide bond, potentially generated in the ER, might disrupt APP trafficking and processing along the secretory pathway. It has been previously reported by Eggert and colleagues that cysteine substitution at position 28 of Aβ caused a significant limitation in APP metabolism, generating less proteolytic products such as APPsα/β and Aβ-peptides (Eggert et al. 2009). We therefore assessed the surface levels of APP695 K28C by a biotinylation approach (Fig. 24B), whereas cell lysates were collected and employed for western blotting analysis with 9E10 antibody.

Figure 24

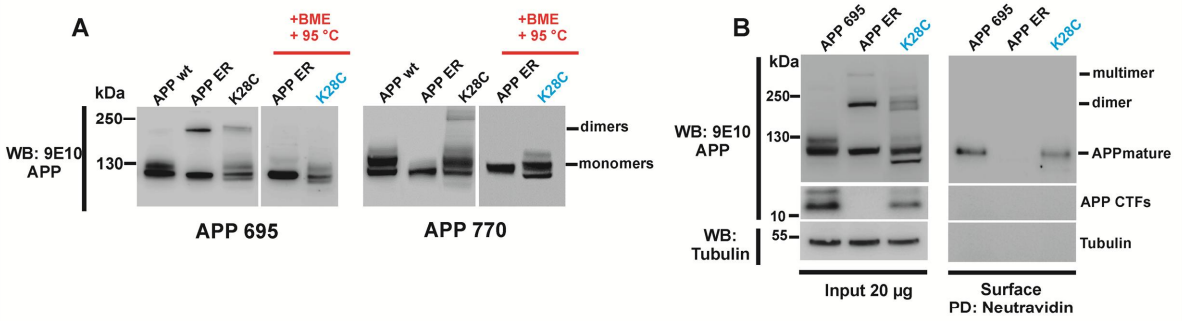

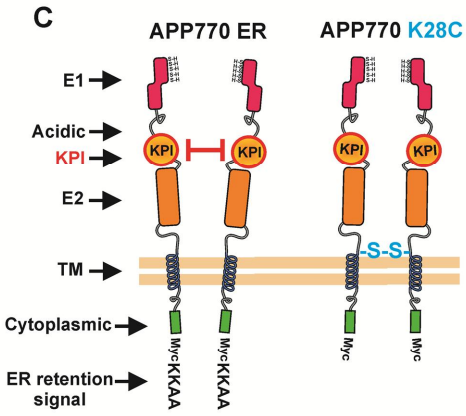

Fig.24: APP dimerization of KPI isoforms can be induced by an engineered disulfide-bond

(A) Artificial cysteine mutations at the transmembrane domain can trigger dimer formation, independent of APP isoforms. CHO-K1 cells were transiently transfected with the K28C mutant (Aβ numbering) of APP695 and APP770. The lysates were run alongside of K1 cells stably overexpressing APPwt or ER retention constructs (APP ER) of both isoforms and analysed under non reducing, versus reducing conditions (+BME/+95°C), followed by western blotting with 9E10 antibody. Cysteine substitution of the basic lysine residue leads to the formation of an additional slow migrating band for both isoforms, which comigrate the size of dimers, generated in the ER. Note, artificial cysteine dimerization is induced independent of APP isoforms. APP770 K28C shows an explicit slower migrating band, round 250 kDa, when membrane proximal lysine (K) was changed to a cysteine (C) residue, whereas no dimers appeared when APP770 was retained in the ER. Induced dimerization is eliminated by the reduction of samples with BME and heat (+BME/+ 95°C) **(B)** The APP K28C construct is transported normally to the cell surface. CHO-K1 cells stably overexpressing either APP695wt or APP ER, or transiently overexpressing APP695 K28C, were labeled with sulfo NHS-SS-biotin. Biotinylated samples (250 µg of total lysates) were precipitated with neutravidin agarose beads and analysed by SDS-PAGE and western blot (PD: neutravidin; right panel). APP and its cleavage products (CTFs) were detected with monoclonal 9E10 antibody, whereas Tubulin served as a loading control or verifies cleanness of the biotinylation. Note that the artificial cysteine mutation (K28C) reveals a clear high molecular weight band, migrating as a doublet, possibly indicating two putative glycosylation patterns (ER and Golgi) of the dimer. **(C)** Schematic illustration depicting a putative mechanism for covalently stabilized APP 770 (KPI) dimers with an induced, intermolecular disulfide bond. APP 770 ER containing a KPI domain and the respective domains are indicated. APP770 or 751 does not form homodimers in the ER, due to the KPI domain which might provide a sterical hindrance, impeding the interacion of two cysteine-rich E1 domains. However, dimerization of KPI APP can be triggered by the introduction of cysteine residues at the transmembrane domain of APP, leading to the formation of a covalent intermolecular disulfide bond (-S-S-).

Indeed, the APP K28C mutant was able to reach the plasmamembrane, comparable to APP695 wt (Fig. 24B, right panel), whereas trafficking of our ER retention mutant was efficiently inhibited. Moreover, induction of covalent disulfide bond-formation did not interfere with maturation of APP, since K28C mutants migrated as a set of two bands, revealing *N*-and *O*-glycosylated species.

Furthermore the generation of C-terminal fragments (CTFs) verified passage through secretory compartments and *secretase*-dependent proteolytic processing of APP. We therefore conclude that dimerization itself does not necessarily interfere with APP trafficking or maturation, nor seems dimerization a precondition for plasmamembrane localization.

4.16 *Trans*-dimerization at the cell surface is independent of the APP isoform

Having established that *cis*-directed dimerization of KPI-APP was impeded within the ER, but inducible with an engineered disulfide-bond (compare Figs. 22 and 24), we next questioned whether interaction between different APP isoforms could occur when present on adjacent cells, designated as *trans*-cellular dimerization. It has been well described that different cell adhesion molecules (CAMs) like cadherins and nectins are important for interneuronal synapse formation (Takai et al. 2003). Consistently, a role for APP in neuronal cell-cell adhesion has been suggested (Breen et al. 1991), and *trans*-interaction properties of APP family proteins was demonstrated to promote cell adhesion in *Drosophila Schneider* (S2) cells (Soba et al. 2005). Since only the neuronal APP695 isoform has been investigated regarding *trans*-dimerization, we employed the well-established cellular aggregation assay to investigate intercellular ectodomain interaction of the different APP isoforms, using *Drosophila Schneider* (S2) cells (Fossgreen et al. 1998; Soba et al. 2005). S2 cells were chosen as a model system because they lack strong cell adhesion properties and show only weak cell-cell interaction, furthermore overexpressed transmembrane proteins are efficiently transported to the plasma membrane and show high cell surface expression (Soba et al. 2005). These properties make them an ideal model system to study cell adhesion proteins, as has been successfully done in previous studies (Fausto-Sterling et al. 1985; Tsiotra et al. 1996; Soba et al. 2005). Expression of two interacting proteins in two separated pools of S2 cells caused coclustering after mixing of both cell pools, like it has been shown for the Notch receptor and its ligand, Delta (Klueg and Muskavitch 1999). Whereas cells expressing only GFP did not co-aggregate (Soba et al. 2005), thus cell clustering gives a direct readout whether two proteins can interact at the surface. Additionally, S2 cells express APP α- and γ-site cleaving enzymes (Fossgreen et al. 1998), but lack endogenous expression of the APP homologue APPL, thus mimicking a knockout condition for APP family proteins. In line with previous findings (Soba et al. 2005; Kaden et al. 2008) we have confirmed the E1-domain as the major dimerization interface of two APP molecules (compare Fig. 20). Consequently, we assumed that the presence of the KPI-domain should not affect intercellular *trans*-dimerization properties of APP751 or APP770 (see illustration in Fig. 25D), since it has been shown by Soba and colleagues that APP695 can *trans*-interact with another APP molecule or one of its homologues APLP1 or APLP2. To compare the homophilic *trans*-cellular dimerization properties of all APP isoforms (695, 751 and 770), the respective cDNAs were cloned into in the GAL4 responsive *Drosophila* pUAST expression vector, described in Soba et al., 2005. S2 cells were transiently cotransfected with pMT-Gal4 and the different pUAST-APP constructs and expression of Gal4 and thus APP was induced 48 h after transfection with 500 µM $CuSO_4$, thus allowing Cu^{2+}-inducible high level expression of Gal4 under control of the metallothioneine promoter (Klueg et al. 2002). As negative control, S2 cells were

transfected with the N-terminal truncated APP695ΔE1, which has been shown to interfere with dimerization of APP and its homologues (Soba et al. 2005; Kaden et al. 2008).

Figure 25

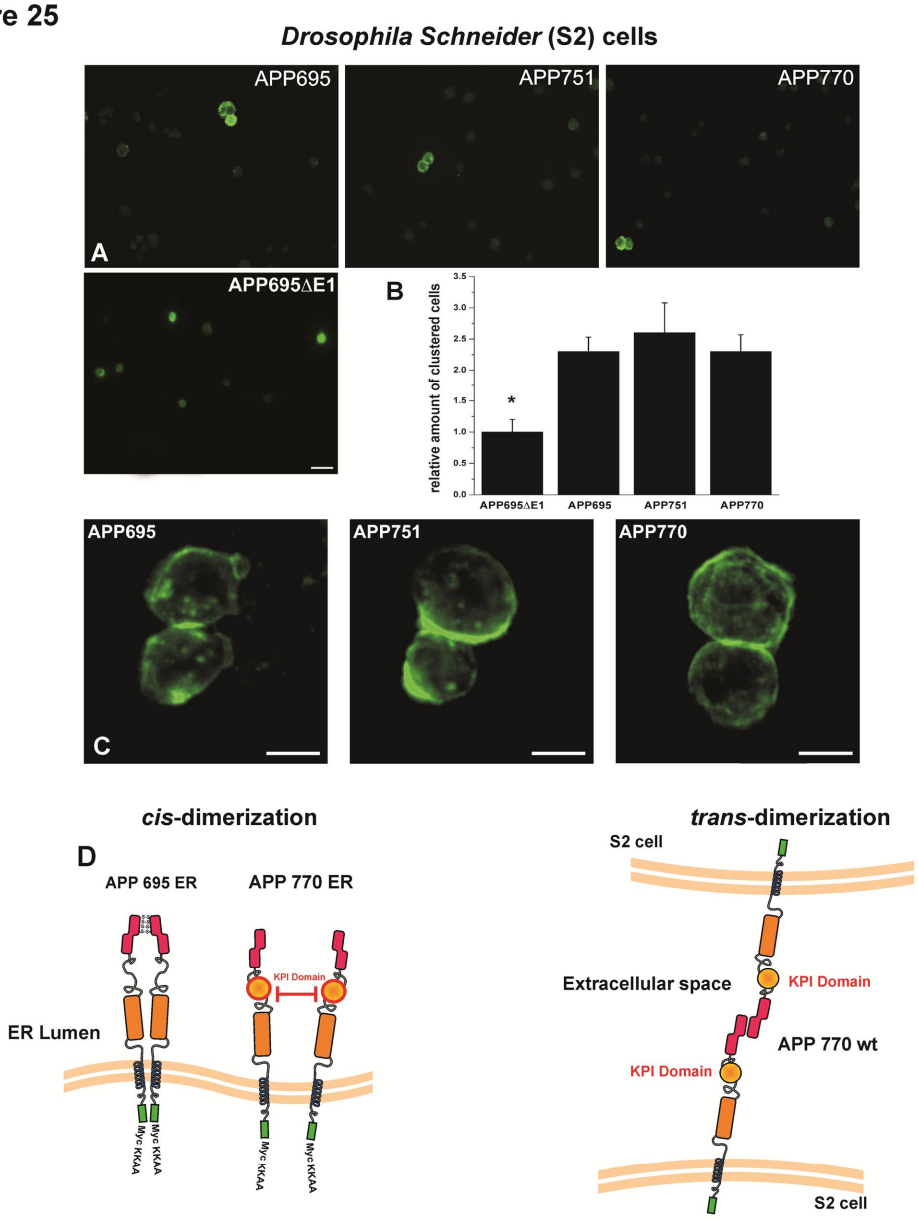

Fig.25: APP *trans*-dimerization at the cell surface is not influenced by the KPI domain

(A) *Drosophila Schneider* S2 cells were transiently transfected with vectors encoding all human APP isoforms (695, 751, 770). As negative control, S2 cells were transfected with APP695ΔE1, truncated at the N-terminus. Cells were immunostained with anti APP antibody (CT-20) and secondary anti-rabbit AlexaFluor488. Note that untransfected cells (no green fluorescence), or APP695ΔE1 expressing cells do not aggregate. **(B)** Quantification of clustered cells is shown. For quantification, clusters of two or more transfected cells were scored as positive and relative amount of aggregated cells is shown. Statistical significance was tested using a students´ t-test. (n≥ 3, ± SD) *p<0.05, t-test. Note that expression of either APP isoform caused equal homotypic clustering of S2 cells. Scale bar equals 20 µm. **(C)** A single confocal section of S2 cells, representing homotypic aggregation of each APP isoform is shown. Scale bar equals 5 µm. **(D)** Hypothetical model depicting dimerization properties of APP isoforms within different cellular compartments. APP695 isoform can form homodimers in the ER lumen, favored by oxidizing conditions. However, APP770 failed to dimerize in the same manner, possibly due to the presence of a KPI domain which might adopt an inhibibitory, intramolecular structure, thereby impeding lateral *cis*-directed homodimerization within the same plasma membrane. At the surface of Drosophila S2 cells dimerization can occur independent of the particular APP isoform in *trans*-direction (right panel). The experiment was performed in cooperation with Katja Wagner from the lab of Prof. Stefan Kins, Kaiserslautern.

Transfected single cell suspensions were aggregated for 2h, and analyzed by immunocytochemistry with polyclonal anti-APP antibody, CT-20 and secondary anti-rabbit AlexaFluor488 (Fig. 25A and C). Despite a very low transfection efficiency (10-15%), quantification of these results revealed that virtually no cell clusters containing two or more APP695ΔE1 expressing cells were present (set as 1; $p<0.05$), while about two-fold more of all APP isoform expressing cells formed homotypic aggregates, significantly more than with the truncated APP version (Fig. 25B). We observed almost equal clustering ratios for cells expressing either APP isoform (Fig. 25B), whereas cells expressing APP695ΔE1 did not reveal specific clustering (Figs. 25A and C), similar to untransfected S2 cells (shown in dark, no green fluorescence). Furthermore single confocal sections revealed accumulated APP immunoreactivity at cell–cell contact sites of homotypic clusters (Fig. 25C), in line with previously published data (Soba et al. 2005). Together, these results demonstrated that cell-cell interaction by ectodomain mediated adhesion occurred independent of a KPI domain. However, APP dimerization was in particular depended on E1 domain at both, the cell surface (*trans*), as well as within the cell (*cis*) (compare Fig. 20). In our studies, only APP695 was able to form lateral intracellular (in the ER), as well as intercellular *trans*-dimers at the cell surface. However, the KPI domain of APP isoforms 751 and 770 only hindered lateral interaction but not homophilic *trans*-interactions, since two E1 domains can still dimerize when faced in opponent orientation (Fig. 25D, illustration).

4.17 Heterointeraction between APP and its homologue APLP1 is initiated and increased in the ER

Various experimental approaches have demonstrated that APP is capable of forming heterodimers with its homologues, APLP1 and APLP2 (Soba et al. 2005; Kaden et al. 2009), both intracellular in *cis*- and intercellular in *trans*-manner (Soba et al. 2005). Previous studies conducted by Soba and co-workers used extensive co-Immunoprecipitation- and aggregation assays with *Drosophila Schneider* (S2) cells, whereas Kaden and colleagues employed a FRET technique in living HEK-293T cells (Kaden et al. 2009). While these approaches suggested the existence of APP/APLP homo-and heterophilic interactions, they did not address in which cellular compartment they might take place. So far, we could identify the ER as the cellular compartment providing ideal oxidizing conditions for triggering APP695 homodimerization via intermolecular disulfide-bridge formation. Therefore, it was of interest whether the interaction between APP695 and APLP1 was achieved by a similar mechanism, since both proteins lack a KPI domain and co-exist in neurons (Zhou et al. 2011). As a first biochemical approach, we performed cell surface biotinylations in our CHO-K1 cells, stably overexpressing either APP695 wt or APP695 ER. Additionally, we transiently co-transfected the human APLP1 cDNA (Fig. 26A), since CHO cells lack endogenous APLP1. Biotinylated proteins were isolated with NeutrAvidin coated agarose beads and probed with 9E10 antibody for APP, or polyclonal anti-APLP1 antibody. Surprisingly, the input controls revealed a significant reduction of more than 60% in APP695 ER homodimers (Fig. 26C), accompanied by a ~50% increase in APP monomers upon the co-expression of APLP1 (Fig. 26A, upper panel, lane 4), compared to vector transfected controls.

Figure 26

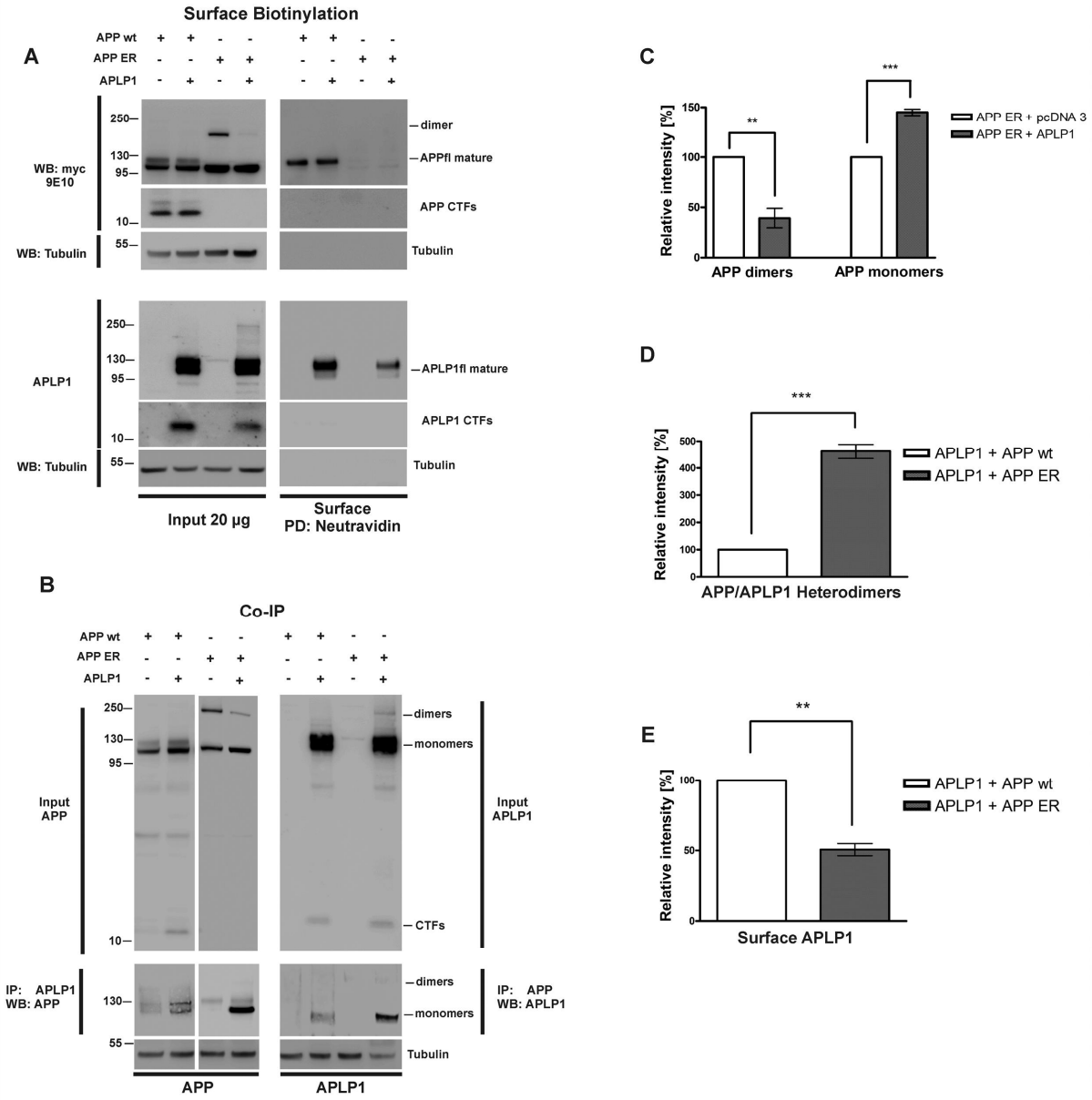

Fig. 26: Heterodimerization between APP and APLP1 is initiated and increased in the ER

(A) Surface Biotinylation of CHO-K1 cells stably overexpressing either APP695 wt or APP695 ER, transiently co-transfected with human APLP1 cDNA, or empty vector (-). Cells were labeled with sulfo NHS-SS-biotin and equal amounts of cell lysates (250 µg) were precipitated with neutravidin beads (PD: neutravidin; right panel). APP full length and CTFs were detected with 9E10 antibody. APLP1 full length and C-terminal fragments were stained with the polyclonal APLP1 antibody 171615 (Calbiochem) and α-Tubulin served as a loading control. Biotinylated proteins were eluted with BME containing SDS sample buffer and heated at 95 °C, whereas input controls were not heat denatured, prior to electrophoresis. Note that hetreointeraction of APLP1 and APP695 ER diminishes APP homodimers in the ER and lowers surface levels of mature APLP1, as shown on one representative western blot. **(B)** CHO-K1 cells stably overexpressing either APP695 wt or APP695 ER were transiently cotransfected with human APLP1 cDNA, or empty vector (-), equal amounts of total protein lysates (250 µg) were immunoprecipitated with either 9E10 antibody (for APP), or 171615 antibody (for APLP1). Co-purified proteins were detected with antibodies as indicated (IP: APLP1, WB: 9E10 for APP, lower panel; left) and reverse (IP: 9E10, WB: APLP1, lower part; right). Input controls were analyzed with the same antibodies (upper blots) and Tubulin served as loading control. Note that heterointeraction of APP and APLP1 is increased, when APP is retained in the ER. **(C)** Diagram shows relative changes [in %] in APP dimers and monomers when co-transfected with pcDNA3 or APLP1. Data represent ±SEM as indicated (n≥ 3). **(D)** Graph shows formation of APP/APLP1 heterodimers, expressed as percentage increase over APP wt and represents mean ±SEM as indicated (n≥3). **(E)** Diagram shows significant reduction in APLP1 surface levels when co-expressed with APP ER from three independent experiments. Statistical significance: ***p<0.001, **p<0.01, t-test.

In addition to the inverse relationship in APP ER monomer-dimer equilibrium, we detected an explicit slower migrating band for APLP1, when expressed along with APP ER. However, this band co-migrating ~220 kDa was absent when APLP1 was overexpressed in APP wt cells (Fig. 26A, input APLP1). Taken together, these results strongly suggested that the formation of APP/APLP1 heterodimers was initiated within the ER, indicating that a portion of existing APP homodimers was converted back to monomers, whereas the rest appeared as heterodimers together with APLP1. Consistently, we found significantly less mature APLP1 at the cell surface, when co-expressed with APP695 ER (Fig. 26A, bottom panel, lane 2 and 4), corresponding to a 50% reduction, compared to APP695 wt (Fig. 26E). This indicated that the interaction of APP and APLP1 occurred already in the ER and that APP potentially retained a portion of APLP1 in the ER as a consequence of forming stable heterocomplexes. Furthermore, only mature APP or APLP1 appeared at the cell surface, whereas *secretase* derived metabolites (CTFs) were only visible in the lysate controls. To provide further evidence for the interaction between APP and its homologue APLP1, we performed co-immunoprecipitation studies in our stable CHO-K1 cells upon co-expression of human APLP1 (Fig. 26B). Lysate controls and co-purified proteins clearly indicated a strong interaction between both proteins in the ER. In line with previous results, APP homodimerization in the ER was reduced upon APLP1 co-expression (Fig. 26B lysate WB 9E10, lane 4), compared to APP695 ER alone. At the same time we observed again the formation of a distinct higher molecular weight band for APLP1 in cell lysates, only when co-expressed with APP695 ER, as seen previously (Fig. 26A, bottom blot). Consistently with the biotinylation approach this band most likely represented APP/APLP1 heterocomplexes, since it co-migrates with the size of APP homodimers (~220 kDa) and both homologues have about the same molecular mass. Furthermore APP- and APLP1-directed co-immunoprecipitation experiments confirmed the specific interaction between both proteins in the ER (Fig. 26B, lower panels). In fact the amount of co-purified proteins (immature form) was increased when APP was retained in the ER. In support of our proposed model, these findings clearly demonstrated that APP695 and APLP1 form heterocomplexes as early as in the ER, most likely via a mechanism, reminiscent of APP homodimerization – triggered by disulfide-bond formation between the respective cysteine-bearing E1 domains of both proteins.

5 Discussion

In previous studies investigating the oligomerization state of APP, most of the employed methods, such as chemical cross-linking, engineering of artificial cysteine bonds (Scheuermann et al. 2001; Munter et al. 2007), or generating APP-FKBP chimeras as an inducible dimerization system (Eggert et al. 2009), did not resemble the natural membrane surrounding within eukaryotic cells. To date, most studies dealing with APP dimerization focused on the impact on Aβ generation (Scheuermann et al. 2001; Munter et al. 2007; Eggert et al. 2009), revealing a lot of inconsistent results regarding its production (Munter et al. 2007; Kienlen-Campard et al. 2008; Eggert et al. 2009). It has been shown that homodimerization of APP is driven by motifs either present in the extracellular domain (E1 domain, E2 domain), or in the juxtamembrane and transmembrane (JM/TM) domain by GxxxG motifs. For the full-length protein, it was demonstrated that dimerization was accomplished by the N-terminal region of APP, referred to as the E1 region, encompassing a growth factor-like domain (GFLD) and a copper-binding domain (CuBD) (Soba et al. 2005; Kaden et al. 2009). Moreover, it has been reported that APP dimerization was partially inhibited by a peptide that mimics a surface exposed loop between Cys 98 and 105 of APP (Kaden et al. 2008). These observations raised important questions about APP processing and function: What is the role of dimerization in APP processing and function? And particularly how and where in the cell is APP dimerization initiated? Furthermore it remained to be determined whether all APP isoforms exhibit the same dimerization characteristics regarding intracellular *cis,* -as well as intercellular *trans*-interactions, since previous research largely investigated the neuronal APP isoform 695. We therefore focused in our study on the actual subcellular origin of APP homodimerization, an underlying mechanism, and a possible impact on dimerization properties of its homologue APLP1. Moreover, we analyzed the dimerization capacity of all three different APP isoforms (KPI- versus non-KPI APP), according to the subcellular compartment.

Despite accumulating data towards APP dimerization, the physiological significance and subcellular localization of its generation are still under debate. Preliminary evidence that APP oligomerization might occur as early as in the ER was obtained when chemically cross-linked [^{35}S]sulfate-labeled APP migrated slower than [^{35}S]methionine-labeled, after being monomerized by reducing agents, suggesting that dimerization was initiated before maturation of N-linked oligosaccharides or tyrosine sulfation (Scheuermann et al. 2001). Nevertheless, the precise mode of dimerization remained somewhat elusive, predominantly hydrophobic interactions between the TM- or ectodomains have been suggested so far (Soba et al. 2005; Munter et al. 2007; Kaden et al. 2008; Kaden et al. 2009). Interestingly, few studies showed that e.g. C99 (Kienlen-Campard et al. 2008) or myc and GFP-tagged APP migrates as a dimer on SDS-polyacrylamide gels Scheuermann et al. 2001), suggesting that stronger interactions might also play a role for APP dimerization.

To further elaborate the precise origin of APP dimer formation and to assess the putative dimerization potential of APP in different cellular destinations, we made use of well known cytosolic dilysine-based motifis, -KKAA and -KKFF, which are critical for endoplasmic reticulum (ER) localization, exit, or retrieval of type I membrane proteins (Andersson et al. 1999). It has been shown

that -KK serves as a binding signal for COP I vesicles (retrograde), whereas -FF interacts directly with COP II vesicles, acting as an ER exit determinant (Andersson et al. 1999). Thereby, the C-terminal KKFF retention signal secures ER exit, but retains APP in the early secretory pathway (Itin et al. 1995), resulting in retrieval back from early Golgi and intermediate compartments to the ER by the retrograde pathway (Pelham et al. 1989 Teasdale et al. 1996; Andersson et al. 1999). On the other hand, substitution of the phenylalanines (FF) by alanines (AA) inhibits anterograde transport, mimicking a permanent ER retention (Cosson and Letourneur 1994; Letourneur et al. 1994; Cosson et al. 1996; Kappeler et al. 1997). It has been demonstrated that the ER-Golgi-intermediate-compartement marker protein, ERGIC-53, normally carrying a dilphenylalanine signal (KKFF), was strictly localized to the ER when the two C-terminal phenylalanines were changed to alanines (KKAA) (Andersson et al. 1999). These data supported the notion that KKAA is a true ER retention signal, preventing transport to the *cis*-Golgi (Kappeler et al. 1997; Andersson et al. 1999).

5.1 Oxidizing conditions in the endoplasmic reticulum promote APP dimerization, mediated through disulfide bond(s)

We began by generating APP695 chimeras, containing the C-terminal KKAA dilysine ER retention-motif (APP ER) or the "leaky" amino acid sequence KKFF, containing the phenylalanine ER exit determinant, allowing its traffic to the *cis*-Golgi, therefore designated as APP Golgi (Itin et al. 1995; Itin et al. 1995; Norkin et al. 2002). We employed a cell culture model in CHO-K1 (mammal) cells, stably overexpressing APP chimeric proteins tagged with C-terminal doublelysine retention motifs. When cell lysates were analyzed biochemically, we could successfully demonstrate in a highly reproducible manner that chimeric APP695 containing the C-terminal dilysine signals were in fact retained within early secretory compartments, as demonstrated by the lack of Golgi-specific carbohydrate modifications, and the absence of APP at the cell surface (Fig. 8). On SDS-PAGE, KK*XX*-tagged APP chimeras migrated exclusively as one band representing immature, *N*-glycosylated species, whereas APP wildtype appeared as a set of two bands, equivalent to immature and mature forms (i.e. not fully and fully glycosylated forms) (Figs. 8 and 9), indicative of its travel along the secretory route to the cell surface (Fig. 9A). Moreover, intracellular retention of APP ER (KKAA) and APP Golgi (KKFF) was confirmed by limted metabolism of APP, normally happening while passage the secretory pathway (Fig. 9B). APP KK*XX* chimeras showed an almost complete suppression in total Aβ secretion (Fig. 9B), which was in agreement with an earlier study that showed the direct retention of C99 in the ER, causing an almost complete inhibition in the secretion of Aβ and APPs (Maltese et al. 2001). Since all three *secretases* (α, β, and γ) also traffic and mature through the secretory pathway, most notably within the Golgi (Schlondorff et al. 2000; Dries and Yu 2008), retained APP cannot be cleaved, furthermore inhibiting the release of the AICD (Fig. 9B). However, the membrane enriched fraction showed at least minor CTF generation for APP Golgi, confirming the "leakiness" of the KKFF motif, denoting that APP had at least access to the *cis*-Golgi compartment (Pelham et al. 1989), where α-*secretase* cleavage occurred only to a little extend (Lammich et al. 1999). Taken together, these results confirm previous studies that APP processing occurs mainly at the cell surface and is negligible along the secretory pathway, i.e. in the ER or proximal Golgi (Caporaso et al. 1992;

Lammich et al. 1999). Supporting of that was the vast increased half-life of APP ER, compared to APP wt (Fig. 18), confirming that despite an identical biosynthesis, the limited access to processing enzymes dramatically increased APP stability.

However, most interestingly was the observation of an explicit upper migrating band for APP 695 when it was retained in the ER by the KKAA motif, co-migrating at the expected molecular weight of a putative APP dimer (~220 kDa). Strikingly, this upper band was absent from APP695 KKFF (Golgi), tagged with the "leaky" retention motif. The fact that APP ER displayed an SDS-stable high molecular weight species, suggested to us that APP could form highly stable dimers, possibly through a disulfide bond(s), under appropriate cellular conditions, that remained stable during standard protein isolation and lysis methods. To further investigate the mechanism of APP dimer formation, we prepared cell extracts from CHO-K1 cells, stably overexpressing APP ER, using conventional SDS-sample buffer containing β-mercaptoethanol (BME) and heated the samples for 10 minutes at various temperatures, from 0 to 85°C. We found that the APP dimer, detected in the absence of heating, was progressively reduced entirely to the monomeric form, which increased simultaneous upon high temperatures (Fig. 12A and B). However, in the absence of BME, APP migrates as dimers, additional to the monomeric form, even when samples were heated for 10 minutes (Fig. 8C). These results indicated that under standard detergent lysis conditions, APP might form disulfide-bound dimers which can only be fully reduced by extended heat denaturing in the presence of BME (Fig. 12A).

Together these findings implicated that APP dimerization was apparently initiated in the ER, likely by disulfide-bond formation, supported by oxidative conditions. However, dimerization properties seemed to be less efficient, when APP progressed further within the secretory pathway, as demonstrated by APP Golgi, comprising an ER exit determinant. Therefore, we provide the first evidence that it was possible to visualize APP dimer formation in the early secretory pathway in CHO-K1 cells, by exposing it to a suitable redox milieu. We reason that permanent retention of APP in the ER selectively increased the quantity of APP molecules, directed into the ER lumen, resulting in a strong formation of SDS-stable homodimers, likely associated by intermolecular disulfide bond(s). Therefore, these stable dimers became visible on western blot analysis. In contrast, when APP could traffic beyond the ER compartment, as shown for the KKFF mutant, dimerization was less concentrated and not visible at steady state levels on western blot analysis. This implicated that dimerization of APP is a dynamic process, normally in a monomer-dimer equilibrium, which can be shifted towards a more dimeric state within the ER, where ideal conditions for disulfide bond formation are provided (Freedman et al. 1984; Turano et al. 2002) (see illustration in Fig.27). These data indicated for the first time that the APP dimerization most likely occurred in the ER lumen via intermolecular cysteine bond. Moreover, the ER contains high amounts of *protein disulfide isomerase* (PDI), the physiological catalyst of native disulfide bond formation of nascent peptides in the cells (Wang 1998), as an important aspect of protein folding and assembly within the ER (Freedman et al. 1984). These bonds do not form in the cytosol, which is characterized by a reducing environment that maintains cysteine residues in their reduced (-SH) state (Frand et al. 2000). In the ER, however, an oxidizing environment promotes disulfide (S-S) bond formation, which is facilitated by the enzyme

PDI, located in the ER lumen (Freedman et al. 1984; Turano et al. 2002). Since the formation of disulfide bonds is a process which requires suitably oxidizing conditions, we postulate that cysteine residues, only present in E1 domain of APP, can produce stable, covalently linked protein homodimers (see Fig. 27). Research efforts so far have shown that APP dimerization was mostly due to the interaction of two E1 domains, whereas the precise mode of action remained elusive. Therefore we provide a model, favoring interchain disulfide bond formation between two APP molecules, although we do not exclude that APP can also dimerize in other cellular compartments, e.g. at the cell surface. Since APP has been suggested to exist in a monomer-dimer equilibrium (Soba et al. 2005), it seems possible that it might dimerize at the surface or within the Golgi by other mechanisms than disulfide bridges, e.g. hydrophobic interactions. Therefore, disulfide-bridges might represent one mechanism of how APP can form homodimers within the cell, however not excluding the existence of different dimer species, possibly associated by hydrogen bonds between the TM domains of two molecules in close proximity (Kienlen-Campard et al. 2008). By retaining APP in the ER, via a specific KKAA motif, we selectively enriched the local concentration of APP molecules directed into the oxidizing ER lumen, which enabled us to visualize a dimer formation as beginning in the ER. Moreover, dimerization was less intense and not visible with our experimental conditions, when APP was shuttled between ER and Golgi compartment, due to the KKFF ER exit determinant. We therefore consider that APP exists in a monomer-to-dimer equilibrium, which may vary in different cell compartments, or possibly depends on the redox state of a given cell. We hypothesize that under physiological conditions a small APP portion dimerizes in the ER via disulfide bonds, likely representing a sub-population of APP dimers. In support of our proposed model that covalent S-S bonds are likely involved in APP-APP interactions, was the finding that in the presence of the reducing agent DTT, in the medium of living cells, prevented the formation of newly synthesized APP dimers (Fig. 12C). As a next step we assured that dimer formation was indeed due to the subcellular localization of APP, rather than the retention motif itself. Therefore we made use of LRP1, another transmembrane protein, which we also tagged with a C-terminal KKAA ER retention signal (Fig. 10A and B). Unlike APP, the N-terminal truncated version of LRP1 (LRP-CT) did not reveal SDS-stable dimers upon ER retention, despite a plethora of cysteine residues, which indicated that this mode of dimerization was specific for APP. Many studies that analyze disulfide bond formation in proteins use N-ethylmaleimide (NEM) to prevent thiol/disulfide exchange (Senkevich et al. 2002; Herscovitch et al. 2008). Therefore, we applied 40 mM NEM in the lysis buffer to prevent post-lysis disulfide bond formation of free cysteine residues (Fig. 10C). Since the upper band did not disappear upon NEM treatment, we conclude that APP dimers must have been assembled within the cell and disulfide bonds were generated during the folding process in the ER, prior to lysis.

Figure 27

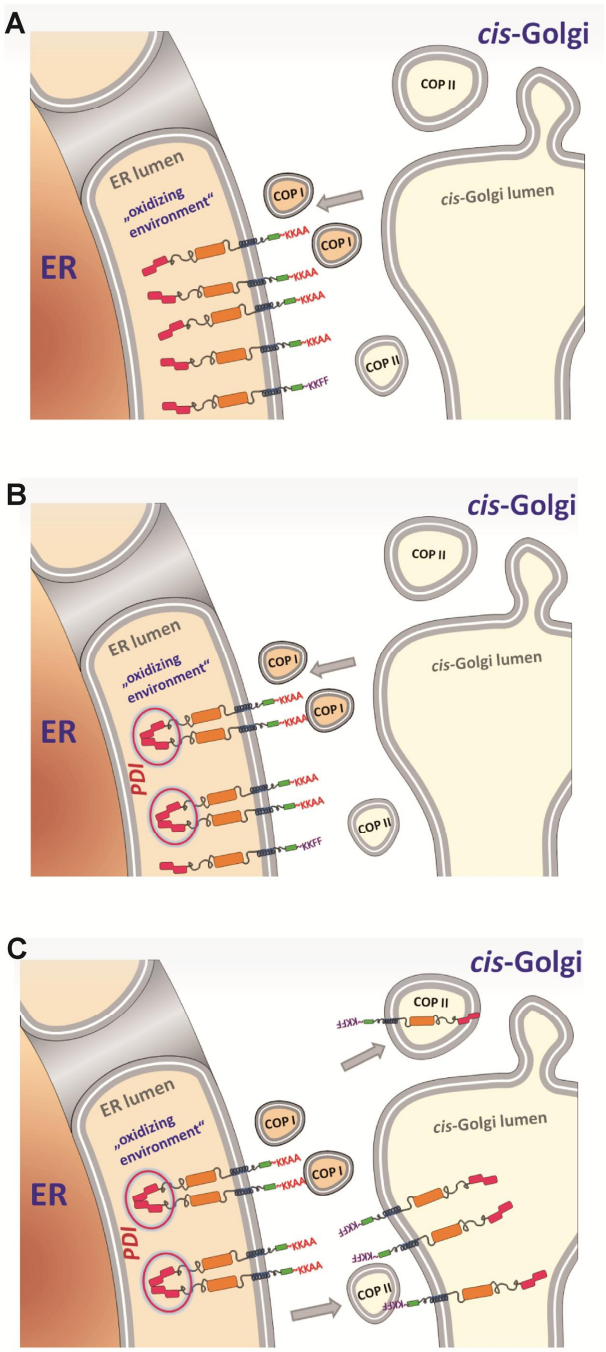

Fig. 27: Schematic depiction of APP dimer formation in the endoplasmic reticulum

(A) We generated APP695 chimeras, either containing the C-terminal KKAA dilysine ER retention-motif or the "leaky" amino acid sequence KKFF, comprising the double-phenylalanine ER exit determinant. The KKAA motif likely intercats with COP I vesicles, mediating a strong retention/retrieval to the ER, whereas the KKFF signal allows further progress to the *cis*-Golgi. By retaining APP in the ER, the local concentration of molecules directed into the oxidizing ER lumen, was selectively enriched which facilitates to visualize a dimer formation as beginning in the ER.

(B) An oxidizing environment as provided by the ER pomotes disulfide (S-S) bond formation, which is facilitated by the enzyme *protein disulfide isomerase* (PDI), located in the ER lumen. Since the formation of native disulfide bonds is a process, requiring suitably oxidizing conditions, we postulate that cysteine residues, only present in E1 domain of APP, can produce stable, covalently linked protein dimers. However, dimerization properties seemed to be less efficient, and therefore not visible, when APP progressed further within the secretory pathway, as demonstrated by APP KKFF (Golgi).

(C) We hypothesize that there exists an APP monomer-to-dimer equilibrium, which may vary in different cell compartments, or possibly depends on the redox state of a given cell. Therefore, we predict that under physiological conditions a only small APP portion dimerizes in the ER via disulfide bonds, likely representing a sub-population of APP dimers. Due to the rapid travel along the secretory route, this fraction becomes not visible when APP travels fast along the secretory route.

To confirm that the higher molecular weight form of APP that we detected under non-reducing conditions was indeed an APP homodimer, and no heterodimer with any other protein of the similar molecular weight, we employed differently tagged APP constructs. When both APP variants were co-expressed in CHO-K1 cells, a high molecular weight band was detected under non-reducing conditions with either myc-, or HA antibody (Fig.11). Thus, confirming that the upper band corresponds to a dimer, equally composed of APP myc and APP HA, also indicating that APP can form homodimers in a cellular context. Furthermore, the finding that dimerization happened between various tagged APP species (myc/HA), excludes unspecific aggregation with cellular proteins, other than APP itself. This is in agreement with the study by Scheuerman and colleagues who were unable

to detect the presence of any proteins other than APP itself in oligomers, after cross-linking proteins in membrane enriched fractions, suggesting that oligomeric APP normally exists in cells, as well defined dimers or higher multimers (Scheuermann et al. 2001).

To obtain additional evidence for the dimerization of APP within the ER we used brefeldin A (BFA) as a specific inhibitor of anterograde membrane transport, blocking protein secretion at an early step in the secretory pathway (Takatsuki and Tamura 1985; Misumi et al. 1986; Nebenfuhr et al. 2002). We were able to accomplish dimerization of APP695 wt (without a KKAA motif) when we treated cells with BFA, verifying that not the KKAA signal itself induced dimerization, but exposure to a sufficient redox environment (Figs. 13 and 14). We found that the generated dimers were resistant to SDS treatment, suggesting that stable intermolecular disulfide bonds between cysteine residues within opposed APP molecules might maintain dimerization. However, the KKAA retention motif caused a stronger APP dimer formation, compared to cell cultures of APP wt treated with BFA (Fig. 13). This could be partially explained by the fact that the retention motif was specific for APP, whereas BFA led to a general blockade of protein export (Fig. 13). Moreover, BFA causes an apparent dissolution of the Golgi-complex, leading to a particular resorption of the Golgi compartment into the ER (Caporaso et al. 1992), thus altering enzyme compositions or pH values within the ER, which might reduce APP dimer formation. Interestingly, additional treatment of APP ER cell cultures with BFA further stabilized the preexisting dimers, and the monomer-dimer equilibrium was shifted in favor of dimers (Fig. 14). This clearly indicated that APP dimerization represents a dynamic process which can be modified in early secretory compartments.

Perturbations that alter ER homeostasis can lead to the accumulation of unfolded proteins, which activate an intracellular signaling pathway – the unfolded protein response (UPR) (reviewed in Kaufman 1999), resulting in up-regulation of transcription factors and expression of ER-resident chaperones, in order to deal with accumulated protein aggregates (Schroder and Kaufman 2005). Pharmacological methods e.g. treatment with brefeldin A (BFA) and tunicamycin (TM) can be used to induce ER stress and activate the UPR as monitored by increased levels in ER chaperones, such as Bip/Grp78 (Preston et al. 2009). According to that we assured that our cell model system, stably overexpressing APP ER, was not accessible to increased ER stress, since we selectively enriched the bulk of APP molecules within the ER. In fact, analysis of steady state protein levels revealed that the APP surplus in the ER only caused a minor Bip/Grp78 up-regulation, which was negligible when compared to APP wt overexpression (Fig 15). In contrast, tunicamycin, an inhibitor of N-glycosylation (Schroder and Kaufman 2005), or BFA act as real ER stress activators, rapidly and significantly up-regulating the expression of Bip/Grp78 more than 3-fold, when compared to APP wt (Fig. 15B). These results demonstrated that the overexpression of APP ER did not trigger an ER related stress response, but that overexpression of proteins causes a temporary ER overload, slightly activating the ER folding machinery. To obtain further independent evidence that APP oligomerization starts in the ER, we applied the strategy of Bimolecular Fluorescence Complementation (BiFC), using split GFP constructs. This fluorescent-based technique allows the detection of APP-APP interactions and provdes information on its subcellular location. Therefore, non-fluorescent fragments of GFP were separately fused to the C-termini of APP695 wt, which then reconstitute the active fluorophore, when the

interacting partners associate (Cabantous and Waldo 2006). Consequently, we could show that APP695 wt (without an ER retention signal) initially interacted in the ER, by performing co-staining with the ER marker Bip/Grp78 (Fig 16A). However, on SDS-PAGE and western blots this fraction of APP wt dimers was only detected upon inhibition of ER-export. Due to its rapid passage through the secretory pathway, the local concentration of APP in the ER was not high enough to monitore a beginning dimer formation under normal conditions. Therefore, this fraction of SDS-stable dimers was only visible after concentrating APP in the ER by using a specific retention signal, or inhibiting protein export with BFA. Nevertheless, both methods apparently identified the ER as the origin of stable APP dimers.

However, several studies demonstrated the existence of APP-APP interactions at the plasmamembrane, either by co-IPs after cross linking surface bound APP, or by FRET anylasis (Soba et al. 2005; Kaden et al. 2009). Furthermore, recent studies have reported that the isolated E1 domain of APP, as well as the full length protein, can from tightly bound dimers upon interaction with heparin at the cell surface (Gralle et al. 2006; Dahms et al. 2010). In support of this view, the addition of *heparinase* has been shown to disrupt cell-surface APP dimers in an over-expressing cell model (Gralle et al. 2009). Since we identified the ER as source for disulfide bound APP dimers, we aimed to show that such dimers exist indeed within other cell compartments and can be transported further to the plasmamembrane. As a first attempt to visualize disulfide-bound APP dimers at the cell surface, we have initially co-expressed a dominant negative mutant of Adapter Protein 180 (AP180 D/N) (Fig. 9A). This construct comprises the clathrin-binding domain at the C-terminal region of AP180 (65 kDa), and its expression is known to inhibit clathrin-mediated endocytosis (Zhao et al. 2001). Although AP180 D/N led to a clear increase of mature APP at the cell surface, we did not detect any SDS-resistant dimers when we simply inhibited endocytosis (Fig 9A). In order to prove that disulfide bound dimers occur at the cell surface, after being generated in the ER, we chose a different approach combining brefeldin A (BFA) and chlorpromazin (CPZ) treatments. We first slowed down protein export from the ER with BFA to allow the formation of stable APP dimers. Subsequently, progression to the surface was permitted after the removal of BFA and application of chlorpromazine (CPZ), which inhibited further endocytosis from the surface (Wang et al. 1993). Indeed, we could capture minor amounts of disulfide linked dimers at the cell surface, which disappeared upon reduction with BME (Fig. 17A and B). Most interestingly, we observed a slight size shift in dimer bands, which likely displayed different glycosylation patterns of immature and mature dimers. Taken together, this indicated that APP dimers were initially generated in the ER, but matured during transport and remained stably associated along the secretory pathway to the plasma membrane. We therefore hypothesize that dimer formation via disulfide bonds starts in the ER, but since APP travels rapidly along the secretory route, this fraction became only visible upon inhibition of ER export, demonstrated by the KKAA retention construct or BFA. Since it was uncertain how long these dimers might reside at the cell surface, or how rapid they can be endocytosed, this particular portion of APP dimers became visible upon inhibition of internalization with CPZ. Therefore, our cell culture model exemplified APP dimerization as it might occur under different cellular conditions. We could particularly visualize dimerization itself and identified the ER as the subcellular compartment of its

origin, where ideal oxidizing conditions might favor disulfide bond formation between APP molecules within the same cell (Freedman et al. 1984; Freedman et al. 1988; Turano et al. 2002). Beside other proposed mechanisms for APP dimerization (Soba et al. 2005, Munter et al. 2007), we assume that intermolecular disulfide linkage between cysteines, located in the E1 domain, might represent another mechanism of how at least an APP sub-fraction can dimerize.

5.2 APP dimerization depends on the N-terminal E1 domain

The findings so far strongly argue for a mechanism that drives APP dimerization by its N-terminal cysteine rich E1-domain. To accomplish a more comprehensive picture, which parts of the protein can influence dimerization, we first focused on the C-terminal, cytoplasmic region. Since we have shown that APP dimerized very efficiently in an oxidizing environment, we were interested whether one can interfere with the topology of APP dimers in the ER, by overexpressing adapter or scaffold proteins, binding to the NP*X*Y-motif in the APP C-terminus (Kimberly et al. 2001; Miller et al. 2006). A number of proteins has been reported to interact with the GYENPTY motif in the APP cytosolic domain, including Mint-1/X11 and X11 like proteins (Mint-2 and Mint-3) (Rogelj et al. 2006), Fe65 (as well as Fe65-like proteins, Fe65L1 and Fe65L2) (Guenette et al. 1996; Kimberly et al. 2001) and c-Jun N-terminal kinase (JNK)-interacting protein (JIP) (Annaert and De Strooper 2002), through the phosphotyrosine-binding (PTB) domain (Ando et al. 1999; Kimberly et al. 2005). In response to the overexpression of either X11α or Fe65 in APP ER cells, we found a strengthened dimerization which was even stronger for X11α (Fig. 19A). This was consistent with findings that both adapter proteins stabilized either APP intracellular fragments (AICD), or increased the half-life of full length APP (Kimberly et al. 2001; Pietrzik et al. 2004). It was demonstrated that cells overexpressing X11 showed intracellular APP accumulation, resulting in less processing, diminished Aβ production, and impaired maturation by reduced *O*-glycosylation (Tomita et al. 1999). As mentioned before, we found that none of the tested proteins was able to break up APP dimerization, in contrary binding of Fe65 or X11α particularly increased APP stability of both, monomers and dimers. Moreover, these results also indicated that APP ER did not represent a folding intermediate or misfolded protein, because it was still capable of binding C-terminal cytoslic adapter proteins, as confirmed by co-IPs with Fe65. This assured that adapter proteins had access to the cytosolic part of APP, since the N-terminus is directed into the ER lumen and the C-terminus remains exposed into the cytoplasm. Consistent with our model these findings point out that APP dimerization was likely achieved and sustained via its N-terminal part.

To further support our proposed model that disulfide bond(s) might stabilize a subpopulation of APP dimers, we next focused on the N-terminal part. Two current studies have previously claimed that the E1 domain serves as the main interaction site of full length APP dimerization (Soba et al. 2005; Kaden et al. 2009). This region encompasses the growth factor-like domain (GFLD) and a copper-binding domain (CuBD) (Small et al. 1994; Rossjohn et al. 1999), which contain together 12 cysteine residues, potentially promoting stable covalently linked dimers or higher multimers. To verify that the E1 domain represents the main interface for APP homo-interactions, we generated stable cell lines, overexpressing APP695 deletion constructs, lacking the N-terminal growth factor-like-, and

copper-binding-domains (ΔE1) consequently omitting all of the cysteines. Strikingly, the generated deletion constructs were incapable of forming stable high molecular weight species, regardless of ER retention or not (Fig. 20A), indicating that the E1 domain was indispensible for generating SDS-resistant APP homodimers. This outcome was in agreement with results obtained by Soba and colleagues, where they found that all mutant APP/APLPs lacking the E1 domain, or the entire ectodomain, were weakly, or not coimmunoprecipitated (Soba et al. 2005). However, deletion of the central carbohydrate (E2) domain did not abolish APP homo-or APP/APLP heterointeractions in coimmunoprecipitation experiments (Soba et al. 2005). Another study by Kaden and colleagues confirmed most of the previous results, using a FRET approach in living HEK293T cells, using CFP-and YFP-tagged deletion mutans Kaden et al. 2009). In addition to the aforementioned studies we provide further strong evidence that the E1 domain, harboring a variety of cysteine residues, is essentially involved in APP dimer formation.

To dissect single cysteines within the APP E1 domain, which might contribute to APP dimer formation, we focused on on a specific region within the E1 domain, encompassing amino acids (aa) 96-118 (see illustration in Fig. 21A), which form a surface exposed loop between Cys98 and Cys105 of APP (Kaden et al. 2008). Kaden and co-workers were able to demonstrate that a molar excess of a peptide that mimics the surface exposed loop, interfered slightly with oligomerization of the N-terminal domain of recombinant APP (residues 18-350) (Kaden et al. 2008). Surface plasmon resonance analysis revealed that this peptide was specifically bound to the N-terminal domain of APP, and that binding was entirely dependent on the oxidation of the thiol groups. Interestingly, application of a mutant-loop peptide, where cysteine residues were replaced by serines, had no effect on N-terminal APP interactions. However, they reasoned that APP dimerization might be accomplished via hydrophobic and electrostatic interactions between two E1 domains (Kaden et al. 2008). Since we postulate that the E1 domain, and in particular cysteine residues, are responsible for dimer formation of APP in the ER, it was of interest which of the respective cysteines might participate in intermolecular disulfide linkage of APP molecules. We tested this in a cellular context, and generated the corresponding serine substitutions at positions 98 and 105 of APP695 (Fig. 21A). Interestingly, replacement of these cysteines prevented homodimerization in the ER, indicating once more that dimers are stabilized by disulfide formation. Thus, given that these dimers are the result of intermolecular disulfide bridges, we conclude that the disulfide-bound loop also plays a crucial role in the covalent dimerization of full length APP. In contrary to the previous study by Kaden and colleagues we have employed the full length protein instead of an isolated, soluble, truncated APP fragment, thus reflecting physiological conditions more closely. However, we cannot exclude that mutation of other cysteines in the E1 domain might lead to the same result. Taken together, these findings indicated that Cys 98 or Cys 105 participate in intermolecular disulfide bond formation of APP. We therefore postulate that these bonds might occur between Cys98/Cys98 and/or Cys105/Cys105. However, we have no crystallographic or biophysical evidence, supporting that hypothesis.

Other research effort, dissecting the regions potentially involved in APP homodimerization, has focused more on the juxtamembrane (JM) and transmembrane (TM) sequence. APP contains three

glycine-xxx-glycine (GxxxG) motifs at the extracellular JM/TM boundary, which is a unique feature of the APP TM domain, since the other APP family members (APLPs) do not contain GxxxG motifs in their TM region (Kienlen-Campard et al. 2010). These GxxxG motifs were originally shown to mediate very close apposition and dimerization of TM helices of the glycophorin A (GpA) protein, whereby glycine allows the close association of interacting helices, due to its small size (Senes et al. 2001). These observations were of particular interest since the GxxxG motifs in the APP TM domain may participate in dimerization, reminiscent of GpA. Initially, Munter and colleagues found that mutation of G625 and G629 (APP695 numbering) to bulky isoleucines diminished the ability of the APP TM sequence to dimerize in ToxR assays (Munter et al. 2007), which enable the study of TM helix-helix oligomerization in a bacterial membrane environment by measuring the activation of a reporter gene (Russ and Engelmann 1999). However, studies in CHO (mammal) cells indicated that the mutation of the G625 and G629 residues to isoleucine seemed to allow dimerization of the entire C99 protein in cell lines, whereas mutations to leucines (GG 625/629 LL) even triggered the formation of homodimers of the APP C-terminal fragments, instead weakening interaction (Kienlen-Campard et al. 2008). Nevertheless, both studies reported that mutation of the central glycine residues (G625 and G629) in the middle GxxxG motif, led to significantly decreased Aβ production (Munter et al. 2007; Kienlen-Campard et al. 2008). Similarly, compounds that directly interfere with APP TMS dimerization were recently shown to lower Aβ levels likewise (Richter et al. 2010). Nevertheless, having confirmed the importance of the E1 domain for APP interactions, we speculate that we should not monitor the oligomerization of C99 upon ER retention, since potential cysteine residues are absent. On the other hand there was still the possibility that the remaining E2 domain (still present in the ΔE1 constructs) could structurally interfere with close apposition of the APP TM domains. Indeed, when we analyzed the C99 wt and C99 ER (containing the C-terminal KKAA motif) constructs under non-reducing conditions we did not observe any SDS-resistant C99 multimers (Fig. 20B), confirming our previous results that SDS-stable dimer formation is dependent on the E1 domain. However, we cannot exclude that other associations, weaker than disulfide bonds, might also contribute to APP dimerization, such as hydrogen bonds between two proximal TM helices. Unexpectedly, Kienlen-Campard and colleagues have showen that the GG 625/629 LL mutation in the APP βCTF/C99 likely triggered the formation of SDS-resistant C99 dimers (Kienlen-Campard et al. 2008), instead of diminishing dimerization, thus contradicting previous observations in a bacterial membrane system (Munter et al. 2007). Consequently, bulkier leucine residues might not be compatible with the close helix packing, allowed by the GxxxG motifs in ToxR assays. However, they possibly alter the helix orientation, thus promoting SDS-stable C99 dimers as seen on western blot experiments by Kienlen-Campard. Given that no intermolecular disulfide bonds were involved in C99 oligomerization (no cysteines present), we speculate that dimerization of APP TM helices might probably serve as a prerequisite to achieve close apposition of two APP full length molecules, facilitating interactions between E1 domains. Taken together, these results indicate that TM dimerization/oligomerization might be cell specific or dependent on the structure and the composition of the membrane-bilayer in which it was anchored. Finally, it has to be considered that these results have been obtained by expressing exclusively the C-terminal part of APP (C99) and not the full-length protein, therefore the role of the GxxxG motifs in homodimerization of the holoprotein protein is rather speculative, as

demonstrated by inconsistent results (Munter et al. 2007; Kienlen-Campard et al. 2008). Moreover, the study by Munter and co-workers revealed that even perturbed dimerization of APP TM domains had no influence on dimerization of the full-length protein, as demonstrated by FRET experiments with the respective G625/G629 isoleucine mutants (Munter et al. 2007). Consequently, dimerization of full-length APP was dependent on contact sites within the E1 domain, which is in support of our model. Nevertheless, other studies reported that the E2 was required for APP-APP interactions, although revealing somewhat inconsistent results. Wang and Ha were able to crystallize an antiparallel dimer of a recombinant (bacterial) produced E2 domain (aa 365-566) (Wang and Ha 2004). In contrast, another study by Dulubova and colleagues used a truncated version of the E2 domain (aa 460-576) which crystallized exclusively monomeric, possibly due to the lack of crucial amino acids, normally participating in dimer formation, or various purification protocols (Dulubova et al. 2004).

5.3 The KPI-containing APP isoforms display reduced *cis*-dimerization in the same cell, but not at the surface of different cells in *trans*-direction

All studies so far have largely focused on the dimerization properties of the neuronal isoform APP695 lacking the KPI domain, therefore it was of interest if the longer isoforms behave in the same manner as APP695. The longer two APP isoforms contain a so called Kunitz type protease inhibitor (KPI) domain, which was the first APP fragment to be crystallized in 1990 (Hynes et al. 1990), encoded by a single exon (exon 7 of APP), which is translated into a 57-amino-acid insert (see Fig. 3) in the middle of the APP sequence (Oltersdorf et al. 1989; Hynes et al. 1990). Due to the fact that the KPI domain encompasses six further cysteine residues, in addition to the 12 cysteines already present in the E1 domain, one might imagine an increased dimerization potential by disulfide linkage. Surprisingly, when APP770 or APP751 were retained in the ER, no *cis*-directed homodimer formation was observed on western blots (Fig. 22A and B). Interestingly, the KPI-containing isoform APP770 showed almost no co-interaction in the ER using immunoprecipitation studies (see Fig. 23). However, when the wt constructs were used, exclusively mature APP770 HA was co-purified with its myc-tagged counterpart, whereas APP695 co-precipitated with both glycosylation species. This indicated that KPI-APP can as such interact within the same cell, but interaction probably occurred downstream of the ER, e.g. the plasma membrane, therefore only fully glycosylated forms were recovered in co-IPs. Conversely, we were able to induce *cis*-dimerization of APP770 in the ER, using a previously described (Scheuermann et al. 2001; Eggert et al. 2009) constitutive engineered dimerization mutant (APP770 K28C, Fig. 24A). This led us to the assumption that the KPI might somehow exhibit a sterical obstruction, possibly diverging two E1 domains, thus interfering with dimerization. Nevertheless, the close proximity of two APP TM domains might be sufficient to cross-link the full length proteins by the constitutive K28C mutant (Fig. 24C). Interestingly, this cysteine mutant also reached the cell surface (Fig. 24B), yet the disulfide bond can only be formed in the ER via oxidation, confirming our hypothesis that once generated, covalent dimers are trafficked normally in the cell (Fig. 17). Moreover, this suggested close apposition between APP molecules, otherwise this constitutive disulfide bond could have never been generated via oxidation in the ER.

Having demonstrated that dimer formation of KPI-APP seemed to be inhibited in the ER, but was induced by an engineered disulfide bond, we questioned whether APP isoforms might also display diverse *trans*-dimerization capacities at the surface, affecting cell adhesion. We employed a well described cell aggregation assay in *Drosophila Schneider* (S2)-cells, previously established by Soba et al., where they could demonstrate that APP695 can form homo-as well as hetero-complexes with APLPs at the surface of different cells (Soba et al. 2005). However, expression of all three different APP isoforms in S2-cells led to equal cell clustering (Fig. 25A and C), whereas the absence of the extracellular E1 domain abolished specific aggregation of transfected S2 cells (Fig. 25B), consistent with observations by Soba and colleagues. Therefore, we speculate that the KPI domain might hinder exclusively *cis*-dimerization of APP within the same cell, whereas *trans*-dimers at the surface of two or more cells, was unperturbed (see illustration Fig. 26D). These findings raised the question, how the differences in *cis/trans* interactions between isoforms can be explained? Interestingly, it has been shown by small-angle X-ray scattering (SAXS; method to obtain high resolution three dimensional protein structures) that a domain, corresponding to the KPI domain of APP770, emerges laterally from one end of the molecule and was freely exposed on the APP surface (Gralle et al. 2006; Gralle et al. 2007). Therefore, we speculate that the KPI domain might adapt different structural features depending on the redox state maintained in a subcellular compartment or microdomain. It might be possible that the six cysteine residues present in the KPI domain (Menendez-Gonzales et al. 2005), cause a special folding due to intramolecular disulfide bonds (Rossjohn et al. 1999) in the ER, but not at the cell surface. Consequently, such conformational changes might potentially hinder dimerization of two adjacent APP molecules only in *cis*-direction (Figs. 23 and 24). In contrast, APP *trans*-dimerization was sterically obstructed by the presence of the KPI domain since two opposite E1 domains can still interact (see hypothetical illustration in Fig. 25D). While it was possible to enforce lateral *cis*-dimerization by introducing a constitutive disulfide bond at the TM border of APP (K28C), irrespective of a KPI domain, we speculate that the vicinity of two molecules (or TM helices), was crucial for *cis*-dimerization (Munter et al. 2007). If two APP molecules are located in close proximity within the same membrane, the redox state of the ER might be sufficient to link them between cysteine residues of the E1 domain, or likewise by an engineered disulfide bond. Nevertheless, we assume that *trans*-dimerization in this aggregation assay is primarily established by hydrophobic interactions, instead of S-S bonds, since cell surface PDI has so far only been identified in few cell types, shown to modify disulfide bonds e.g. in β-integrins, thus regulating adhesion and migration (Turano et al. 2002). Therefore, these results enable us to speculate that formation of the disulfide-bonded APP dimer can be modulated by the particular isoform, i.e the presence or absence of a KPI domain.

5.4 Heterodimer formation between APP and APLP1 is initiated in the ER

Previous studies revealed that APP and APLP1 exhibit strikingly different subcellular localizations with APP being distributed more intracellularly and APLP1 mainly localized to the cell surface (Soba et al. 2005; Kaden et al. 2009). Consequently, various co-immunoprecipitation approaches by Soba and co-workers implicated that mature, but mostly immature, APP/APLP forms are interacting in COS7 cells,

since recovered proteins displayed a primarily immature glycosylation pattern. This suggested that the large intracellular pool of APP family proteins can form lateral *cis*-dimers, thus the majority of APP/APLP interaction most likely takes place in intracellular compartments e.g. the ER (Soba et al. 2005). To gain further insight into dimerization mechanisms between APP and APLPs we investigated whether we might observe a similar mechanism with one of its homologues. Due to the previously described different cellular distributions, we were curious whether APP might have a retentive influence over APLP1, likely by forming heterodimers as early as in the ER. Indeed, APP was able to retain a portion of APLP1 in the ER, revealed by biotinylation experiments (Fig. 26A and E), consequently preexisting APP homodimers were reduced and monomers increased, vice versa (Fig. 26C). Additionally, co-immunoprecipitations confirmed a stronger interaction between both homologues when APP was retained in the ER (Fig.26B). Most interestingly, we detected the formation of SDS-stable APP/APLP1 heterodimers, suggesting an equivalent mechanism for heterodimer formation, possibly involving disulfide bond(s). Therefore we provide first evidence that it was possible to visualize a beginning dimer formation between both APP and APLP1 early in the secretory pathway, despite diverse subcellular distributions and differerences in their degree of cell surface localization. Taken together, APP could retain and stabilize APLP1 in intracellular compartments, indicating that interactions between the APP family proteins might occur as early as in the ER. This was particularly interesting, due to the fact that hetero-complex formation between APP and APLPs was shown to diminish Aβ production. Therefore, the ER might provide an interesting target possibly favoring dimer equilibrium from homo- to hetreo-complexes, thus influencing Aβ generation.

6 Summary

The amyloid precursor protein (APP) is a type I transmembrane protein, which resembles a cell surface receptor, comprising a large ectodomain, a single spanning transmembrane part and a short C-terminal, cytoplasmic domain. It belongs to a conserved gene family, including the two homologues APP-like proteins (APLP) 1 and 2. Several independent studies have shown that APP can form homodimers within the cell, driven by motifs present in the extracellular domain, as well as in the juxtamembrane (JM) and transmembrane (TM) domains of the molecule. Different experimental approaches have been attempted to elucidate the role of APP dimerization in a physiological or pathological context, as in promoting cell-cell adhesion, or influencing APP cleavage and the release of Aβ, respectively, whereby the exact molecular mechanism and the origin of dimer formation remains elusive. We therefore focused in our study on the actual subcellular origin of APP homo-dimerization within the cell, an underlying mechanism, and a possible impact on dimerization properties of its homologue APLP1. Furthermore, we analyzed homodimerization of different APP isoforms, in particular APP695, APP751 and APP770, which differ in the presence of a Kunitz-type protease inhibitor domain (KPI) in the extracellular region.

In order to assess the cellular origin of dimerization under different cellular conditions, we have established a mammalian cell culture model-system in CHO-K1 cells, stably overexpressing human APP, harboring dilysine based organelle sorting motifs at the very C-terminus (KKAA-Endoplasmic Reticulum (ER); KKFF-Golgi). Consequently, retention within early secretory compartments was accomplished. In this study we show that APP exists as disulfide-bound, SDS-stable dimers, when it was retained in the ER, unlike when it trafficked further to the *cis*-Golgi. These stable APP complexes were isolated from cells, and analyzed by SDS–polyacrylamide gel electrophoresis under non-reducing conditions, whereas strong denaturing and reducing conditions dissolved those dimers. Our findings suggested that APP homodimer formation starts early in the secretory pathway and that the unique oxidizing environment of the ER likely promotes intermolecular disulfide bond formation between APP molecules. We particularly visualized APP dimerization employing a variety of biochemical experiments and investigated the origin of its generation by using a Bimolecular Fluorescence Complementation (BiFC) approach with split GFP-APP chimeras. Moreover, we demonstrate that intermolecular disulfide linkage between cysteine residues, exclusively located in the extracellular E1 domain, represents another mechanism of how an APP sub-fraction can dimerize within the cell. Indeed, deleting either the E1 domain or the entire N-terminal part (C99) abolished APP homodimers in our system, indicating that this region of the APP ectodomain is indispensible for homointeraction. Additionally, mutational studies revealed that cysteines at positions 98 and 105, embedded in the conserved loop region within the E1 domain, are critical for interchain disulfide bond formation. Furthermore, we show that once generated in the oxidative environment of the ER, APP dimers remain stably associated during transport, reaching the plasma membrane. In addition, we provide evidence that APP isoforms encompassing the KPI domain exhibit a strongly reduced capacity to form *cis*-directed dimers in the ER, but interact in later cellular compartments. To assess the *trans*-cellular dimerization potential of each APP isoform, we analyzed cell clustering at the

surface of *Drosophila Schneider* (S2)-cells in an aggregation assay, strongly suggesting that all APP isoforms display the same *trans*-cellular complexes, regardless of the isoform. Moreover, we detected the formation of SDS-stable APP/APLP1 hetero-complexes, suggesting an equivalent mechanism for heterodimer formation, likely involving disulfide bond(s), generated in the ER.

In conclusion, our results provide novel observations with important implications for the regulation of APP dimerization: First, we demonstrate that cell-bound APP can initially dimerize after biosynthesis in the ER (*cis*-dimerization). Second, we show for the first time that APP dimers, containing either single or more intermolecular disulfide bonds can exist in cells, and that cysteines in the E1 domain participate in either stabilizing APP intramolecular, when it is monomeric, or intermolecular by cross-linking two molecules via disulfide bonds as early as in the ER. Moreover, we provide evidence that disulfide-bound APP dimers can traffick to the cell surface, possibly as a prerequisite for its correct orientation and exposure at the plasmamembrane, if APP has receptor-like functions. Third, we clearly identified striking differences between APP isoforms, revealing reduced *cis*-dimerization capacity for KPI-containing APP within the same cell. We therefore believe that there exists an equilibrium of APP monomer-to-dimer, which may vary in different cell types e.g. depending on the redox state of a given cell. Furthermore, our results enable us to speculate that formation of the disulfide-bonded APP dimer can be modulated by the particular isoform, i.e. the presence or absence of a KPI domain. Fourth, by investigating the impact of APP retention in the ER on APLP1 cellular distribution and processing, we show that both proteins form heterocomplexes as early as the ER and APP was able to retain a portion of APLP1 in early secretory compartments. Therefore, dynamic alterations of APP between monomeric, homodimeric, and possibly heterodimeric status could at least partially explain some of the variety in the functions of APP.

This data is partly published in Cell Mol Life Sci. 2011 Nov 22. [Epub ahead of print]

7 References

Akabas, M. H., D. A. Stauffer, M. Xu and A. Karlin (1992). "Acetylcholine receptor channel structure probed in cysteine-substitution mutants." Science 258(5080): 307-310.

Alzheimer, A. (1907). "Über eine eigenartige Erkrankung der Hirnrinde." Allgemeine Zeitschrift Psychiatr Physchisch-Gerichtliche Medizin 64: 146-148.

Ando, K., K. I. Iijima, J. I. Elliott, Y. Kirino and T. Suzuki (2001). "Phosphorylation-dependent regulation of the interaction of amyloid precursor protein with Fe65 affects the production of beta-amyloid." J Biol Chem 276(43): 40353-40361.

Anfinsen, C. B. and H. A. Scheraga (1975). "Experimental and theoretical aspects of protein folding." Adv Protein Chem 29: 205-300.

Anliker, B. and U. Muller (2006). "The functions of mammalian amyloid precursor protein and related amyloid precursor-like proteins." Neurodegener Dis 3(4-5): 239-246.

Annaert, W. and B. De Strooper (2002). "A cell biological perspective on Alzheimer's disease." Annu Rev Cell Dev Biol 18: 25-51.

Aoe, T., E. Cukierman, A. Lee, D. Cassel, P. J. Peters and V. W. Hsu (1997). "The KDEL receptor, ERD2, regulates intracellular traffic by recruiting a GTPase-activating protein for ARF1." Embo J 16(24): 7305-7316.

Arner, E. S. and A. Holmgren (2000). "Physiological functions of thioredoxin and thioredoxin reductase." Eur J Biochem 267(20): 6102-6109.

Baek, S. H., K. A. Ohgi, D. W. Rose, E. H. Koo, C. K. Glass and M. G. Rosenfeld (2002). "Exchange of N-CoR corepressor and Tip60 coactivator complexes links gene expression by NF-kappaB and beta-amyloid precursor protein." Cell 110(1): 55-67.

Bailey, D. and P. O'Hare (2007). "Transmembrane bZIP transcription factors in ER stress signaling and the unfolded protein response." Antioxid Redox Signal 9(12): 2305-2321.

Bannykh, S. I. and W. E. Balch (1997). "Membrane dynamics at the endoplasmic reticulum-Golgi interface." J Cell Biol 138(1): 1-4.

Barlowe, C. (1998). "COPII and selective export from the endoplasmic reticulum." Biochim Biophys Acta 1404(1-2): 67-76.

Barlowe, C. and R. Schekman (1993). "SEC12 encodes a guanine-nucleotide-exchange factor essential for transport vesicle budding from the ER." Nature 365(6444): 347-349.

Baulac, S., M. J. LaVoie, W. T. Kimberly, J. Strahle, M. S. Wolfe, D. J. Selkoe and W. Xia (2003). "Functional gamma-secretase complex assembly in Golgi/trans-Golgi network: interactions among presenilin, nicastrin, Aph1, Pen-2, and gamma-secretase substrates." Neurobiol Dis 14(2): 194-204.

Beher, D., L. Hesse, C. L. Masters and G. Multhaup (1996). "Regulation of amyloid protein precursor (APP) binding to collagen and mapping of the binding sites on APP and collagen type I." J Biol Chem 271(3): 1613-1620.

Bertolotti, A., Y. Zhang, L. M. Hendershot, H. P. Harding and D. Ron (2000). "Dynamic interaction of BiP and ER stress transducers in the unfolded-protein response." Nat Cell Biol 2(6): 326-332.

Bertram, L., C. M. Lill and R. E. Tanzi (2010). "The genetics of Alzheimer disease: back to the future." Neuron 68(2): 270-281.

Bertram, L. and R. E. Tanzi (2004). "The current status of Alzheimer's disease genetics: what do we tell the patients?" Pharmacol Res 50(4): 385-396.

Bertrand, E., E. Brouillet, I. Caille, C. Bouillot, G. M. Cole, A. Prochiantz and B. Allinquant (2001). "A short cytoplasmic domain of the amyloid precursor protein induces apoptosis in vitro and in vivo." Mol Cell Neurosci 18(5): 503-511.

Beyer, A. S., B. von Einem, D. Schwanzar, I. E. Keller, A. Hellrung, D. R. Thal, M. Ingelsson, A. Makarova, M. Deng, E. S. Chhabra, C. Propper, T. M. Bockers, B. T. Hyman and C. A. von Arnim (2010). "Engulfment adapter PTB domain containing 1 interacts with and affects processing of the amyloid-beta precursor protein." Neurobiol Aging.

Borg, J. P., J. Ooi, E. Levy and B. Margolis (1996). "The phosphotyrosine interaction domains of X11 and FE65 bind to distinct sites on the YENPTY motif of amyloid precursor protein." Mol Cell Biol 16(11): 6229-6241.

Bork, P. and B. Margolis (1995). "A phosphotyrosine interaction domain." Cell 80(5): 693-694.

Braakman, I., H. Hoover-Litty, K. R. Wagner and A. Helenius (1991). "Folding of influenza hemagglutinin in the endoplasmic reticulum." J Cell Biol 114(3): 401-411.

Breen, K. C., M. Bruce and B. H. Anderton (1991). "Beta amyloid precursor protein mediates neuronal cell-cell and cell-surface adhesion." J Neurosci Res 28(1): 90-100.

Brookmeyer, R., E. Johnson, K. Ziegler-Graham and H. M. Arrighi (2007). "Forecasting the global burden of Alzheimer's disease." Alzheimers Dement 3(3): 186-191.

Brown, M. S., J. Ye, R. B. Rawson and J. L. Goldstein (2000). "Regulated intramembrane proteolysis: a control mechanism conserved from bacteria to humans." Cell 100(4): 391-398.

Burdick, D., B. Soreghan, M. Kwon, J. Kosmoski, M. Knauer, A. Henschen, J. Yates, C. Cotman and C. Glabe (1992). "Assembly and aggregation properties of synthetic Alzheimer's A4/beta amyloid peptide analogs." J Biol Chem 267(1): 546-554.

Bush, A. I., G. Multhaup, R. D. Moir, T. G. Williamson, D. H. Small, B. Rumble, P. Pollwein, K. Beyreuther and C. L. Masters (1993). "A novel zinc(II) binding site modulates the function of the beta A4 amyloid protein precursor of Alzheimer's disease." J Biol Chem 268(22): 16109-16112.

Cabantous, S. and G. S. Waldo (2006). "In vivo and in vitro protein solubility assays using split GFP." Nat Methods 3(10): 845-854.

Cao, X. and T. C. Sudhof (2001). "A transcriptionally [correction of transcriptively] active complex of APP with Fe65 and histone acetyltransferase Tip60." Science 293(5527): 115-120.

Cao, X. and T. C. Sudhof (2004). "Dissection of amyloid-beta precursor protein-dependent transcriptional transactivation." J Biol Chem 279(23): 24601-24611.

Capell, A., D. Beher, S. Prokop, H. Steiner, C. Kaether, M. S. Shearman and C. Haass (2005). "Gamma-secretase complex assembly within the early secretory pathway." J Biol Chem 280(8): 6471-6478.

Caporaso, G. L., S. E. Gandy, J. D. Buxbaum and P. Greengard (1992). "Chloroquine inhibits intracellular degradation but not secretion of Alzheimer beta/A4 amyloid precursor protein." Proc Natl Acad Sci U S A 89(6): 2252-2256.

Caughey, B. and P. T. Lansbury (2003). "Protofibrils, pores, fibrils, and neurodegeneration: separating the responsible protein aggregates from the innocent bystanders." Annu Rev Neurosci 26: 267-298.

Chartier-Harlin, M. C., F. Crawford, K. Hamandi, M. Mullan, A. Goate, J. Hardy, H. Backhovens, J. J. Martin and C. V. Broeckhoven (1991). "Screening for the beta-amyloid precursor protein mutation (APP717: Val----Ile) in extended pedigrees with early onset Alzheimer's disease." Neurosci Lett 129(1): 134-135.

Chen, W. J., J. L. Goldstein and M. S. Brown (1990). "NPXY, a sequence often found in cytoplasmic tails, is required for coated pit-mediated internalization of the low density lipoprotein receptor." J Biol Chem 265(6): 3116-3123.

Chyung, J. H., D. M. Raper and D. J. Selkoe (2005). "Gamma-secretase exists on the plasma membrane as an intact complex that accepts substrates and effects intramembrane cleavage." J Biol Chem 280(6): 4383-4392.

Citron, M., T. Oltersdorf, C. Haass, L. McConlogue, A. Y. Hung, P. Seubert, C. Vigo-Pelfrey, I. Lieberburg and D. J. Selkoe (1992). "Mutation of the beta-amyloid precursor protein in familial Alzheimer's disease increases beta-protein production." Nature 360(6405): 672-674.

Citron, M., D. Westaway, W. Xia, G. Carlson, T. Diehl, G. Levesque, K. Johnson-Wood, M. Lee, P. Seubert, A. Davis, D. Kholodenko, R. Motter, R. Sherrington, B. Perry, H. Yao, R. Strome, I. Lieberburg, J. Rommens, S. Kim, D. Schenk, P. Fraser, P. St George Hyslop and D. J. Selkoe (1997). "Mutant presenilins of Alzheimer's disease increase production of 42-residue amyloid beta-protein in both transfected cells and transgenic mice." Nat Med 3(1): 67-72.

Cordell, B. (1994). "beta-Amyloid formation as a potential therapeutic target for Alzheimer's disease." Annu Rev Pharmacol Toxicol 34: 69-89.

Cosson, P., C. Demolliere, S. Hennecke, R. Duden and F. Letourneur (1996). "Delta- and zeta-COP, two coatomer subunits homologous to clathrin-associated proteins, are involved in ER retrieval." Embo J 15(8): 1792-1798.

Cosson, P. and F. Letourneur (1994). "Coatomer interaction with di-lysine endoplasmic reticulum retention motifs." Science 263(5153): 1629-1631.

Coulson, E. J., K. Paliga, K. Beyreuther and C. L. Masters (2000). "What the evolution of the amyloid protein precursor supergene family tells us about its function." Neurochem Int 36(3): 175-184.

Dahms, S. O., S. Hoefgen, D. Roeser, B. Schlott, K. H. Guhrs and M. E. Than (2010). "Structure and biochemical analysis of the heparin-induced E1 dimer of the amyloid precursor protein." Proc Natl Acad Sci U S A 107(12): 5381-5386.

Daigle, I. and C. Li (1993). "apl-1, a Caenorhabditis elegans gene encoding a protein related to the human beta-amyloid protein precursor." Proc Natl Acad Sci U S A 90(24): 12045-12049.

Dancourt, J. and C. Barlowe (2010). "Protein sorting receptors in the early secretory pathway." Annu Rev Biochem 79: 777-802.

Dawson, G. R., G. R. Seabrook, H. Zheng, D. W. Smith, S. Graham, G. O'Dowd, B. J. Bowery, S. Boyce, M. E. Trumbauer, H. Y. Chen, L. H. Van der Ploeg and D. J. Sirinathsinghji (1999). "Age-related cognitive deficits, impaired long-term potentiation and reduction in synaptic marker density in mice lacking the beta-amyloid precursor protein." Neuroscience 90(1): 1-13.

Dobson, C. M. (2004). "Experimental investigation of protein folding and misfolding." Methods 34(1): 4-14.

Dries, D. R. and G. Yu (2008). "Assembly, maturation, and trafficking of the gamma-secretase complex in Alzheimer's disease." Curr Alzheimer Res 5(2): 132-146.

Duden, R., V. Allan and T. Kreis (1991). "Involvement of beta-COP in membrane traffic through the Golgi complex." Trends Cell Biol 1(1): 14-19.

Duden, R., L. Kajikawa, L. Wuestehube and R. Schekman (1998). "epsilon-COP is a structural component of coatomer that functions to stabilize alpha-COP." Embo J 17(4): 985-995.

Duilio, A., R. Faraonio, G. Minopoli, N. Zambrano and T. Russo (1998). "Fe65L2: a new member of the Fe65 protein family interacting with the intracellular domain of the Alzheimer's beta-amyloid precursor protein." Biochem J 330 (Pt 1): 513-519.

Dulubova, I., A. Ho, I. Huryeva, T. C. Sudhof and J. Rizo (2004). "Three-dimensional structure of an independently folded extracellular domain of human amyloid-beta precursor protein." Biochemistry 43(30): 9583-9588.

Duncan, B. A. and A. P. Siegal (1998). "Early diagnosis and management of Alzheimer's disease." J Clin Psychiatry 59 Suppl 9: 15-21.

Dyrks, T., A. Weidemann, G. Multhaup, J. M. Salbaum, H. G. Lemaire, J. Kang, B. Muller-Hill, C. L. Masters and K. Beyreuther (1988). "Identification, transmembrane orientation and biogenesis of the amyloid A4 precursor of Alzheimer's disease." Embo J 7(4): 949-957.

Edbauer, D., E. Winkler, J. T. Regula, B. Pesold, H. Steiner and C. Haass (2003). "Reconstitution of gamma-secretase activity." Nat Cell Biol 5(5): 486-488.

Eggert, S., B. Midthune, B. Cottrell and E. H. Koo (2009). "Induced dimerization of the amyloid precursor protein leads to decreased amyloid-beta protein production." J Biol Chem 284(42): 28943-28952.

Eggert, S., K. Paliga, P. Soba, G. Evin, C. L. Masters, A. Weidemann and K. Beyreuther (2004). "The proteolytic processing of the amyloid precursor protein gene family members APLP-1 and APLP-2 involves alpha-, beta-, gamma-, and epsilon-like cleavages: modulation of APLP-1 processing by n-glycosylation." J Biol Chem 279(18): 18146-18156.

Ehehalt, R., P. Keller, C. Haass, C. Thiele and K. Simons (2003). "Amyloidogenic processing of the Alzheimer beta-amyloid precursor protein depends on lipid rafts." J Cell Biol 160(1): 113-123.

Endres, K., R. Postina, A. Schroeder, U. Mueller and F. Fahrenholz (2005). "Shedding of the amyloid precursor protein-like protein APLP2 by disintegrin-metalloproteinases." Febs J 272(22): 5808-5820.

Esch, F. S., P. S. Keim, E. C. Beattie, R. W. Blacher, A. R. Culwell, T. Oltersdorf, D. McClure and P. J. Ward (1990). "Cleavage of amyloid beta peptide during constitutive processing of its precursor." Science 248(4959): 1122-1124.

Fausto-Sterling, A., F. A. Muckenthaler, L. Hsieh and P. L. Rosenblatt (1985). "Some determinants of cellular adhesiveness in an embryonic cell line from Drosophila melanogaster." J Exp Zool 234(1): 47-55.

Feinberg, E. H., M. K. Vanhoven, A. Bendesky, G. Wang, R. D. Fetter, K. Shen and C. I. Bargmann (2008). "GFP Reconstitution Across Synaptic Partners (GRASP) defines cell contacts and synapses in living nervous systems." Neuron 57(3): 353-363.

Ferber, E. C., M. Kajita, A. Wadlow, L. Tobiansky, C. Niessen, H. Ariga, J. Daniel and Y. Fujita (2008). "A role for the cleaved cytoplasmic domain of E-cadherin in the nucleus." J Biol Chem 283(19): 12691-12700.

Ferri, C. P., M. Prince, C. Brayne, H. Brodaty, L. Fratiglioni, M. Ganguli, K. Hall, K. Hasegawa, H. Hendrie, Y. Huang, A. Jorm, C. Mathers, P. R. Menezes, E. Rimmer and M. Scazufca (2005). "Global prevalence of dementia: a Delphi consensus study." Lancet 366(9503): 2112-2117.

Fiore, F., N. Zambrano, G. Minopoli, V. Donini, A. Duilio and T. Russo (1995). "The regions of the Fe65 protein homologous to the phosphotyrosine interaction/phosphotyrosine binding domain of Shc bind the intracellular domain of the Alzheimer's amyloid precursor protein." J Biol Chem 270(52): 30853-30856.

Fossgreen, A., B. Bruckner, C. Czech, C. L. Masters, K. Beyreuther and R. Paro (1998). "Transgenic Drosophila expressing human amyloid precursor protein show gamma-secretase activity and a blistered-wing phenotype." Proc Natl Acad Sci U S A 95(23): 13703-13708.

Frand, A. R., J. W. Cuozzo and C. A. Kaiser (2000). "Pathways for protein disulphide bond formation." Trends Cell Biol 10(5): 203-210.

Freedman, R. B., B. E. Brockway and N. Lambert (1984). "Protein disulphide-isomerase and the formation of native disulphide bonds." Biochem Soc Trans 12(6): 929-932.

Fujiwara, T., K. Oda, S. Yokota, A. Takatsuki and Y. Ikehara (1988). "Brefeldin A causes disassembly of the Golgi complex and accumulation of secretory proteins in the endoplasmic reticulum." J Biol Chem 263(34): 18545-18552.

Furukawa, K., B. L. Sopher, R. E. Rydel, J. G. Begley, D. G. Pham, G. M. Martin, M. Fox and M. P. Mattson (1996). "Increased activity-regulating and neuroprotective efficacy of alpha-secretase-derived secreted amyloid precursor protein conferred by a C-terminal heparin-binding domain." J Neurochem 67(5): 1882-1896.

Gendron, T. F. and L. Petrucelli (2009). "The role of tau in neurodegeneration." Mol Neurodegener 4: 13.

Giovacchini, G., R. Bonwetsch, P. Herscovitch, R. E. Carson and W. H. Theodore (2007). "Cerebral blood flow in temporal lobe epilepsy: a partial volume correction study." Eur J Nucl Med Mol Imaging 34(12): 2066-2072.

Glenner, G. G. and C. W. Wong (1984). "Alzheimer's disease and Down's syndrome: sharing of a unique cerebrovascular amyloid fibril protein." Biochem Biophys Res Commun 122(3): 1131-1135.

Goate, A., M. C. Chartier-Harlin, M. Mullan, J. Brown, F. Crawford, L. Fidani, L. Giuffra, A. Haynes, N. Irving, L. James and et al. (1991). "Segregation of a missense mutation in the amyloid precursor protein gene with familial Alzheimer's disease." Nature 349(6311): 704-706.

Godfroid, E. and J. N. Octave (1990). "Glycosylation of the amyloid peptide precursor containing the Kunitz protease inhibitor domain improves the inhibition of trypsin." Biochem Biophys Res Commun 171(3): 1015-1021.

Goedert, M., M. G. Spillantini, R. Jakes, D. Rutherford and R. A. Crowther (1989). "Multiple isoforms of human microtubule-associated protein tau: sequences and localization in neurofibrillary tangles of Alzheimer's disease." Neuron 3(4): 519-526.

Goedert, M., C. M. Wischik, R. A. Crowther, J. E. Walker and A. Klug (1988). "Cloning and sequencing of the cDNA encoding a core protein of the paired helical filament of Alzheimer disease: identification as the microtubule-associated protein tau." Proc Natl Acad Sci U S A 85(11): 4051-4055.

Goodson, H. V., C. Valetti and T. E. Kreis (1997). "Motors and membrane traffic." Curr Opin Cell Biol 9(1): 18-28.

Gorman, P. M., S. Kim, M. Guo, R. A. Melnyk, J. McLaurin, P. E. Fraser, J. U. Bowie and A. Chakrabartty (2008). "Dimerization of the transmembrane domain of amyloid precursor proteins and familial Alzheimer's disease mutants." BMC Neurosci 9: 17.

Goutte, C., M. Tsunozaki, V. A. Hale and J. R. Priess (2002). "APH-1 is a multipass membrane protein essential for the Notch signaling pathway in Caenorhabditis elegans embryos." Proc Natl Acad Sci U S A 99(2): 775-779.

Gralle, M. and S. T. Ferreira (2007). "Structure and functions of the human amyloid precursor protein: the whole is more than the sum of its parts." Prog Neurobiol 82(1): 11-32.

Gralle, M., C. L. Oliveira, L. H. Guerreiro, W. J. McKinstry, D. Galatis, C. L. Masters, R. Cappai, M. W. Parker, C. H. Ramos, I. Torriani and S. T. Ferreira (2006). "Solution conformation and heparin-induced dimerization of the full-length extracellular domain of the human amyloid precursor protein." J Mol Biol 357(2): 493-508.

Grundke-Iqbal, I., K. Iqbal, Y. C. Tung, M. Quinlan, H. M. Wisniewski and L. I. Binder (1986). "Abnormal phosphorylation of the microtubule-associated protein tau (tau) in Alzheimer cytoskeletal pathology." Proc Natl Acad Sci U S A 83(13): 4913-4917.

Gu, Y., H. Misonou, T. Sato, N. Dohmae, K. Takio and Y. Ihara (2001). "Distinct intramembrane cleavage of the beta-amyloid precursor protein family resembling gamma-secretase-like cleavage of Notch." J Biol Chem 276(38): 35235-35238.

Guenette, S. Y., J. Chen, P. D. Jondro and R. E. Tanzi (1996). "Association of a novel human FE65-like protein with the cytoplasmic domain of the beta-amyloid precursor protein." Proc Natl Acad Sci U S A 93(20): 10832-10837.

Haass, C., M. G. Schlossmacher, A. Y. Hung, C. Vigo-Pelfrey, A. Mellon, B. L. Ostaszewski, I. Lieberburg, E. H. Koo, D. Schenk, D. B. Teplow and et al. (1992). "Amyloid beta-peptide is produced by cultured cells during normal metabolism." Nature 359(6393): 322-325.

Hansson, E. M., K. Stromberg, S. Bergstedt, G. Yu, J. Naslund, J. Lundkvist and U. Lendahl (2005). "Aph-1 interacts at the cell surface with proteins in the active gamma-secretase complex and membrane-tethered Notch." J Neurochem 92(5): 1010-1020.

Hardy, J. (1997). "Amyloid, the presenilins and Alzheimer's disease." Trends Neurosci 20(4): 154-159.

Hardy, J. (2002). "Testing times for the "amyloid cascade hypothesis"." Neurobiol Aging 23(6): 1073-1074.

Hardy, J. and D. J. Selkoe (2002). "The amyloid hypothesis of Alzheimer's disease: progress and problems on the road to therapeutics." Science 297(5580): 353-356.

Hatahet, F. and L. W. Ruddock (2009). "Protein disulfide isomerase: a critical evaluation of its function in disulfide bond formation." Antioxid Redox Signal 11(11): 2807-2850.

Haucke, V. (2003). "Vesicle budding: a coat for the COPs." Trends Cell Biol 13(2): 59-60.

Hayano, T., K. Inaka, M. Otsu, Y. Taniyama, K. Miki, M. Matsushima and M. Kikuchi (1993). "PDI and glutathione-mediated reduction of the glutathionylated variant of human lysozyme." FEBS Lett 328(1-2): 203-208.

Heber, S., J. Herms, V. Gajic, J. Hainfellner, A. Aguzzi, T. Rulicke, H. von Kretzschmar, C. von Koch, S. Sisodia, P. Tremml, H. P. Lipp, D. P. Wolfer and U. Muller (2000). "Mice with combined gene knock-outs reveal essential and partially redundant functions of amyloid precursor protein family members." J Neurosci 20(21): 7951-7963.

Hebert, S. S., L. Serneels, A. Tolia, K. Craessaerts, C. Derks, M. A. Filippov, U. Muller and B. De Strooper (2006). "Regulated intramembrane proteolysis of amyloid precursor protein and regulation of expression of putative target genes." EMBO Rep 7(7): 739-745.

Herrup, K. (2010). "Reimagining Alzheimer's disease--an age-based hypothesis." J Neurosci 30(50): 16755-16762.

Herscovitch, M., W. Comb, T. Ennis, K. Coleman, S. Yong, B. Armstead, D. Kalaitzidis, S. Chandani and T. D. Gilmore (2008). "Intermolecular disulfide bond formation in the NEMO dimer requires Cys54 and Cys347." Biochem Biophys Res Commun 367(1): 103-108.

Herz, J. and H. H. Bock (2002). "Lipoprotein receptors in the nervous system." Annu Rev Biochem 71: 405-434.

Herz, J., U. Hamann, S. Rogne, O. Myklebost, H. Gausepohl and K. K. Stanley (1988). "Surface location and high affinity for calcium of a 500-kd liver membrane protein closely related to the LDL-receptor suggest a physiological role as lipoprotein receptor." Embo J 7(13): 4119-4127.

Hesse, L., D. Beher, C. L. Masters and G. Multhaup (1994). "The beta A4 amyloid precursor protein binding to copper." FEBS Lett 349(1): 109-116.

Hilbich, C., B. Kisters-Woike, J. Reed, C. L. Masters and K. Beyreuther (1991). "Aggregation and secondary structure of synthetic amyloid beta A4 peptides of Alzheimer's disease." J Mol Biol 218(1): 149-163.

Hillson, D. A., N. Lambert and R. B. Freedman (1984). "Formation and isomerization of disulfide bonds in proteins: protein disulfide-isomerase." Methods Enzymol 107: 281-294.

Hogl, S., P. H. Kuhn, A. Colombo and S. F. Lichtenthaler (2011). "Determination of the proteolytic cleavage sites of the amyloid precursor-like protein 2 by the proteases ADAM10, BACE1 and gamma-secretase." PLoS One 6(6): e21337.

Homayouni, R., D. S. Rice, M. Sheldon and T. Curran (1999). "Disabled-1 binds to the cytoplasmic domain of amyloid precursor-like protein 1." J Neurosci 19(17): 7507-7515.

Hotoda, N., H. Koike, N. Sasagawa and S. Ishiura (2002). "A secreted form of human ADAM9 has an alpha-secretase activity for APP." Biochem Biophys Res Commun 293(2): 800-805.

Howell, B. W., L. M. Lanier, R. Frank, F. B. Gertler and J. A. Cooper (1999). "The disabled 1 phosphotyrosine-binding domain binds to the internalization signals of transmembrane glycoproteins and to phospholipids." Mol Cell Biol 19(7): 5179-5188.

Hsu, V. W. and J. S. Yang (2009). "Mechanisms of COPI vesicle formation." FEBS Lett 583(23): 3758-3763.

Hu, C. D., A. V. Grinberg and T. K. Kerppola (2005). "Visualization of protein interactions in living cells using bimolecular fluorescence complementation (BiFC) analysis." Curr Protoc Protein Sci Chapter 19: Unit 19 10.

Hung, A. Y. and D. J. Selkoe (1994). "Selective ectodomain phosphorylation and regulated cleavage of beta-amyloid precursor protein." Embo J 13(3): 534-542.

Hussain, I., D. Powell, D. R. Howlett, D. G. Tew, T. D. Meek, C. Chapman, I. S. Gloger, K. E. Murphy, C. D. Southan, D. M. Ryan, T. S. Smith, D. L. Simmons, F. S. Walsh, C. Dingwall and G. Christie (1999). "Identification of a novel aspartic protease (Asp 2) as beta-secretase." Mol Cell Neurosci 14(6): 419-427.

Hwang, C., A. J. Sinskey and H. F. Lodish (1992). "Oxidized redox state of glutathione in the endoplasmic reticulum." Science 257(5076): 1496-1502.

Hyman, B. T., H. Damasio, A. R. Damasio and G. W. Van Hoesen (1989). "Alzheimer's disease." Annu Rev Public Health 10: 115-140.

Hyman, B. T., R. E. Tanzi, K. Marzloff, R. Barbour and D. Schenk (1992). "Kunitz protease inhibitor-containing amyloid beta protein precursor immunoreactivity in Alzheimer's disease." J Neuropathol Exp Neurol 51(1): 76-83.

Hyman, B. T., G. W. Van Hoesen, K. Beyreuther and C. L. Masters (1989). "A4 amyloid protein immunoreactivity is present in Alzheimer's disease neurofibrillary tangles." Neurosci Lett 101(3): 352-355.

Hynes, T. R., M. Randal, L. A. Kennedy, C. Eigenbrot and A. A. Kossiakoff (1990). "X-ray crystal structure of the protease inhibitor domain of Alzheimer's amyloid beta-protein precursor." Biochemistry 29(43): 10018-10022.

Iqbal, K., C. Alonso Adel, S. Chen, M. O. Chohan, E. El-Akkad, C. X. Gong, S. Khatoon, B. Li, F. Liu, A. Rahman, H. Tanimukai and I. Grundke-Iqbal (2005). "Tau pathology in Alzheimer disease and other tauopathies." Biochim Biophys Acta 1739(2-3): 198-210.

Itin, C., F. Kappeler, A. D. Linstedt and H. P. Hauri (1995). "A novel endocytosis signal related to the KKXX ER-retrieval signal." Embo J 14(10): 2250-2256.

Itin, C., R. Schindler and H. P. Hauri (1995). "Targeting of protein ERGIC-53 to the ER/ERGIC/cis-Golgi recycling pathway." J Cell Biol 131(1): 57-67.

Jackson, M. R., T. Nilsson and P. A. Peterson (1990). "Identification of a consensus motif for retention of transmembrane proteins in the endoplasmic reticulum." Embo J 9(10): 3153-3162.

Jackson, M. R., T. Nilsson and P. A. Peterson (1993). "Retrieval of transmembrane proteins to the endoplasmic reticulum." J Cell Biol 121(2): 317-333.

Jager, S., S. Leuchtenberger, A. Martin, E. Czirr, J. Wesselowski, M. Dieckmann, E. Waldron, C. Korth, E. H. Koo, M. Heneka, S. Weggen and C. U. Pietrzik (2009). "alpha-secretase mediated conversion of the amyloid precursor protein derived membrane stub C99 to C83 limits Abeta generation." J Neurochem 111(6): 1369-1382.

Jarrett, J. T., E. P. Berger and P. T. Lansbury, Jr. (1993). "The carboxy terminus of the beta amyloid protein is critical for the seeding of amyloid formation: implications for the pathogenesis of Alzheimer's disease." Biochemistry 32(18): 4693-4697.

Kaden, D., L. M. Munter, M. Joshi, C. Treiber, C. Weise, T. Bethge, P. Voigt, M. Schaefer, M. Beyermann, B. Reif and G. Multhaup (2008). "Homophilic interactions of the amyloid precursor protein (APP) ectodomain are regulated by the loop region and affect beta-secretase cleavage of APP." J Biol Chem 283(11): 7271-7279.

Kaden, D., P. Voigt, L. M. Munter, K. D. Bobowski, M. Schaefer and G. Multhaup (2009). "Subcellular localization and dimerization of APLP1 are strikingly different from APP and APLP2." J Cell Sci 122(Pt 3): 368-377.

Kakuda, N., S. Funamoto, S. Yagishita, M. Takami, S. Osawa, N. Dohmae and Y. Ihara (2006). "Equimolar production of amyloid beta-protein and amyloid precursor protein intracellular domain from beta-carboxyl-terminal fragment by gamma-secretase." J Biol Chem 281(21): 14776-14786.

Kang, J., H. G. Lemaire, A. Unterbeck, J. M. Salbaum, C. L. Masters, K. H. Grzeschik, G. Multhaup, K. Beyreuther and B. Muller-Hill (1987). "The precursor of Alzheimer's disease amyloid A4 protein resembles a cell-surface receptor." Nature 325(6106): 733-736.

Kang, J. and B. Muller-Hill (1990). "Differential splicing of Alzheimer's disease amyloid A4 precursor RNA in rat tissues: PreA4(695) mRNA is predominantly produced in rat and human brain." Biochem Biophys Res Commun 166(3): 1192-1200.

Kappeler, F., D. R. Klopfenstein, M. Foguet, J. P. Paccaud and H. P. Hauri (1997). "The recycling of ERGIC-53 in the early secretory pathway. ERGIC-53 carries a cytosolic endoplasmic reticulum-exit determinant interacting with COPII." J Biol Chem 272(50): 31801-31808.

Kerppola, T. K. (2006). "Visualization of molecular interactions by fluorescence complementation." Nat Rev Mol Cell Biol 7(6): 449-456.

Khalifa, N. B., J. Van Hees, B. Tasiaux, S. Huysseune, S. O. Smith, S. N. Constantinescu, J. N. Octave and P. Kienlen-Campard (2010). "What is the role of amyloid precursor protein dimerization?" Cell Adh Migr 4(2): 268-272.

Kienlen-Campard, P., B. Tasiaux, J. Van Hees, M. Li, S. Huysseune, T. Sato, J. Z. Fei, S. Aimoto, P. J. Courtoy, S. O. Smith, S. N. Constantinescu and J. N. Octave (2008). "Amyloidogenic processing but not amyloid precursor protein (APP) intracellular C-terminal domain production requires a precisely oriented APP dimer assembled by transmembrane GXXXG motifs." J Biol Chem 283(12): 7733-7744.

Killar, L., J. White, R. Black and J. Peschon (1999). "Adamalysins. A family of metzincins including TNF-alpha converting enzyme (TACE)." Ann N Y Acad Sci 878: 442-452.

Kim, H. S., E. M. Kim, J. P. Lee, C. H. Park, S. Kim, J. H. Seo, K. A. Chang, E. Yu, S. J. Jeong, Y. H. Chong and Y. H. Suh (2003). "C-terminal fragments of amyloid precursor protein exert neurotoxicity by inducing glycogen synthase kinase-3beta expression." Faseb J 17(13): 1951-1953.

Kimberly, W. T., J. B. Zheng, S. Y. Guenette and D. J. Selkoe (2001). "The intracellular domain of the beta-amyloid precursor protein is stabilized by Fe65 and translocates to the nucleus in a notch-like manner." J Biol Chem 276(43): 40288-40292.

Kirchhausen, T. (2000). "Clathrin." Annu Rev Biochem 69: 699-727.

Kitaguchi, N., Y. Takahashi, Y. Tokushima, S. Shiojiri and H. Ito (1988). "Novel precursor of Alzheimer's disease amyloid protein shows protease inhibitory activity." Nature 331(6156): 530-532.

Klausner, R. D., J. G. Donaldson and J. Lippincott-Schwartz (1992). "Brefeldin A: insights into the control of membrane traffic and organelle structure." J Cell Biol 116(5): 1071-1080.

Klueg, K. M., D. Alvarado, M. A. Muskavitch and J. B. Duffy (2002). "Creation of a GAL4/UAS-coupled inducible gene expression system for use in Drosophila cultured cell lines." Genesis 34(1-2): 119-122.

Klueg, K. M. and M. A. Muskavitch (1999). "Ligand-receptor interactions and trans-endocytosis of Delta, Serrate and Notch: members of the Notch signalling pathway in Drosophila." J Cell Sci 112 (Pt 19): 3289-3297.

Kochhar, S., P. E. Hunziker, P. Leong-Morgenthaler and H. Hottinger (1992). "Evolutionary relationship of NAD(+)-dependent D-lactate dehydrogenase: comparison of primary structure of 2-hydroxy acid dehydrogenases." Biochem Biophys Res Commun 184(1): 60-66.

Kolset, S. O., K. Prydz, K. Fjeldstad, F. Safaiyan, T. T. Vuong, E. Gottfridsson and M. Salmivirta (2002). "Effect of brefeldin A on heparan sulphate biosynthesis in Madin-Darby canine kidney cells." Biochem J 362(Pt 2): 359-366.

Koo, E. H. and S. L. Squazzo (1994). "Evidence that production and release of amyloid beta-protein involves the endocytic pathway." J Biol Chem 269(26): 17386-17389.

Korenberg, J. R., S. M. Pulst, R. L. Neve and R. West (1989). "The Alzheimer amyloid precursor protein maps to human chromosome 21 bands q21.105-q21.05." Genomics 5(1): 124-127.

Kosik, K. S., C. L. Joachim and D. J. Selkoe (1986). "Microtubule-associated protein tau (tau) is a major antigenic component of paired helical filaments in Alzheimer disease." Proc Natl Acad Sci U S A 83(11): 4044-4048.

Kounnas, M. Z., R. D. Moir, G. W. Rebeck, A. I. Bush, W. S. Argraves, R. E. Tanzi, B. T. Hyman and D. K. Strickland (1995). "LDL receptor-related protein, a multifunctional ApoE receptor, binds secreted beta-amyloid precursor protein and mediates its degradation." Cell 82(2): 331-340.

Kusano, I., A. Kageyama, T. Tamura, T. Oda and T. Muramatsu (2001). "Enhancement of diphtheria toxin-induced apoptosis in Vero cells by combination treatment with brefeldin A and okadaic acid." Cell Struct Funct 26(5): 279-288.

Lai, A., S. S. Sisodia and I. S. Trowbridge (1995). "Characterization of sorting signals in the beta-amyloid precursor protein cytoplasmic domain." J Biol Chem 270(8): 3565-3573.

Lammich, S., E. Kojro, R. Postina, S. Gilbert, R. Pfeiffer, M. Jasionowski, C. Haass and F. Fahrenholz (1999). "Constitutive and regulated alpha-secretase cleavage of Alzheimer's amyloid precursor protein by a disintegrin metalloprotease." Proc Natl Acad Sci U S A 96(7): 3922-3927.

Landes, A. M., S. D. Sperry, M. E. Strauss and D. S. Geldmacher (2001). "Apathy in Alzheimer's disease." J Am Geriatr Soc 49(12): 1700-1707.

LeBlanc, A. C., H. Y. Chen, L. Autilio-Gambetti and P. Gambetti (1991). "Differential APP gene expression in rat cerebral cortex, meninges, and primary astroglial, microglial and neuronal cultures." FEBS Lett 292(1-2): 171-178.

Lee, J., M. K. Shin, D. K. Ryu, S. Kim and W. S. Ryu (2010). "Insertion and deletion mutagenesis by overlap extension PCR." Methods Mol Biol 634: 137-146.

Letourneur, F., E. C. Gaynor, S. Hennecke, C. Demolliere, R. Duden, S. D. Emr, H. Riezman and P. Cosson (1994). "Coatomer is essential for retrieval of dilysine-tagged proteins to the endoplasmic reticulum." Cell 79(7): 1199-1207.

Li, Q. and T. C. Sudhof (2004). "Cleavage of amyloid-beta precursor protein and amyloid-beta precursor-like protein by BACE 1." J Biol Chem 279(11): 10542-10550.

Li, S., M. Jin, T. Koeglsperger, N. E. Shepardson, G. M. Shankar and D. J. Selkoe (2011). "Soluble Abeta oligomers inhibit long-term potentiation through a mechanism involving excessive activation of extrasynaptic NR2B-containing NMDA receptors." J Neurosci 31(18): 6627-6638.

Lichtenthaler, S. F., G. Multhaup, C. L. Masters and K. Beyreuther (1999). "A novel substrate for analyzing Alzheimer's disease gamma-secretase." FEBS Lett 453(3): 288-292.

Ling, Y. H., T. Li, R. Perez-Soler and M. Haigentz, Jr. (2009). "Activation of ER stress and inhibition of EGFR N-glycosylation by tunicamycin enhances susceptibility of human non-small cell lung cancer cells to erlotinib." Cancer Chemother Pharmacol 64(3): 539-548.

Lippincott-Schwartz, J., L. C. Yuan, J. S. Bonifacino and R. D. Klausner (1989). "Rapid redistribution of Golgi proteins into the ER in cells treated with brefeldin A: evidence for membrane cycling from Golgi to ER." Cell 56(5): 801-813.

Lodish, H. F. and N. Kong (1993). "The secretory pathway is normal in dithiothreitol-treated cells, but disulfide-bonded proteins are reduced and reversibly retained in the endoplasmic reticulum." J Biol Chem 268(27): 20598-20605.

Lorent, K., L. Overbergh, D. Moechars, B. De Strooper, F. Van Leuven and H. Van den Berghe (1995). "Expression in mouse embryos and in adult mouse brain of three members of the amyloid precursor protein family, of the alpha-2-macroglobulin receptor/low density lipoprotein receptor-related protein and of its ligands apolipoprotein E, lipoprotein lipase, alpha-2-macroglobulin and the 40,000 molecular weight receptor-associated protein." Neuroscience 65(4): 1009-1025.

Malo, M., C. Vurpillot, M. Tomasi, J. Bruner, J. Stinnakre and M. Israel (2000). "Effect of brefeldin A on acetylcholine release from glioma C6BU-1 cells." Neuropharmacology 39(11): 2214-2221.

Marks, N. and M. J. Berg (2003). "APP processing enzymes (secretases) as therapeutic targets: insights from the use of transgenics (Tgs) and transfected cells." Neurochem Res 28(7): 1049-1062.

Mazzarella, R. A., M. Srinivasan, S. M. Haugejorden and M. Green (1990). "ERp72, an abundant luminal endoplasmic reticulum protein, contains three copies of the active site sequences of protein disulfide isomerase." J Biol Chem 265(2): 1094-1101.

McEvoy, L. K., C. Fennema-Notestine, J. C. Roddey, D. J. Hagler, Jr., D. Holland, D. S. Karow, C. J. Pung, J. B. Brewer and A. M. Dale (2009). "Alzheimer disease: quantitative structural neuroimaging for detection and prediction of clinical and structural changes in mild cognitive impairment." Radiology 251(1): 195-205.

McLoughlin, D. M. and C. C. Miller (2008). "The FE65 proteins and Alzheimer's disease." J Neurosci Res 86(4): 744-754.

Misumi, Y., K. Miki, A. Takatsuki, G. Tamura and Y. Ikehara (1986). "Novel blockade by brefeldin A of intracellular transport of secretory proteins in cultured rat hepatocytes." J Biol Chem 261(24): 11398-11403.

Mok, S. S., G. Sberna, D. Heffernan, R. Cappai, D. Galatis, H. J. Clarris, W. H. Sawyer, K. Beyreuther, C. L. Masters and D. H. Small (1997). "Expression and analysis of heparin-binding regions of the amyloid precursor protein of Alzheimer's disease." FEBS Lett 415(3): 303-307.

Moss, M. L., S. L. Jin, J. D. Becherer, D. M. Bickett, W. Burkhart, W. J. Chen, D. Hassler, M. T. Leesnitzer, G. McGeehan, M. Milla, M. Moyer, W. Rocque, T. Seaton, F. Schoenen, J. Warner and D. Willard (1997). "Structural features and biochemical properties of TNF-alpha converting enzyme (TACE)." J Neuroimmunol 72(2): 127-129.

Mullan, M., F. Crawford, K. Axelman, H. Houlden, L. Lilius, B. Winblad and L. Lannfelt (1992). "A pathogenic mutation for probable Alzheimer's disease in the APP gene at the N-terminus of beta-amyloid." Nat Genet 1(5): 345-347.

Muller, U., N. Cristina, Z. W. Li, D. P. Wolfer, H. P. Lipp, T. Rulicke, S. Brandner, A. Aguzzi and C. Weissmann (1994). "Behavioral and anatomical deficits in mice homozygous for a modified beta-amyloid precursor protein gene." Cell 79(5): 755-765.

Mullis, K. B. and F. A. Faloona (1987). "Specific synthesis of DNA in vitro via a polymerase-catalyzed chain reaction." Methods Enzymol 155: 335-350.

Multhaup, G., A. I. Bush, P. Pollwein and C. L. Masters (1994). "Interaction between the zinc (II) and the heparin binding site of the Alzheimer's disease beta A4 amyloid precursor protein (APP)." FEBS Lett 355(2): 151-154.

Multhaup, G., H. Mechler and C. L. Masters (1995). "Characterization of the high affinity heparin binding site of the Alzheimer's disease beta A4 amyloid precursor protein (APP) and its enhancement by zinc(II)." J Mol Recognit 8(4): 247-257.

Multhaup, G., T. Ruppert, A. Schlicksupp, L. Hesse, E. Bill, R. Pipkorn, C. L. Masters and K. Beyreuther (1998). "Copper-binding amyloid precursor protein undergoes a site-specific fragmentation in the reduction of hydrogen peroxide." Biochemistry 37(20): 7224-7230.

Multhaup, G., A. Schlicksupp, L. Hesse, D. Beher, T. Ruppert, C. L. Masters and K. Beyreuther (1996). "The amyloid precursor protein of Alzheimer's disease in the reduction of copper(II) to copper(I)." Science 271(5254): 1406-1409.

Munro, S. and H. R. Pelham (1987). "A C-terminal signal prevents secretion of luminal ER proteins." Cell 48(5): 899-907.

Munter, L. M., P. Voigt, A. Harmeier, D. Kaden, K. E. Gottschalk, C. Weise, R. Pipkorn, M. Schaefer, D. Langosch and G. Multhaup (2007). "GxxxG motifs within the amyloid precursor protein transmembrane sequence are critical for the etiology of Abeta42." Embo J 26(6): 1702-1712.

Murrell, J. R., A. M. Hake, K. A. Quaid, M. R. Farlow and B. Ghetti (2000). "Early-onset Alzheimer disease caused by a new mutation (V717L) in the amyloid precursor protein gene." Arch Neurol 57(6): 885-887.

Naruse, S., G. Thinakaran, J. J. Luo, J. W. Kusiak, T. Tomita, T. Iwatsubo, X. Qian, D. D. Ginty, D. L. Price, D. R. Borchelt, P. C. Wong and S. S. Sisodia (1998). "Effects of PS1 deficiency on membrane protein trafficking in neurons." Neuron 21(5): 1213-1221.

Nebenfuhr, A., C. Ritzenthaler and D. G. Robinson (2002). "Brefeldin A: deciphering an enigmatic inhibitor of secretion." Plant Physiol 130(3): 1102-1108.

Neumann, S., S. Schobel, S. Jager, A. Trautwein, C. Haass, C. U. Pietrzik and S. F. Lichtenthaler (2006). "Amyloid precursor-like protein 1 influences endocytosis and proteolytic processing of the amyloid precursor protein." J Biol Chem 281(11): 7583-7594.

Nilsberth, C., A. Westlind-Danielsson, C. B. Eckman, M. M. Condron, K. Axelman, C. Forsell, C. Stenh, J. Luthman, D. B. Teplow, S. G. Younkin, J. Naslund and L. Lannfelt (2001). "The 'Arctic' APP mutation (E693G) causes Alzheimer's disease by enhanced Abeta protofibril formation." Nat Neurosci 4(9): 887-893.

Nilsson, T., M. Jackson and P. A. Peterson (1989). "Short cytoplasmic sequences serve as retention signals for transmembrane proteins in the endoplasmic reticulum." Cell 58(4): 707-718.

Norkin, L. C., H. A. Anderson, S. A. Wolfrom and A. Oppenheim (2002). "Caveolar endocytosis of simian virus 40 is followed by brefeldin A-sensitive transport to the endoplasmic reticulum, where the virus disassembles." J Virol 76(10): 5156-5166.

Nunan, J. and D. H. Small (2000). "Regulation of APP cleavage by alpha-, beta- and gamma-secretases." FEBS Lett 483(1): 6-10.

Oddo, S., V. Vasilevko, A. Caccamo, M. Kitazawa, D. H. Cribbs and F. M. LaFerla (2006). "Reduction of soluble Abeta and tau, but not soluble Abeta alone, ameliorates cognitive decline in transgenic mice with plaques and tangles." J Biol Chem 281(51): 39413-39423.

Okochi, M., H. Steiner, A. Fukumori, H. Tanii, T. Tomita, T. Tanaka, T. Iwatsubo, T. Kudo, M. Takeda and C. Haass (2002). "Presenilins mediate a dual intramembranous gamma-secretase cleavage of Notch-1." Embo J 21(20): 5408-5416.

Oltersdorf, T., L. C. Fritz, D. B. Schenk, I. Lieberburg, K. L. Johnson-Wood, E. C. Beattie, P. J. Ward, R. W. Blacher, H. F. Dovey and S. Sinha (1989). "The secreted form of the Alzheimer's amyloid precursor protein with the Kunitz domain is protease nexin-II." Nature 341(6238): 144-147.

Orci, L., M. Stamnes, M. Ravazzola, M. Amherdt, A. Perrelet, T. H. Sollner and J. E. Rothman (1997). "Bidirectional transport by distinct populations of COPI-coated vesicles." Cell 90(2): 335-349.

Otte, S. and C. Barlowe (2004). "Sorting signals can direct receptor-mediated export of soluble proteins into COPII vesicles." Nat Cell Biol 6(12): 1189-1194.

Pahlsson, P., S. H. Shakin-Eshleman and S. L. Spitalnik (1992). "N-linked glycosylation of beta-amyloid precursor protein." Biochem Biophys Res Commun 189(3): 1667-1673.

Paliga, K., G. Peraus, S. Kreger, U. Durrwang, L. Hesse, G. Multhaup, C. L. Masters, K. Beyreuther and A. Weidemann (1997). "Human amyloid precursor-like protein 1--cDNA cloning, ectopic expression in COS-7 cells and identification of soluble forms in the cerebrospinal fluid." Eur J Biochem 250(2): 354-363.

Palmert, M. R., T. E. Golde, M. L. Cohen, D. M. Kovacs, R. E. Tanzi, J. F. Gusella, M. F. Usiak, L. H. Younkin and S. G. Younkin (1988). "Amyloid protein precursor messenger RNAs: differential expression in Alzheimer's disease." Science 241(4869): 1080-1084.

Pardossi-Piquard, R., A. Petit, T. Kawarai, C. Sunyach, C. Alves da Costa, B. Vincent, S. Ring, L. D'Adamio, J. Shen, U. Muller, P. St George Hyslop and F. Checler (2005). "Presenilin-dependent transcriptional control of the Abeta-degrading enzyme neprilysin by intracellular domains of betaAPP and APLP." Neuron 46(4): 541-554.

Parlati, F., O. Varlamov, K. Paz, J. A. McNew, D. Hurtado, T. H. Sollner and J. E. Rothman (2002). "Distinct SNARE complexes mediating membrane fusion in Golgi transport based on combinatorial specificity." Proc Natl Acad Sci U S A 99(8): 5424-5429.

Parvathy, S., I. Hussain, E. H. Karran, A. J. Turner and N. M. Hooper (1999). "Cleavage of Alzheimer's amyloid precursor protein by alpha-secretase occurs at the surface of neuronal cells." Biochemistry 38(30): 9728-9734.

Pelham, H. R. (1988). "Evidence that luminal ER proteins are sorted from secreted proteins in a post-ER compartment." Embo J 7(4): 913-918.

Pelham, H. R. (1991). "Multiple targets for brefeldin A." Cell 67(3): 449-451.

Pelham, H. R. (1996). "The dynamic organisation of the secretory pathway." Cell Struct Funct 21(5): 413-419.

Pelletier, L., P. Guillaumot, B. Freche, C. Luquain, D. Christiansen, S. Brugiere, J. Garin and S. N. Manie (2006). "Gamma-secretase-dependent proteolysis of CD44 promotes neoplastic transformation of rat fibroblastic cells." Cancer Res 66(7): 3681-3687.

Perez, R. G., S. Soriano, J. D. Hayes, B. Ostaszewski, W. Xia, D. J. Selkoe, X. Chen, G. B. Stokin and E. H. Koo (1999). "Mutagenesis identifies new signals for beta-amyloid precursor protein endocytosis, turnover, and the generation of secreted fragments, including Abeta42." J Biol Chem 274(27): 18851-18856.

Pietrzik, C. U., T. Busse, D. E. Merriam, S. Weggen and E. H. Koo (2002). "The cytoplasmic domain of the LDL receptor-related protein regulates multiple steps in APP processing." Embo J 21(21): 5691-5700.

Pietrzik, C. U., I. S. Yoon, S. Jaeger, T. Busse, S. Weggen and E. H. Koo (2004). "FE65 constitutes the functional link between the low-density lipoprotein receptor-related protein and the amyloid precursor protein." Journal of Neuroscience 24(17): 4259-4265.

Pigiet, V. P. and B. J. Schuster (1986). "Thioredoxin-catalyzed refolding of disulfide-containing proteins." Proc Natl Acad Sci U S A 83(20): 7643-7647.

Ponte, P., P. Gonzalez-DeWhitt, J. Schilling, J. Miller, D. Hsu, B. Greenberg, K. Davis, W. Wallace, I. Lieberburg and F. Fuller (1988). "A new A4 amyloid mRNA contains a domain homologous to serine proteinase inhibitors." Nature 331(6156): 525-527.

Preston, A. M., E. Gurisik, C. Bartley, D. R. Laybutt and T. J. Biden (2009). "Reduced endoplasmic reticulum (ER)-to-Golgi protein trafficking contributes to ER stress in lipotoxic mouse beta cells by promoting protein overload." Diabetologia 52(11): 2369-2373.

Price, J. M., E. T. Sutton, A. Hellermann and T. Thomas (1997). "beta-Amyloid induces cerebrovascular endothelial dysfunction in the rat brain." Neurol Res 19(5): 534-538.

Qahwash, I., K. L. Weiland, Y. Lu, R. W. Sarver, R. F. Kletzien and R. Yan (2003). "Identification of a mutant amyloid peptide that predominantly forms neurotoxic protofibrillar aggregates." J Biol Chem 278(25): 23187-23195.

Ramelot, T. A. and L. K. Nicholson (2001). "Phosphorylation-induced structural changes in the amyloid precursor protein cytoplasmic tail detected by NMR." J Mol Biol 307(3): 871-884.

Richards, S. J., C. Hodgman and M. Sharpe (1995). "Reported sequence homology between Alzheimer amyloid770 and the MRC OX-2 antigen does not predict function." Brain Res Bull 38(3): 305-306.

Richter, L., L. M. Munter, J. Ness, P. W. Hildebrand, M. Dasari, S. Unterreitmeier, B. Bulic, M. Beyermann, R. Gust, B. Reif, S. Weggen, D. Langosch and G. Multhaup (2010). "Amyloid beta 42 peptide (Abeta42)-lowering compounds directly bind to Abeta and interfere with amyloid precursor protein (APP) transmembrane dimerization." Proc Natl Acad Sci U S A 107(33): 14597-14602.

Ring, S., S. W. Weyer, S. B. Kilian, E. Waldron, C. U. Pietrzik, M. A. Filippov, J. Herms, C. Buchholz, C. B. Eckman, M. Korte, D. P. Wolfer and U. C. Muller (2007). "The secreted beta-amyloid precursor protein ectodomain APPs alpha is sufficient to rescue the anatomical, behavioral, and electrophysiological abnormalities of APP-deficient mice." J Neurosci 27(29): 7817-7826.

Robakis, N. K., H. M. Wisniewski, E. C. Jenkins, E. A. Devine-Gage, G. E. Houck, X. L. Yao, N. Ramakrishna, G. Wolfe, W. P. Silverman and W. T. Brown (1987). "Chromosome 21q21 sublocalisation of gene encoding beta-amyloid peptide in cerebral vessels and neuritic (senile) plaques of people with Alzheimer disease and Down syndrome." Lancet 1(8529): 384-385.

Rogelj, B., J. C. Mitchell, C. C. Miller and D. M. McLoughlin (2006). "The X11/Mint family of adaptor proteins." Brain Res Rev 52(2): 305-315.

Rosen, D. R., L. Martin-Morris, L. Q. Luo and K. White (1989). "A Drosophila gene encoding a protein resembling the human beta-amyloid protein precursor." Proc Natl Acad Sci U S A 86(7): 2478-2482.

Rosendahl, M. S., S. C. Ko, D. L. Long, M. T. Brewer, B. Rosenzweig, E. Hedl, L. Anderson, S. M. Pyle, J. Moreland, M. A. Meyers, T. Kohno, D. Lyons and H. S. Lichenstein (1997). "Identification and characterization of a pro-tumor necrosis factor-alpha-processing enzyme from the ADAM family of zinc metalloproteases." J Biol Chem 272(39): 24588-24593.

Rossjohn, J., R. Cappai, S. C. Feil, A. Henry, W. J. McKinstry, D. Galatis, L. Hesse, G. Multhaup, K. Beyreuther, C. L. Masters and M. W. Parker (1999). "Crystal structure of the N-terminal, growth factor-like domain of Alzheimer amyloid precursor protein." Nat Struct Biol 6(4): 327-331.

Rothman, J. E. and F. T. Wieland (1996). "Protein sorting by transport vesicles." Science 272(5259): 227-234.

Russ, W. P. and D. M. Engelman (1999). "TOXCAT: a measure of transmembrane helix association in a biological membrane." Proc Natl Acad Sci U S A 96(3): 863-868.

Russo, C., V. Venezia, E. Repetto, M. Nizzari, E. Violani, P. Carlo and G. Schettini (2005). "The amyloid precursor protein and its network of interacting proteins: physiological and pathological implications." Brain Res Brain Res Rev 48(2): 257-264.

Sabo, S. L., A. F. Ikin, J. D. Buxbaum and P. Greengard (2001). "The Alzheimer amyloid precursor protein (APP) and FE65, an APP-binding protein, regulate cell movement." Journal of Cell Biology 153(7): 1403-1414.

Sambamurti, K., L. M. Refolo, J. Shioi, M. A. Pappolla and N. K. Robakis (1992). "The Alzheimer's amyloid precursor is cleaved intracellularly in the trans-Golgi network or in a post-Golgi compartment." Ann N Y Acad Sci 674: 118-128.

Sandbrink, R., R. Banati, C. L. Masters, K. Beyreuther and G. Konig (1993). "Expression of L-APP mRNA in brain cells." Ann N Y Acad Sci 695: 183-189.

Sandbrink, R., U. Monning, C. L. Masters and K. Beyreuther (1997). "Expression of the APP gene family in brain cells, brain development and aging." Gerontology 43(1-2): 119-131.

Santiago-Garcia, J., J. Mas-Oliva, T. L. Innerarity and R. E. Pitas (2001). "Secreted forms of the amyloid-beta precursor protein are ligands for the class A scavenger receptor." J Biol Chem 276(33): 30655-30661.

Sastre, M., R. S. Turner and E. Levy (1998). "X11 interaction with beta-amyloid precursor protein modulates its cellular stabilization and reduces amyloid beta-protein secretion." J Biol Chem 273(35): 22351-22357.

Sato, K., M. Sato and A. Nakano (2001). "Rer1p, a retrieval receptor for endoplasmic reticulum membrane proteins, is dynamically localized to the Golgi apparatus by coatomer." J Cell Biol 152(5): 935-944.

Scacchi, R., L. De Bernardini, E. Mantuano, L. M. Donini, T. Vilardo and R. M. Corbo (1995). "Apolipoprotein E (APOE) allele frequencies in late-onset sporadic Alzheimer's disease (AD), mixed dementia and vascular dementia: lack of association of epsilon 4 allele with AD in Italian octogenarian patients." Neurosci Lett 201(3): 231-234.

Scheinfeld, M. H., E. Ghersi, P. Davies and L. D'Adamio (2003). "Amyloid beta protein precursor is phosphorylated by JNK-1 independent of, yet facilitated by, JNK-interacting protein (JIP)-1." J Biol Chem 278(43): 42058-42063.

Scheinfeld, M. H., E. Ghersi, K. Laky, B. J. Fowlkes and L. D'Adamio (2002). "Processing of beta-amyloid precursor-like protein-1 and -2 by gamma-secretase regulates transcription." J Biol Chem 277(46): 44195-44201.

Scheuermann, S., B. Hambsch, L. Hesse, J. Stumm, C. Schmidt, D. Beher, T. A. Bayer, K. Beyreuther and G. Multhaup (2001). "Homodimerization of amyloid precursor protein and its implication in the amyloidogenic pathway of Alzheimer's disease." J Biol Chem 276(36): 33923-33929.

Schlessinger, J. (2002). "Ligand-induced, receptor-mediated dimerization and activation of EGF receptor." Cell 110(6): 669-672.

Schlondorff, J., J. D. Becherer and C. P. Blobel (2000). "Intracellular maturation and localization of the tumour necrosis factor alpha convertase (TACE)." Biochem J 347 Pt 1: 131-138.

Schmechel, D. E., D. Goldgaber, D. S. Burkhart, J. R. Gilbert, D. C. Gajdusek and A. D. Roses (1988). "Cellular localization of messenger RNA encoding amyloid-beta-protein in normal tissue and in Alzheimer disease." Alzheimer Dis Assoc Disord 2(2): 96-111.

Schroder, M. and R. J. Kaufman (2005). "ER stress and the unfolded protein response." Mutat Res 569(1-2): 29-63.

Seabrook, G. R., D. W. Smith, B. J. Bowery, A. Easter, T. Reynolds, S. M. Fitzjohn, R. A. Morton, H. Zheng, G. R. Dawson, D. J. Sirinathsinghji, C. H. Davies, G. L. Collingridge and R. G. Hill (1999). "Mechanisms contributing to the deficits in hippocampal synaptic plasticity in mice lacking amyloid precursor protein." Neuropharmacology 38(3): 349-359.

Selkoe, D. J. (1991). "The molecular pathology of Alzheimer's disease." Neuron 6(4): 487-498.

Selkoe, D. J. (2002). "Deciphering the genesis and fate of amyloid beta-protein yields novel therapies for Alzheimer disease." J Clin Invest 110(10): 1375-1381.

Senes, A., I. Ubarretxena-Belandia and D. M. Engelman (2001). "The Calpha ---H...O hydrogen bond: a determinant of stability and specificity in transmembrane helix interactions." Proc Natl Acad Sci U S A 98(16): 9056-9061.

Senkevich, T. G., C. L. White, E. V. Koonin and B. Moss (2002). "Complete pathway for protein disulfide bond formation encoded by poxviruses." Proc Natl Acad Sci U S A 99(10): 6667-6672.

Shen, X., V. Meza-Carmen, E. Puxeddu, G. Wang, J. Moss and M. Vaughan (2008). "Interaction of brefeldin A-inhibited guanine nucleotide-exchange protein (BIG) 1 and kinesin motor protein KIF21A." Proc Natl Acad Sci U S A 105(48): 18788-18793.

Simons, A., T. Ruppert, C. Schmidt, A. Schlicksupp, R. Pipkorn, J. Reed, C. L. Masters, A. R. White, R. Cappai, K. Beyreuther, T. A. Bayer and G. Multhaup (2002). "Evidence for a copper-binding superfamily of the amyloid precursor protein." Biochemistry 41(30): 9310-9320.

Sinha, S., J. P. Anderson, R. Barbour, G. S. Basi, R. Caccavello, D. Davis, M. Doan, H. F. Dovey, N. Frigon, J. Hong, K. Jacobson-Croak, N. Jewett, P. Keim, J. Knops, I. Lieberburg, M. Power, H. Tan, G. Tatsuno, J. Tung, D. Schenk, P. Seubert, S. M. Suomensaari, S. Wang, D. Walker, J. Zhao, L. McConlogue and V. John (1999). "Purification and cloning of amyloid precursor protein beta-secretase from human brain." Nature 402(6761): 537-540.

Sinha, S. and I. Lieberburg (1999). "Cellular mechanisms of beta-amyloid production and secretion." Proc Natl Acad Sci U S A 96(20): 11049-11053.

Sisodia, S. S., E. H. Koo, P. N. Hoffman, G. Perry and D. L. Price (1993). "Identification and transport of full-length amyloid precursor proteins in rat peripheral nervous system." J Neurosci 13(7): 3136-3142.

Sloane, P. D., S. Zimmerman, C. Suchindran, P. Reed, L. Wang, M. Boustani and S. Sudha (2002). "The public health impact of Alzheimer's disease, 2000-2050: potential implication of treatment advances." Annu Rev Public Health 23: 213-231.

Slomnicki, L. P. and W. Lesniak (2008). "A putative role of the Amyloid Precursor Protein Intracellular Domain (AICD) in transcription." Acta Neurobiol Exp (Wars) 68(2): 219-228.

Slunt, H. H., G. Thinakaran, C. Von Koch, A. C. Lo, R. E. Tanzi and S. S. Sisodia (1994). "Expression of a ubiquitous, cross-reactive homologue of the mouse beta-amyloid precursor protein (APP)." J Biol Chem 269(4): 2637-2644.

Small, D. H., V. Nurcombe, G. Reed, H. Clarris, R. Moir, K. Beyreuther and C. L. Masters (1994). "A heparin-binding domain in the amyloid protein precursor of Alzheimer's disease is involved in the regulation of neurite outgrowth." J Neurosci 14(4): 2117-2127.

Smith, R. P., D. A. Higuchi and G. J. Broze, Jr. (1990). "Platelet coagulation factor XIa-inhibitor, a form of Alzheimer amyloid precursor protein." Science 248(4959): 1126-1128.

Soba, P., S. Eggert, K. Wagner, H. Zentgraf, K. Siehl, S. Kreger, A. Lower, A. Langer, G. Merdes, R. Paro, C. L. Masters, U. Muller, S. Kins and K. Beyreuther (2005). "Homo- and heterodimerization of APP family members promotes intercellular adhesion." Embo J 24(20): 3624-3634.

Sonnichsen, B., R. Watson, H. Clausen, T. Misteli and G. Warren (1996). "Sorting by COP I-coated vesicles under interphase and mitotic conditions." J Cell Biol 134(6): 1411-1425.

Soriano, S., D. C. Lu, S. Chandra, C. U. Pietrzik and E. H. Koo (2001). "The amyloidogenic pathway of amyloid precursor protein (APP) is independent of its cleavage by caspases." J Biol Chem 276(31): 29045-29050.

Sprecher, C. A., F. J. Grant, G. Grimm, P. J. O'Hara, F. Norris, K. Norris and D. C. Foster (1993). "Molecular cloning of the cDNA for a human amyloid precursor protein homolog: evidence for a multigene family." Biochemistry 32(17): 4481-4486.

Sudol, M., H. I. Chen, C. Bougeret, A. Einbond and P. Bork (1995). "Characterization of a novel protein-binding module--the WW domain." FEBS Lett 369(1): 67-71.

Suzuki, N., T. T. Cheung, X. D. Cai, A. Odaka, L. Otvos, Jr., C. Eckman, T. E. Golde and S. G. Younkin (1994). "An increased percentage of long amyloid beta protein secreted by familial amyloid beta protein precursor (beta APP717) mutants." Science 264(5163): 1336-1340.

Takai, Y., K. Shimizu and T. Ohtsuka (2003). "The roles of cadherins and nectins in interneuronal synapse formation." Curr Opin Neurobiol 13(5): 520-526.

Takatsuki, A. and G. Tamura (1985). "[Inhibitors affecting synthesis and intracellular translocation of glycoproteins as probes]." Tanpakushitsu Kakusan Koso 30(6): 417-440.

Taler, V. and N. A. Phillips (2008). "Language performance in Alzheimer's disease and mild cognitive impairment: a comparative review." J Clin Exp Neuropsychol 30(5): 501-556.

Tamayev, R., D. Zhou and L. D'Adamio (2009). "The interactome of the amyloid beta precursor protein family members is shaped by phosphorylation of their intracellular domains." Mol Neurodegener 4: 28.

Tanzi, R. E., J. F. Gusella, P. C. Watkins, G. A. Bruns, P. St George-Hyslop, M. L. Van Keuren, D. Patterson, S. Pagan, D. M. Kurnit and R. L. Neve (1987). "Amyloid beta protein gene: cDNA, mRNA distribution, and genetic linkage near the Alzheimer locus." Science 235(4791): 880-884.

Tanzi, R. E., A. I. McClatchey, E. D. Lamperti, L. Villa-Komaroff, J. F. Gusella and R. L. Neve (1988). "Protease inhibitor domain encoded by an amyloid protein precursor mRNA associated with Alzheimer's disease." Nature 331(6156): 528-530.

Tarr, P. E., R. Roncarati, G. Pelicci, P. G. Pelicci and L. D'Adamio (2002). "Tyrosine phosphorylation of the beta-amyloid precursor protein cytoplasmic tail promotes interaction with Shc." J Biol Chem 277(19): 16798-16804.

Taru, H. and T. Suzuki (2004). "Facilitation of stress-induced phosphorylation of beta-amyloid precursor protein family members by X11-like/Mint2 protein." J Biol Chem 279(20): 21628-21636.

Teasdale, R. D. and M. R. Jackson (1996). "Signal-mediated sorting of membrane proteins between the endoplasmic reticulum and the golgi apparatus." Annu Rev Cell Dev Biol 12: 27-54.

Thinakaran, G. and E. H. Koo (2008). "Amyloid precursor protein trafficking, processing, and function." J Biol Chem 283(44): 29615-29619.

Thinakaran, G. and S. S. Sisodia (1994). "Amyloid precursor-like protein 2 (APLP2) is modified by the addition of chondroitin sulfate glycosaminoglycan at a single site." J Biol Chem 269(35): 22099-22104.

Tomita, S. and T. Suzuki (1999). "[Structure and function of proteins interacting with the cytoplasmic domain of APP]." Seikagaku 71(11): 1336-1340.

Trommsdorff, M., J. P. Borg, B. Margolis and J. Herz (1998). "Interaction of cytosolic adaptor proteins with neuronal apolipoprotein E receptors and the amyloid precursor protein." J Biol Chem 273(50): 33556-33560.

Tsiotra, P. C., K. Theodorakis, J. Papamatheakis and D. Karagogeos (1996). "The fibronectin domains of the neural adhesion molecule TAX-1 are necessary and sufficient for homophilic binding." J Biol Chem 271(46): 29216-29222.

Tucker, H. M., M. Kihiko-Ehmann and S. Estus (2002). "Urokinase-type plasminogen activator inhibits amyloid-beta neurotoxicity and fibrillogenesis via plasminogen." J Neurosci Res 70(2): 249-255.

Turano, C., S. Coppari, F. Altieri and A. Ferraro (2002). "Proteins of the PDI family: unpredicted non-ER locations and functions." J Cell Physiol 193(2): 154-163.

Turner, P. R., K. O'Connor, W. P. Tate and W. C. Abraham (2003). "Roles of amyloid precursor protein and its fragments in regulating neural activity, plasticity and memory." Prog Neurobiol 70(1): 1-32.

Ulery, P. G., J. Beers, I. Mikhailenko, R. E. Tanzi, G. W. Rebeck, B. T. Hyman and D. K. Strickland (2000). "Modulation of beta-amyloid precursor protein processing by the low density lipoprotein receptor-related protein (LRP). Evidence that LRP contributes to the pathogenesis of Alzheimer's disease." J Biol Chem 275(10): 7410-7415.

Unger, J. W., L. W. Lapham, T. H. McNeill, T. A. Eskin and R. W. Hamill (1991). "The amygdala in Alzheimer's disease: neuropathology and Alz 50 immunoreactivity." Neurobiol Aging 12(5): 389-399.

Van Nostrand, W. E., S. L. Wagner, M. Suzuki, B. H. Choi, J. S. Farrow, J. W. Geddes, C. W. Cotman and D. D. Cunningham (1989). "Protease nexin-II, a potent antichymotrypsin, shows identity to amyloid beta-protein precursor." Nature 341(6242): 546-549.

Vassar, R. (2002). "Beta-secretase (BACE) as a drug target for Alzheimer's disease." Adv Drug Deliv Rev 54(12): 1589-1602.

Vassar, R., B. D. Bennett, S. Babu-Khan, S. Kahn, E. A. Mendiaz, P. Denis, D. B. Teplow, S. Ross, P. Amarante, R. Loeloff, Y. Luo, S. Fisher, J. Fuller, S. Edenson, J. Lile, M. A. Jarosinski, A. L. Biere, E. Curran, T. Burgess, J. C. Louis, F. Collins, J. Treanor, G. Rogers and M. Citron (1999). "Beta-secretase cleavage of Alzheimer's amyloid precursor protein by the transmembrane aspartic protease BACE." Science 286(5440): 735-741.

Vidal, G. A., A. Naresh, L. Marrero and F. E. Jones (2005). "Presenilin-dependent gamma-secretase processing regulates multiple ERBB4/HER4 activities." J Biol Chem 280(20): 19777-19783.

von Koch, C. S., H. Zheng, H. Chen, M. Trumbauer, G. Thinakaran, L. H. van der Ploeg, D. L. Price and S. S. Sisodia (1997). "Generation of APLP2 KO mice and early postnatal lethality in APLP2/APP double KO mice." Neurobiol Aging 18(6): 661-669.

von Rotz, R. C., B. M. Kohli, J. Bosset, M. Meier, T. Suzuki, R. M. Nitsch and U. Konietzko (2004). "The APP intracellular domain forms nuclear multiprotein complexes and regulates the transcription of its own precursor." J Cell Sci 117(Pt 19): 4435-4448.

Waldemar, G., B. Dubois, M. Emre, J. Georges, I. G. McKeith, M. Rossor, P. Scheltens, P. Tariska and B. Winblad (2007). "Recommendations for the diagnosis and management of Alzheimer's disease and other disorders associated with dementia: EFNS guideline." Eur J Neurol 14(1): e1-26.

Waldemar, G., B. Dubois, M. Emre, P. Scheltens, P. Tariska and M. Rossor (2000). "Diagnosis and management of Alzheimer's disease and other disorders associated with dementia. The role of neurologists in Europe. European Federation of Neurological Societies." Eur J Neurol 7(2): 133-144.

Waldron, E., C. Heilig, A. Schweitzer, N. Nadella, S. Jaeger, A. M. Martin, S. Weggen, K. Brix and C. U. Pietrzik (2008). "LRP1 modulates APP trafficking along early compartments of the secretory pathway." Neurobiol Dis 31(2): 188-197.

Walsh, D. M., J. V. Fadeeva, M. J. LaVoie, K. Paliga, S. Eggert, W. T. Kimberly, W. Wasco and D. J. Selkoe (2003). "gamma-Secretase cleavage and binding to FE65 regulate the nuclear translocation of the intracellular C-terminal domain (ICD) of the APP family of proteins." Biochemistry 42(22): 6664-6673.

Wancata, J., M. Musalek, R. Alexandrowicz and M. Krautgartner (2003). "Number of dementia sufferers in Europe between the years 2000 and 2050." Eur Psychiatry 18(6): 306-313.

Wang, C. C. (1998). "Isomerase and chaperone activities of protein disulfide isomerase are both required for its function as a foldase." Biochemistry (Mosc) 63(4): 407-412.

Wang, E., J. G. Pennington, J. R. Goldenring, W. Hunziker and K. W. Dunn (2001). "Brefeldin A rapidly disrupts plasma membrane polarity by blocking polar sorting in common endosomes of MDCK cells." J Cell Sci 114(Pt 18): 3309-3321.

Wang, H., W. J. Luo, Y. W. Zhang, Y. M. Li, G. Thinakaran, P. Greengard and H. Xu (2004). "Presenilins and gamma-secretase inhibitors affect intracellular trafficking and cell surface localization of the gamma-secretase complex components." J Biol Chem 279(39): 40560-40566.

Wang, J., Y. Huang, M. Fang, Y. Zhang, Z. Zheng, Y. Zhao and W. Su (2002). "Brefeldin A, a cytotoxin produced by Paecilomyces sp. and Aspergillus clavatus isolated from Taxus mairei and Torreya grandis." FEMS Immunol Med Microbiol 34(1): 51-57.

Wang, L. H., K. G. Rothberg and R. G. Anderson (1993). "Mis-assembly of clathrin lattices on endosomes reveals a regulatory switch for coated pit formation." J Cell Biol 123(5): 1107-1117.

Wang, P., G. Yang, D. R. Mosier, P. Chang, T. Zaidi, Y. D. Gong, N. M. Zhao, B. Dominguez, K. F. Lee, W. B. Gan and H. Zheng (2005). "Defective neuromuscular synapses in mice lacking amyloid precursor protein (APP) and APP-Like protein 2." J Neurosci 25(5): 1219-1225.

Wang, Y. and Y. Ha (2004). "The X-ray structure of an antiparallel dimer of the human amyloid precursor protein E2 domain." Mol Cell 15(3): 343-353.

Wasco, W., K. Bupp, M. Magendantz, J. F. Gusella, R. E. Tanzi and F. Solomon (1992). "Identification of a mouse brain cDNA that encodes a protein related to the Alzheimer disease-associated amyloid beta protein precursor." Proc Natl Acad Sci U S A 89(22): 10758-10762.

Wasco, W., S. Gurubhagavatula, M. D. Paradis, D. M. Romano, S. S. Sisodia, B. T. Hyman, R. L. Neve and R. E. Tanzi (1993). "Isolation and characterization of APLP2 encoding a homologue of the Alzheimer's associated amyloid beta protein precursor." Nat Genet 5(1): 95-100.

Weidemann, A., G. Konig, D. Bunke, P. Fischer, J. M. Salbaum, C. L. Masters and K. Beyreuther (1989). "Identification, biogenesis, and localization of precursors of Alzheimer's disease A4 amyloid protein." Cell 57(1): 115-126.

Wolfe, M. S., W. Xia, C. L. Moore, D. D. Leatherwood, B. Ostaszewski, T. Rahmati, I. O. Donkor and D. J. Selkoe (1999). "Peptidomimetic probes and molecular modeling suggest that Alzheimer's gamma-secretase is an intramembrane-cleaving aspartyl protease." Biochemistry 38(15): 4720-4727.

Wolozin, B. L., A. Pruchnicki, D. W. Dickson and P. Davies (1986). "A neuronal antigen in the brains of Alzheimer patients." Science 232(4750): 648-650.

Wu, J. and R. J. Kaufman (2006). "From acute ER stress to physiological roles of the Unfolded Protein Response." Cell Death Differ 13(3): 374-384.

Yan, R., M. J. Bienkowski, M. E. Shuck, H. Miao, M. C. Tory, A. M. Pauley, J. R. Brashier, N. C. Stratman, W. R. Mathews, A. E. Buhl, D. B. Carter, A. G. Tomasselli, L. A. Parodi, R. L. Heinrikson and M. E. Gurney (1999). "Membrane-anchored aspartyl protease with Alzheimer's disease beta-secretase activity." Nature 402(6761): 533-537.

Yang, G., Y. D. Gong, K. Gong, W. L. Jiang, E. Kwon, P. Wang, H. Zheng, X. F. Zhang, W. B. Gan and N. M. Zhao (2005). "Reduced synaptic vesicle density and active zone size in mice lacking amyloid precursor protein (APP) and APP-like protein 2." Neurosci Lett 384(1-2): 66-71.

Yazaki, M., K. Tagawa, K. Maruyama, H. Sorimachi, T. Tsuchiya, S. Ishiura and K. Suzuki (1996). "Mutation of potential N-linked glycosylation sites in the Alzheimer's disease amyloid precursor protein (APP)." Neurosci Lett 221(1): 57-60.

Young-Pearse, T. L., J. Bai, R. Chang, J. B. Zheng, J. J. LoTurco and D. J. Selkoe (2007). "A critical function for beta-amyloid precursor protein in neuronal migration revealed by in utero RNA interference." J Neurosci 27(52): 14459-14469.

Yu, G., M. Nishimura, S. Arawaka, D. Levitan, L. Zhang, A. Tandon, Y. Q. Song, E. Rogaeva, F. Chen, T. Kawarai, A. Supala, L. Levesque, H. Yu, D. S. Yang, E. Holmes, P. Milman, Y. Liang, D. M. Zhang, D. H. Xu, C. Sato, E. Rogaev, M. Smith, C. Janus, Y. Zhang, R. Aebersold, L. S. Farrer, S. Sorbi, A. Bruni, P. Fraser and P. St George-Hyslop (2000). "Nicastrin modulates presenilin-mediated notch/glp-1 signal transduction and betaAPP processing." Nature 407(6800): 48-54.

Zambrano, N., J. D. Buxbaum, G. Minopoli, F. Fiore, P. De Candia, S. De Renzis, R. Faraonio, S. Sabo, J. Cheetham, M. Sudol and T. Russo (1997). "Interaction of the phosphotyrosine interaction/phosphotyrosine binding-related domains of Fe65 with wild-type and mutant Alzheimer's beta-amyloid precursor proteins." J Biol Chem 272(10): 6399-6405.

Zhang, Z., C. H. Lee, V. Mandiyan, J. P. Borg, B. Margolis, J. Schlessinger and J. Kuriyan (1997). "Sequence-specific recognition of the internalization motif of the Alzheimer's amyloid precursor protein by the X11 PTB domain." Embo J 16(20): 6141-6150.

Zhao, X., T. Greener, H. Al-Hasani, S. W. Cushman, E. Eisenberg and L. E. Greene (2001). "Expression of auxilin or AP180 inhibits endocytosis by mislocalizing clathrin: evidence for formation of nascent pits containing AP1 or AP2 but not clathrin." J Cell Sci 114(Pt 2): 353-365.

Zhao, G., G. Mao, J. Tan, Y. Dong, M. Z. Cui, S. H. Kim and X. Xu (2004). "Identification of a new presenilin-dependent zeta-cleavage site within the transmembrane domain of amyloid precursor protein." J Biol Chem 279(49): 50647-50650.

Zheng, H., M. Jiang, M. E. Trumbauer, D. J. Sirinathsinghji, R. Hopkins, D. W. Smith, R. P. Heavens, G. R. Dawson, S. Boyce, M. W. Conner, K. A. Stevens, H. H. Slunt, S. S. Sisoda, H. Y. Chen and L. H. Van der Ploeg (1995). "beta-Amyloid precursor protein-deficient mice show reactive gliosis and decreased locomotor activity." Cell 81(4): 525-531.

Zheng, H. and E. H. Koo (2006). "The amyloid precursor protein: beyond amyloid." Mol Neurodegener 1: 5.

Zhou, F., T. van Laar, H. Huang and L. Zhang (2011). "APP and APLP1 are degraded through autophagy in response to proteasome inhibition in neuronal cells." Protein Cell 2(5): 377-383.

8 Appendix

8.1 Publications

Isbert, S., K. Wagner, S. Eggert, A. Schweitzer, G. Multhaup, S. Weggen, S. Kins and C. U. Pietrzik (2011). "APP dimer formation is initiated in the endoplasmic reticulum and differs between isoforms. " Cell Mol Life Sci 2011 Nov 22. [Epub ahead of print]

Jefferson, T., M. Causevic, U. auf dem Keller, O. Schilling, S. Isbert, R. Geyer, W. Maier, S. Tschickardt, T. Jumpertz, S. Weggen, J. S. Bond, C. M. Overall, C. U. Pietrzik and C. Becker-Pauly (2011). "Metalloprotease meprin beta generates nontoxic N-terminal amyloid precursor protein fragments in vivo." J Biol Chem 286(31): 27741-27750.

Luthringer, B., S. Isbert, W. E. Muller, C. Zilberberg, N. L. Thakur, G. Worheide, R. H. Stauber, M. Kelve and M. Wiens (2011). "Poriferan survivin exhibits a conserved regulatory role in the interconnected pathways of cell cycle and apoptosis." Cell Death Differ 18(2): 201-213.

Reekmans, S. M., T. Pflanzner, P. L. Gordts, S. Isbert, P. Zimmermann, W. Annaert, S. Weggen, A. J. Roebroek and C. U. Pietrzik (2010). "Inactivation of the proximal NPXY motif impairs early steps in LRP1 biosynthesis." Cell Mol Life Sci 67(1): 135-145.

Waldron, E., S. Isbert, A. Kern, S. Jaeger, A. M. Martin, S. S. Hebert, C. Behl, S. Weggen, B. De Strooper and C. U. Pietrzik (2008). "Increased AICD generation does not result in increased nuclear translocation or activation of target gene transcription." Exp Cell Res 314(13): 2419-2433.

8.2 Contribution to international meetings

40th Annulal Meeting, Neuroscience 2010; November 10-13, 2010; San Diego, California, USA

Oral Presentation/NANOSYMPOSIUM 11.2 - APP Metabolism and Processing -

"*APP dimer formation in an oxidizing environment as provided by the endoplasmic reticulum"*

Simone Isbert, Daniela Kaden, Gerd Multhaup, Sascha Weggen, Stefan Kins, Claus U. Pietrzik

8.3 Danksagung

8.4 Curriculum Vitae

8.5 Eidesstattliche Erklärung

Die vorliegende Arbeit wurde in der Zeit von Februar 2008 bis November 2011 am Institut für Pathobiochmie angefertigt.

Hiermit versichere ich an Eides statt, dass ich die vorliegende Promotionsarbeit selbstständig verfasst und nur unter Verwendung der angegebenen Hilfsmittel angefertigt habe.

Mainz, den

_____